Impact of Obesity on Metabolism of Some Selected Anesthetic Agents

by

Hamdah Mohammed Al Nebaihi

A thesis submitted in partial fulfillment of the requirements for the degree of

Master of Science

In

Pharmaceutical Sciences

Faculty of Pharmacy and Pharmaceutical Sciences
University of Alberta

Abstract

Over the last few decades the incidence of obesity has increased remarkably in Canada and in the rest of the world, with the highest increases occurring in the excessive weight categories class II (BMI 35– 39.9) and class III (BMI ≥ 40). By 2019, it is anticipated that over 20% of the Canadian adult population will be obese. Obese patients pose significant challenges to anesthesiologists in terms of dose accuracy of anesthetics due to potentially altered pharmacokinetics. In our research project, we aim to investigate the influence of obesity on the proteins level of drug metabolizing enzymes as well as the drug pharmacokinetics parameters of propofol and lidocaine which are commonly used drugs for the induction and maintenance of general and local anesthesia. In addition, we aim to assess the impact of obesity on drug metabolizing enzymes after high fat feedings, and after a switch back to a normal diet.

For lidocaine study, male and female rats (n=8 for each group) were fed high fat diet (HF) for 14 weeks. At the end of 14 weeks period, half of each male and female group were euthanized. In the remaining rats, the diet was switched to standard rat chow. Four weeks after, those rats were euthanized. For each 14 & 18 week groups, control rats (n=4 each) were fed standard chow. Afterwards, we investigated the impact of obesity on the activity of phase I drug metabolizing enzymes using lidocaine as well as the protein contents of cytochrome P450 (CYP) enzymes in female rats. What we found is that after 14 weeks on high fat diet, MEGX (lidocaine active metabolite) maximum formation rate was reduced significantly. Moreover, Expressions of CYP3A1, CYP1A2 and CYP2C12 were also significantly lower compared to control group. Interestingly, the expressions were returned to normal levels when the normal diet was implemented from weeks 14 to 18. We also examined the influence of obesity on phase II enzymes using propofol as well as the protein expression of UGT1A1 (phase II) and CYP2D1 (phase I). In this part of experiment, the animal model comprised male rats fed 14 weeks of either

standard (normal) chow with water (control), 45% high fat chow (HF) and water, normal chow with high fructose corn syrup water (HFCS), and HFCS and HF combined. After 14 weeks on high caloric diet, hepatic microsomal rate of glucuronidation of propofol was significantly low in HF group while HFCS and HFCS+HF showed the opposite effect on glucuronidation activity. Diet rich in fat led to reduction in the activity of UGT1A1 and CYP2D1.

Our findings indicate that diet-induced obesity was associated with reduction in the hepatic microsomal rates of MEGX formation and expression of some metabolizing enzymes. Hepatic microsomal rate of glucuronidation demonstrated a different trend in the enzyme activities with different diet (HF, HFCS and HF+HFCS). Reduction in the fat content of the diet reversed the changes in CYP expression.

Preface

This thesis is an original work by Hamdah Mohammed S Al Nebaihi. The research project, of which this thesis is a part, received research ethics approval from the University of Alberta Research Ethics Board, Project Name “Investigating the impact of obesity on proteins involved in drug disposition”, No. AUP00000825.

This work is dedicated to

My lovely parents Mohammed Al Nebaihi and Nawal Alhaydan, who I have learnt from, grown from and developed many life asset skills that has sustained me throughout this project. In addition, how they've impacted the true definition of what it means to be an independent-hardworking-self-sufficient lady and scholar.

My wonderful brothers Ahmed, Mshari, Naif and Abdullah, my sisters Hessah and Munira who have been a mental and emotional support throughout long nights of research and experiments.

Thank you

Acknowledgment

I would like to express my sincere gratitude to my supervisor **Dr. Dion Brocks** for his understanding, encouragement and unlimited support throughout my Master's program. His guidance has helped me in all the research and writing of the thesis.

I would like to thank my examining committee members **Dr. Ayman El-Kadi and Dr. John Ussher** for their insightful comments, constructive feedbacks and encouragement.

My appreciation is extended to Dr. Ayman El-Kadi for his support and providing unlimited accessibility of his laboratory facilities.

My appreciation is extended to Dr. John Ussher for his support and providing us some murine liver samples.

I would also like to thank my fellow lab mates Yousef Bin Jardan and Marwa Al-Agili for their help and friendly lab environment, especially in the beginning of my Master's program.

I would like to thank my friends Malak Almutairi and Mead Almowaled, and my lab mates Zaid Alma'ayah, Ahmed Alammari and Rami Al Batran for their assistance and help in some experiments during my studies.

I would like to also thank the King Abdullah Scholarship program supported by the Ministry of Higher Education in Saudi Arabia for allowing me to pursue my Master's degree.

Finally, I would also like to thank all the academic and non-academic supporting staff at the Faculty of Pharmacy and Pharmaceutical Sciences, University of Alberta.

Thank you all

Table of Contents

List of tables

List of Figures

List of abbreviation and symbols:

SSRIs	Selective serotonin reuptake inhibitors
MAOIs	Monoamine oxidase inhibitors
LEP	Leptin deficiency
LEPR	Leptin receptor deficiency
SAF	Saturated fatty acids
PUFA	Polyunsaturated fatty acids
NAPQI	N-acetyl-p-benzoquinone imine (Acetaminophen)
NAFLD	Non-alcoholic fatty liver disease
APAP	Acetyl-para-aminophenol
°C	Degree Celsius
DMSO	Dimethyl sulfoxide
ANOVA	Analysis of variance
BMI	Body mass index
TBW	Total body weight
LBW	Lean body weight
BSA	Body surface area
NADPH	Nicotinamide adenine dinucleotide phosphate tetrasodium
UDPGA	Uridine 5′_diphosphoglucuronic acid trisodium salt
Cl	Clearance
Cmax	Maximum plasma drug concentration
CYPs	Cytochrome P450
H2SO4	Sulfuric acid
HCl	Hydrochloric acid
HDL	High-density lipoprotein
HFCS	High fructose corn syrup(Group or liquid used)
HF	Group provided high fat diet 45% kcal of fat and normal water
HF+HFCS	Group provided high fat diet (45% kcal fat) with 13%w/v HFCS
HPLC	High performance liquid chromatography
IBW	Ideal bodyweight
IFN	Interferon γ
IL	Interleukin
IS	Internal standard
iv	Intravenous
Kg	Kilogram

KH2PO4	Potassium dihydrogen phosphate
LBW	Lean body weight
LDL	Low-density lipoprotein
m^2	Square meters
mg	Milligram
min	Minutes
mL	Milli liter
mM	Milli molar
mRNA	Messenger RNA
Na_2CO_3	Sodium carbonate
nmol	Nano mole
PK	Pharmacokinetics
SD	Standard deviation
t ½	Terminal elimination phase half-life
Tmax	Time to reach Cmax
TNFα	Tumor necrosis factor alpha
UGTs	UDP-glucuronosyltransferases
UV	Ultra-violet
Vd	Volume of distribution
WHO	World Health Organization
µg	Microgram
µL	Microliter

Chapter 1: Introduction

1.1 Obesity

Over the last few decades the prevalence of obesity has increased remarkably in Canada and worldwide, with the highest increases occurring in the excessive weight categories class II (BMI 35– 39.9) and class III (BMI ≥ 40) [1][2]. By 2019, it is anticipated that over 20% of the Canadian adult population will be obese [1]. Thus, it is critical to realize the definition of obesity. Obesity can be defined based on the method used to determine the presence of obesity (waist circumference, body mass index, BMI). The World Health Organization (WHO) relies on BMI to classify the obesity which takes into consideration the individual's weight in kilograms divided by individual's height in meters squared (kg/m^2) (Table 1) [3].

Table 1: International classification of adult overweight and obesity according to body mass index

	BMI (kg/m^2)	
Classification	**Principal Cutoff Points**	**Additional Cutoff Points**
Overweight	≥ 25.00	≥ 25.00
Preobese	25.00-29.99	25.00-27.49
		27.50-29.99
Obese	≥30.00	≥30.00
Obese class I	30.00-34.99	30.00-32.49
		32.50-34.99
Obese class II	35.00-39.99	35.00-37.49
		37.50-39.99
Obese class III	≥40.00	≥40

BMI classification by World Health Organization. 2016.

Obesity has negative consequences on the cardiovascular (CV) system as it triggers chronic accumulation of excess body fat which leads to not only metabolic changes and cardiovascular diseases (CVD), but also influencing systems modulating inflammation [4]. It poses a risk factor since it associates with other comorbid diseases including hypertension, dyslipidemia, glucose intolerance, obstructive sleep apnea or hypoventilation, and inflammatory condition [5].

There are many factors that initiate the risk of obesity including medically treatable causes of obesity (Table 2) [6], low energy expenditure [7], and food intake when the consumption of energy-dense foods is high, especially for those with a high glycemic index (GI), are the primary factors leading to increase in the prevalence of the global epidemic of obesity[8]. The high-GI carbohydrates enhance the sensation of hunger and increases energy intake consequently [9][10].

Table 2: Medically treatable causes of obesity

Drug-induced (>97 %)	Anti- seizure (Carbamazepine, valproate, gabapentin) Anti- depressant: Tricyclics (nortriptyline, amitriptyline, doxepin), SSRIs (paroxetine, escitalopram), mirtazapine, MAO-inhibitors, lithium. Anti- psychotic (Olanzapine, clozapine, quetiapine, risperidone). Anti- diabetic (Insulin, sulfonylureas, thiazolidinedione) Steroids (Corticosteroids, Depo-Provera)
Genetic syndromes (<1 %)	Albright hereditary osteodystrophy Alstrom-Hallgren syndrome Bardet-Biedl syndrome Beckwith-Wiederman syndrome

	Carpenter syndrome Cohen syndrome Prader-Willi syndrome
Single-gene disorders (<1 %)	Leptin deficiency (LEP) Leptin receptor deficiency (LEPR) Proopiomelanocortin deficiency Prohormone convertase 1 impairment Melanocortin receptor 4 deficiency
Endocrine disorders (<1 %)	Cortisol Excess (corticosteroid medication, Cushing syndrome) Hypothyroidism Growth hormone deficiency Acquired hypothalamic lesions • Infection • Vascular malformation • Neoplasm • ROHHAD/ROHHADNET syndrome • Trauma

1.2 Physiological changes associated with obesity

Obesity influences drug disposition as it leads to physiological and pathophysiological changes in the body. In comparison with healthy individuals of the same age, gender, and height, obese patients have larger absolute lean body masses and fat mass. Although the lean components represent 20 to 40% of extra weight, the fat mass is doubled in those subjects [11]. Other physiological changes occur as differences come in hormonal release, cardiac

output, blood flow as well as in the expression of proinflammatory cytokines including IL-6, TNF-α and IL-10 [11], [12].

Those alternations in the body are risk factors for developing of serious comorbid diseases including hyperlipidemia, hypertension, insulin resistance and type 2 diabetes, and other cardiovascular diseases [13]. Due to the increase of total body weight load on the joints, the majority of obese patients have an experience with osteoarthritis [14]. It is common that obesity associates with dyspnea as it causes a reduction in chest wall compliance and a reduction of respiratory muscle [15]. In terms of gastrointestinal tract function, it has been reported that gastric emptying rate and drug permeability through the gut wall are elevated in obese subject [16].

Because of some pathophysiological alterations that concomitant with obesity and the majority of obese individuals are treated pharmacologically, it is critical to consider the pharmacokinetics and pharmacodynamics changes of administered drugs in these individuals [16].

1.3 Animal models of obesity

A wide variety of animal models are available to study the impact of obesity on pharmacokinetics. One of these models is based on mutation or knock out of one or more genes that trigger obesity. Poor lifestyle including consumption of high caloric diet and sedentary life style is another factor that boosts weight gain [17].

1.3.1. Diet induced obesity models

Keeping animals on high caloric diet for prolonged periods of time are one of the most commonly used models for induction of obesity. This model was adopted to simulate the most common factor that induces obesity in human beings.

In this model the animals are fed high fat (HF) or high fructose corn syrup (HFCS), or a combination of both (HF+HFCS), which has been reported to exhibit remarkable increases in body weight and adiposity compared to control animals on standard show for the same period of time [18],[19]. Some studies utilize different types of HF, for example, they differ in the source of fatty acids (animal or plant origin) and the type of fatty acid (saturated fatty acids (SFA), polyunsaturated fatty acids (PUFA))[148].

The diet induced obesity models in the literature are distinct from each other in terms of the composition of diet that is used to promote the obesity, the diet duration, and species used, thereby resulting in different extents of obesity as well as biological and physiological changes. Another adopted model is breeding of obese animals from dietary obese models as those offspring have a higher chance of being obese [20].

1.3.2. Models of obesity involving genetic ablation of leptin

This model is induced by mutation of a specific gene that plays role in regulation of leptin signaling pathway and / or leptin receptor. The model where the mutation of ob gene leads to termination of leptin secretion is known as “ob/ob” mouse, and it is characterized with hyperinsulinemia, hyperglycemia, hypothyroidism and hyperphagia. When there is a mutation that causes a defect in leptin receptors, it triggers morbid obesity and is called the leptin receptor deficient “db/db” mouse or the leptin receptor-deficient “fa/fa Zucker rat [21], [22].

1.4. Management of obesity

Lifestyle changes, pharmacotherapy and bariatric surgery are different strategies used to manage obesity.

1.4.1 Self directed or prescribed lifestyle modifications

Lifestyle intervention is an essential approach regardless of augmentation by drugs or surgery [23]. Its concept mainly relies on increasing the physical activity and restriction on caloric intake which has been shown a reduction in body weight from 5 to 7% [24]. Behavioral therapy is a complementary part of lifestyle modification which focuses on goal setting for obese individuals to minimize and monitor their caloric intake [25]. After lifestyle modification, those subjects may experience weight loss in a relatively short period of time; however, they are liable to gain weight again [26].

1.4.2 Other medical interventions

1.4.2.1. Pharmacotherapy

In some cases when the individual is considered to be obese or morbidly obese (BMI ≥ 30 kg/m^2) or overweight (MBI ≥ 27 kg/m^2), they are considered high risk for developing complications. Thus, medical intervention is required to overcome and manage the obesity. There is some medication for short and long-term therapy. Short term therapy which last for 12 weeks or less includes phendimetrazine, phentermine, diethylpropion, and benzphetamine. Those medications work through appetite suppression. Other available medications used for long term are orlistat, liraglutide, lorcaserin, or a combination of naltrexone/bupropion [27].

1.4.2.2. Bariatric surgery

Bariatric surgery is recommended when dietary and/or the medical weight loss failed to manage the morbidly obese patients (BMI ≥ 35 kg//m^2) [27]. Based on a 2011 report, the prevalence of metabolic bariatric procedures worldwide was high with the number of procedures reaching over 340,000 [28]. Several positive outcomes were observed after bariatric surgery in a six year study. Those positive outcomes included sustainable weight loss, diabetes remission, and significant improvement of metabolic and cardiovascular risk factors [29]. However, there were some negative consequences after surgery including malabsorption of essential elements such as vitamin B12 as well as alteration of some drugs disposition [27].

There are several forms of bariatric surgery, such as laparoscopic sleeve gastrectomy (LSG) where a section of stomach is removed, laparoscopic adjustable gastric banding (LAGB), by placing an adjustable band around the upper part of the stomach, and bilio-pancreatic

diversion with duodenal switch (BPD-DS) which simply works through removing two third of distal stomach and connecting ileum to the proximal stomach. In the laparoscopic Roux-en-Y gastric bypass (LRYGBP), the physician tends to make a small upper pouch and a large lower pouch, after which the upper part is connected to small intestine [29]. LRYGBP is the most performed procedure used worldwide (47% of procedures); laparoscopic sleeve gastrectomy (~28%); laparoscopic adjustable gastric banding (~ 18%); and bilio-pancreatic diversion with duodenal switch (2.2%) [30].

1.5. Measures used to calculate drug doses in obese individuals

At the level of health care, there are some concerns regarding the impact of obesity on the pharmacokinetics of drugs and the most suitable measure to calculate safe and effective drug doses for those patients. Some of the used metrics such as body mass index (BMI), lean body mass (LBM), body surface area (BSA), ideal bodyweight (IBW), and adjusted bodyweight rely on other factors including gender, height, and weight. Those measured are known as indirect measures of arthrometrics [31].

Body mass index (BMI), an approved measure of body composition which incorporate total body weight (TBW) in kilograms and height in meters. BMI classifies people as obese if their BMIs greater than or equal to 30 kg/m^2 and as morbidly obese if greater than 40 kg/m^2 [27].

Body surface area (BSA) is used to determine the dosage of wide variety of anticancer agents. Even though the usage of BSA in dosing obese individuals is not well studied, many physicians tend to utilize BSA value of $2m^2$ for patients whose actual BSA too higher. Since

the utility of ideal body weight (IBW) in dosing provides all subjects with the same sex and height the same dose regardless the body composition, it is not an optimal metric to use for drugs that distribute into fatty tissues [31].

Lean body weight (LBW) is a size descriptor of weight that represents the body composition apart from adipose tissue [27]. One of the recently conducted reviews recommends utilizing LBW for guiding dosing in obesity [32]. However, the reasoning is rather simplistic as the authors did not take into account factors such as lipophilicity of drugs or possible changes in factors such as drug metabolizing efficiency in making the conclusion. Indeed, the few drugs they examined were very highly water soluble; such drugs are intrinsically best to dose according to lean or ideal body weight. Other pharmacokinetics studies on obesity advocated that TBW was a good descriptor for assessing dosing needs [33] [34].

1.6. Effect of obesity on drug pharmacokinetics

Because there is no evidence-based guide for drug dosing in morbidly obese patients, it is critical to understand how body composition impacts the pharmacokinetics of drugs [32].

The volume of distribution (Vd), the rate and extent of absorption, and the elimination rate of the drug are all factors that affect the drug concentration in the body [35]. The distribution of drug into body compartments depends on several factors including tissue blood flow, plasma and tissue protein binding, as well as the physiochemical prosperities of the drug such as the molecular size, lipid solubility, and extent of ionization [31]. Other important parameter is clearance (CL) which represents the amount of drug removed from the body per unit time, and

it relies on the phase I and phase II metabolizing enzymes, renal tubular reabsorption and secretion, and globular filtration rate [36].

Obesity is associated with pathophysiological changes in total adipose tissue, hepatic blood flow, hormone productivity, serum lipid concentrations and enzyme activities. Thus, it could influence the pharmacokinetics and pharmacodynamics properties of administered drugs.

1.6.1. Effect of obesity on drug bioavailability and absorption

Absorption is a process where the drug moves from the site of administration to the circulation [37]. Many available studies have studied the effect of obesity on the absorption rate and the bioavailability. The observed changes between obese and non-obese volunteers are a consequence of pathophysiological changes that associated with obesity.

It was reported that the oral bioavailability of propranolol was slightly higher in obese subjects than normal subjects as the oral clearance of propranolol was low compared to healthy volunteers [38]. However, there was no difference in oral absorption rate of cyclosporine, moxifloxacin and dexfenfluramine between obese and nonobese patients [39-41].

In terms of subcutaneous injection, a microdialysis study demonstrated that the penetration ratio of injected cefazolin over short period of time was declined by 30% in obese individuals [42]. Similarly, the absorption of enoxaparin, a low molecular weight heparin, was reduced in obese group compared to control group, but the extent of absorption was completed in all groups [43]. In contrast, one study showed that the absorption rate of rapid-acting insulin that injected subcutaneously did not differ in obese and those nonobese with type 2 diabetes

mellitus [44]. Further studies are required to investigate the effect of obesity on drug absorption.

1.6.2. Effect of obesity on drug distribution

The extent by which a drug is distributed to tissues is largely dictated by the fraction bound to tissues relative to plasma proteins [45]. Indeed, the Vd is often altered in obesity [12] [46]. A number of other factors are involved including tissue blood flow, and physiochemical properties of the drug [16][47]. Drug lipophilicity, molecular weight, degree of ionization, and affinity to protein binding are examples of physiochemical characteristics of the drug that can play a role in drug distribution [31] [48].

The alteration in the volume of distribution might be predicted in obese patients as a result of increased cardiac output, increased fat mass, increased blood volume and reduced tissue perfusion [31] [49] [50]. Intuitively, obesity has more influence on hydrophobic drugs than hydrophilic drugs [51]. Nonetheless, prediction of the changes in the Vd is difficult, and it cannot be based solely on the drug's lipophilicity. This point of view is because when the volume of distribution was normalized with body weight, its value may be increased, reduced, or unchanged [12]. For example, the peripheral volume of distribution for propofol, a relatively lipophilic drug, was not altered in obese individuals [52] [53]. Other drugs such as cyclosporine A showed a decreased Vd in obese subjects. The normalized Vd to body weight in case of using hydrophilic drug was unchanged or decreased, yet the effect of obesity on hydrophilic drugs was smaller than hydrophobic drugs [12].

Albumin, α1-acid glycoprotein, and lipoprotein are plasma proteins that tend to bind to a wide range of circulating drugs. The concentrations of albumin, which has a high affinity for binding to acidic drugs, does not seem to be changed because of being overweight whereas α1-acid glycoprotein levels are elevated [51]. The plasma concentration of unbound thiopental and phenytoin do not appear to deviate in obese subjects as they mainly bind to serum albumin. Drugs that bind to α1-acid glycoprotein might display no changes in unbound drug levels (verapamil, triazolam "intravenous dose") or reduction in free drug concentration (propranolol "intravenous dose")[149][150]. Moreover, the level of triglyceride and cholesterol are high in obese patients, hence inconsistent changes in free drug concentration are expected [54].

Thus, the Vd is not only influenced by lipophilicity of administered drug, it is also affected by plasma protein concentration as well as the body composition. Further studies are needed to investigate the impact of obesity on drug distribution.

1.6.3 Effect of obesity on drug metabolism

Metabolism of exogenous substrates predominantly occurs in the liver through hepatic enzymes that either modify the functional groups of these substrates (phase I metabolism) and/or conjugate the functional groups to endogenous substrates to increase the solubility of these compounds such that they can be more readily eliminated from the body (phase II metabolism) (Figure 1) [55]. Over one-third of obese patients experience histological changes in liver tissue primarily due to steatosis [56]. Non-alcoholic fatty liver disease (NAFLD) may range from simple liver steatosis without inflammation to non-alcoholic steatohepatitis (NASH) with inflammation [57]. Even though the assessment of non-alcoholic steatohepatitis is challenging to some extent, it is estimated that up to 20% of obese individuals and up to 50% of morbidly obese patients have NASH, and its prevalence correlates with body mass

index (kg/m^2) [58]. It is documented that some obese patients have altered enzymatic activity compared to normal individuals because of accumulation and deposition of fat in the liver (fat infiltration) [59]. Thus, it is crucial to understand the enzymes that could be influenced by obesity and to which degree or severity as the changes in the metabolism in obesity have not been well studies.

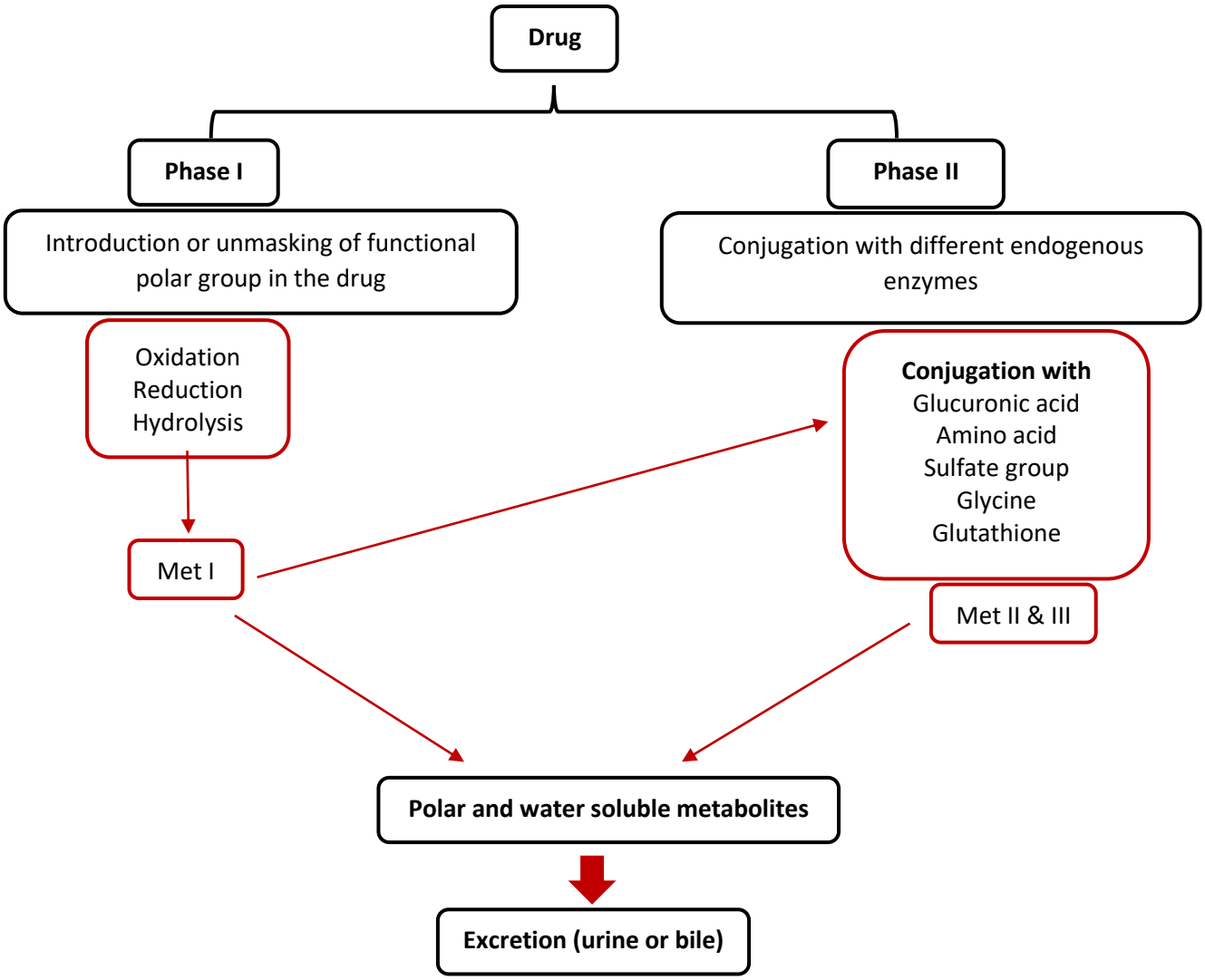

Figure 1: Chemical reactions and enzymes involve in phase I and phase II metabolic reactions. Met = metabolism

1.6.3.1. Phase I Metabolism

The majority of phase I enzymes consist of cytochrome P450 (CYPs), which catalyze the modification of functional groups of substrates (oxidation, reduction, and hydrolysis) [61]. CYPs are predominantly located in the smooth endoplasmic reticulum of hepatocytes, and they participate in approximately three-quarters of total drug metabolism [62].

1.6.3.1.1. Cytochrome P450 (CYP) 3A4

Almost half of drugs that are metabolised in the phase I reaction are catalyzed by CYP3A4 [60]. Several studies have been conducted to evaluate the impact of obesity on the activity of CYP3A4 compared to non-obese patients [36]. Erythromycin, for example, is one of the most commonly used antibiotics [63], and it is reported that its metabolism is markedly decreased in obese individuals compared to non-obese individuals (measured with breath analysis method using [^{14}C]-N-methyl-erythromycin) [64]. This indicates a reduction of CYP3A4 metabolic activity [36]. Similarly, triazolam metabolism was considerably decreased in overweight individuals [65]. Moreover, it was found that obesity is associated with lower clearance of cyclosporine and alprazolam, although this was not statistically significant [39][65].

Michaut concluded that reduction in enzymatic activity of CYP3A4 is considered to be a protective factor against liver injury in obese subjects since the reduction of CYP3A4 is associated with low production of N-acetyl-p-benzoquinone imine (NAPQI), the toxic metabolite of acetyl-para-aminophenol (APAP) [66]. Thus, it is clear that obesity is associated with impairment of CYP3A4 activity.

1.6.3.1.2. CYP2E1

Even though only 5% of phase I metabolism is catalyzed by CYP2E1 [62], numerous studies have been conducted to assess the effect of obesity on CYP2E1 activity and a significant proportion of morbidly obese patients were involved in these studies [36]. Lucas et al. demonstrated that CYP2E1 activity was 40% higher in obese individuals as compared with non-obese individuals [67]. It can also metabolize procarcinogens and industrial solvents, which may lead to reactive oxygen species (ROS), thereby increasing the risk of cancer development [68].

Increased levels of 6-hydroxylation of the muscle relaxant chlorzoxazone is associated with morbidly obese individuals, which is consistent with induction of CYP2E1 [16]. Importantly, obesity and related metabolic disorders are associated with marked alterations of acetaminophen (N-acetyl-para-aminophenol: APAP) pharmacokinetics [66]. Studies by Abernethy et al. demonstrated higher APAP glucuronidation in hepatic microsomes from ob/ob mice compared with wild type mice. Similarly, increasing APAP glucuronidation has also been observed in obese subjects, which suggests a lower risk of APAP toxicity in obese individuals [69]. However, a recent study demonstrated that increased glucuronidation of APAP among obese individuals was associated with increased CYP2E1 activity, thereby enhancing the risk of APAP induced hepatotoxicity [70]. Induction of CYP2E1 is one of the major factors that leads to reactive oxygen species (ROS) overproduction during non-alcoholic steatohepatitis (NASH) [71] (Figure 2).

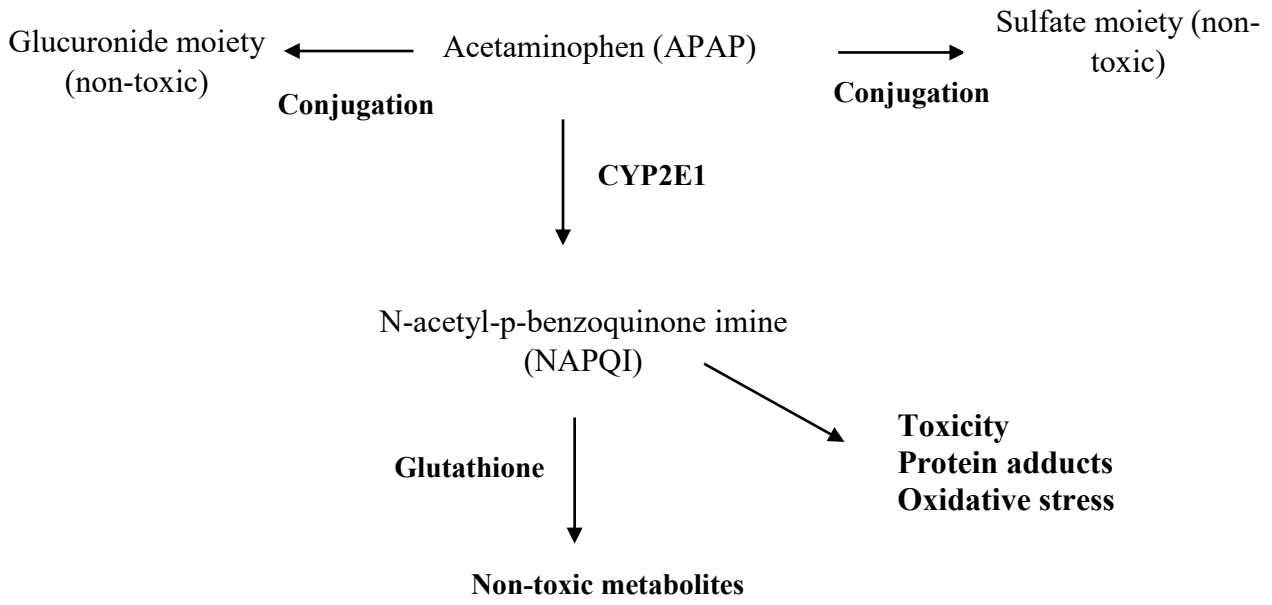

Figure 2: The metabolism of acetaminophen in humans

1.6.3.1.3. CYP2D6

Cytochrome P450 (CYP) 2D6 is a polypeptide that consists of 497 amino acids [72]. Even though CYP2D6 metabolizes a small proportion of phase I drugs (10-15%) [60], its role in drug metabolism is tremendously higher than its relative content [73]. CYP2D6 polymorphisms influence the metabolism rate of about half of medications that are in clinical use; consequently, pharmacokinetic parameters of these medications are altered [74].

Pharmacokinetic parameters of dexfenfluramine and nebivolol, which are CYP2D6 substrates, have been studied in obese and non-obese patients. It has been postulated that clearance of dexfenfluramine and metabolite to parent ratio were higher in obese versus non-obese individuals [40]. Likewise, nebivolol metabolism is relatively high in obese patients compared

to non-obese patients [75]. Since nebivolol metabolism is relatively high, it was suggested that its clearance depends more on liver blood flow than on intrinsic Cytochrome P450 metabolism. However, it has been reported that CYP2D6 phenotype influences the metabolism of nebivolol [76]. Based on these studies, it can be concluded that CYP2D6 activity tends to be higher in obese populations compared to non-obese populations [36].

1.6.3.1.4. CYP1A2

CYP1A2 involves metabolism of a small proportion of total phase I drug metabolism [77]. It was reported that smoking induces expression of CYP1A2, and it is important to consider this point since it was reported that 16.4% of Canadians population consume cigarettes per day [78][79].

Because caffeine and theophylline are specific substrates of CYP1A2, they are used to indicate CYP1A2 activity [80][81]. Several studies have been conducted to evaluate the influence of obesity on CYP1A2 activity [16]. In terms of caffeine metabolism, Caraco et al. found that elimination half-life and clearance of caffeine were similar in non-smoking obese and non-smoking lean individuals [82]. Another caffeine study in adult obese and non-obese subjects did not report a significant difference in caffeine metabolism [83].

Regarding theophylline clearance, it was reported by Jusko et al. that theophylline metabolism did not differ statistically in moderately obese versus healthy-weight individuals [84]. However, after considering the impact of smoking, Blouin et al. confirmed that there is no remarkable difference in theophylline metabolism between smokers and non-smokers obese, and that total body weight provides a better estimation of theophylline clearance than ideal

body weight [85]. Thus, these few studies indicate a trend towards increased CYP1A2 activity in the smoker population compared to the general population. However, CYP1A2 activity does not differ significantly between smokers and non-smokers obese.

1.6.3.1.5. CYP2C9

CYP2C9 catalyzes about 10 % of P450-mediated metabolic reactions of drugs currently on the market [60]. There are some clinically used medications that are substrates for CYP2C9, including Ibuprofen and phenytoin. These have been studied in obese individuals. Ibuprofen and phenytoin in obese patients were studied by Abernethy et al. These studies revealed that clearance of ibuprofen and phenytoin showed an upward trend in obese subjects compared with non-obese subjects, although phenytoin metabolism was not statistically significant [86][87]. Thus, these studies implied slightly increased CYP2C9-mediated metabolism in obese patients versus control group patients.

1.6.3.1.6. CYP2C19

Less than 10% of phase I metabolic reactions are catalyzed by CYP2C19 [60]. Due to genetic polymorphisms, CYP2C19 activity varies among the population [88]. The clearance of diazepam and desmethyldiazepam has been extensively studied. Two studies showed that metabolism of diazepam was decreased in obese subjects compared to non-obese patients, thereby extending the half-life of the drug [89][49]. Another study conducted on desmethyldiazepam demonstrated a reduction in the activity of CYP2C19 among obese

individuals [90]. It was concluded that there is a trend towards decreased CYP2C19 activity in obese versus non-obese patients.

1.6.3.1.7. Other Phase I Metabolic Enzymes

Xanthine Oxidase

Xanthine oxidase is a phase I enzyme that plays an important role with CYP in metabolizing drugs [91]. Mercaptopurine, for instance, is extensively metabolized by xanthine oxidase [92]. Its clearance was evaluated in nine obese children, and it was found that the metabolism rate was significantly elevated compared with non-obese children [93]. Similarly, caffeine clearance was assessed in the same study, and it was shown that the concentration of its metabolite in the urine was significantly increased in obese children versus non-obese children [93] (Figure 3). Generally, after drugs get metabolized through phase I reactions, in which functionalization reactions occur, they move to phase II metabolism where they are conjugated with endogenous substrates [94].

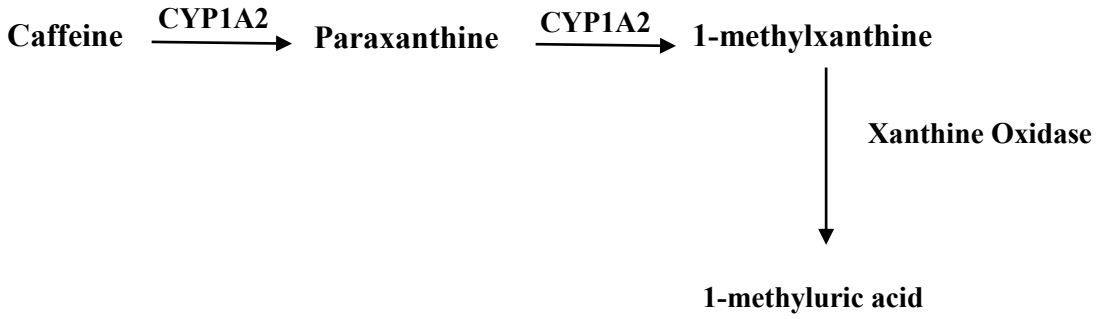

Figure 3: Caffeine metabolism in humans

1.6.3.2.Phase II Metabolism

After phase I metabolic reactions, the produced metabolites or the parent compounds themselves undergo conjugation with glucuronic acid, sulfate, glutathione, or amino acids. These reactions facilitate and enhance their excretion into bile or urine and consequently from the body through increasing water solubility and molecular weight of the compounds, which mostly inactivates their biological activities [95].

1.6.3.2.1. Uridine Diphosphate Glucuronosyltransferase (UGT)

The glucuronidation reaction is catalyzed by the enzyme UDP-glucuronosyltransferase (UGT), and it is involved in metabolism of a large proportion (almost half) of drugs during phase II [60]. This major enzyme family constitutes two families (UGT1 and UGT2) and three subfamilies (UGT1A, UGT2A and UGT2B); it is expressed mainly in the liver and other extrahepatic tissue (gastrointestinal tract, adipose tissue, and kidneys) [96]. As liver is considered to be a major organ where UGT enzymes are expressed, it has been suggested that any histopathological changes or increase in liver size, which often accompanies obesity, could influence UGT activity [97].

Acetaminophen, lorazepam, and oxazepam are examples of drugs that primarily undergo UGT conjugation. Acetaminophen (APAP) is extensively metabolized by UGT, particularly UGT 1A9 and 1B15 [98] (Figure 2). Many studies have been conducted to evaluate the impact of obesity on APAP metabolism. One of these studies was conducted on adolescents with and without non-alcoholic fatty liver disease (NAFLD); it was reported that the magnitude of acetaminophen clearance was higher among obese subjects compared to control subjects [99].

Another study was performed in children with NAFLD. After administration of paracetamol, APAP and its glucuronide metabolite (APAP-G) were measured, and it was observed that the concentration of APAP-G in the serum and urine were remarkably higher in children with NAFLD compared to children without NAFLD [100].

Biotransformation of lorazepam and oxazepam by UGT has also been evaluated among morbidly obese patients, and it was confirmed that obesity is associated with elevated UGT metabolism as the clearance of both drugs was significantly higher in severely obese individuals with a mean body weight of 113 kg [69]. However, one year later in 1984, Abernethy et al. published another study that demonstrated the impact of obesity on other drugs from the same benzodiazepam family, including alprazolam and triazolam. It was found that the clearance rate of both drugs was impaired between the two different groups (obese vs. non-obese). In addition, other studies show a significant reduction in mRNA expression of UGT1A1, 1A6, 2B1in the liver of obese Zucker rats compared to Sprague-Dawley rats [101]. Other study that was conducted on diet induced obesity mice who were on chemotherapy demonstrated a reduction in expression of hepatic UGT1A1 [102].

1.6.3.2.2. Other Phase II Metabolic Enzymes

N-acetyltransferase and glutathione S-transferase, which are included in phase II drug metabolism, have been investigated in obese versus non-obese subjects. N-acetylation of procainamide is catalyzed by N-acetyltransferase [60][103]. After evaluation of the metabolism rate of procainamide in obese and normal-weight patients, it was found that its clearance was insignificantly high in obese individuals [104]. Busulfan is another drug that is metabolized by glutathione S-transferase (GST) [105]. Its clearance was studied in obese and

morbidly obese subjects, and those individuals showed remarkably higher oral clearance rates compared with non-obese subjects [106].

In conclusion, based on provided data and evidence, the effect of obesity on enzymatic activity differs from one enzyme to another. Depending on the enzymatic pathway, phase I enzymatic processes demonstrated increased, decreased, or similar activity in obese subjects compared with non-obese subjects. The activity of CYP3A4-mediated metabolism was consistently decreased, whereas CYP2E1 activity was elevated in obese versus non-obese patients. Although drug metabolism mediated by phase I metabolizing enzymes (CYP2D6, CYP1A2, CYP2C9 except CYP2C19) was high, it was not statistically significant. By contrast, xanthine oxidase clearance was markedly increased in obese versus non-obese children. Phase II clearance, on the other hand, demonstrated inconsistent trend in obese versus non-obese individuals. Since there are limited studies on the impact of severely obese individuals (BMI ≥ 40) on drug metabolism, further studies are needed.

1.6.3.3. Transcriptional factors regulating phase I & II enzymes

Receptor	Cytochrome P450 genes regulated by receptor	Ref
AhR (Aryl hydrocarbon Receptor)	Human: CYP1A1, CYP1A2, CYP1B1 Rat: CYP1A1, CYP1A2, CYP1B1	[228] [229]
CAR (Constitutive androstane receptor)	Human: CYP2B6, CYP2C9, CYP2C19, CYP3A4, CYP3A5, CYP4A Rat: CYP2B1 & CYP2B2	[230] [231] [232]
PXR/SXR Pregnane X receptor (Rodent)/ /Steroid and Xenobiotic Receptorn (human)	Human: CYP1A, CYP2A, CYP3A4, CYP3A5, CYP3A7, CYP2B6, CYP2C9, CYP2C19, CYP2C8, CYP4F Rat: CYP3A1, CYP3A2, CYP3A9, CYP3A18, CYP3A23	[233] [229] [232]

VDR **Vitamin D Receptor**	Human**:** CYP2B6, CYP2C9, CYP3A4, CYP24, CYP27B1 Rat: CYP24A1, CYP27A1, CYP27B1	[234] [229] [235]
PPARα **Peroxisome Proliferator Activated Receptor-α**	Human: CYP1A, CYP2A, CYP4A, CYP2C, CYP2E Rat: CYP4A1	[236] [229]
GH **Growth hormone**	Human: CYP3A4, CYP1A2, CYP2E Rat: CYP 2C11, CYP2C12, CYP2C13, CYP2A2, CYP3A18.	[227] [237]

1.6.4. Effect of obesity on renal excretion

Many drugs and their metabolites are excreted from the body through the kidney. Globular filtration, tubular secretion and tubular reabsorption are the process that drugs go through when they reach the kidney [107]. It was reported that intake of high fat diet for relatively short period of time, 7-9 weeks, participated in significant histologic and functional changes in the kidney. These pathophysiological changes included thickness of glomerular and tubular basement membranes, expansion of Bowman's capsule and cell proliferation in the glomeruli. Consequently, glomerular filtration, arterial blood pressure, and renal plasma flow were markedly increased [108].

It was recorded that the tubular secretion of ciprofloxacin and procainamide was high in obese patients [104]. Similarly, the clearance of ciprofloxacin was noticed to be high in obese group compared with control group which approved the induction of glomerular filtration and tubular secretion in obese individuals [109].

1.7. Obesity and inflammation

Adipose tissue is critical for life as it is responsible for production of proteins that affect lipid and glucose metabolism, appetite and satiety, blood pressure regulation, inflammation, and immune functions [110].

Some of those proteins are beneficial to the body. Adipocyte hormones including adiponectin and leptin counter insulin resistance and hyperphagia phenomenon (satiety center) via enhancing insulin sensitivity and energy expenditure, respectively. Some other proteins, On the other hand, demonstrate disadvantageous effect on the body such as interleukin-6 (IL-6) and tumor necrosis factor α (TNF-α) which contribute to inflammation and insulin resistance as well as renin and angiotensinogen which leads to developing hypertension [110].

Tissues including skeletal muscles, mammary epithelium, and stomach are involved in the synthesis of leptin; however, the majority of leptin is released from adipose tissue. Leptin regulates appetite and energy expenditure through its action on the hypothalamus [111]. Hyperleptinemia was reported in obese individuals [112].

Adiponectin facilitates fatty acid oxidation and stimulates insulin secretion via down regulation of C-reactive protein, TNFα and IL-6 protein and up regulation of interleukin-10 and interleukin-1 receptor antagonist (IL-1RA) [113], [114]. It was reported that obesity is associated with reduction in level of adiponectin [114].

Obesity is accompanied with elevation in IL-6 and TNFα which leads to induction of low-grade inflammation [115][116]. The pro inflammatory cytokines IL-6 is released from skeletal muscle and adipose tissue. High level of IL-6 leads to overproduction of C-reactive protein (acute-phase proteins) in response to inflammation [115]. TNFα is another pro inflammatory

cytokine which is produced by adipose tissue [116]. It is one of the factors that trigger insulin resistant and type II diabetes especially with central obesity [117].

There is a correlation between those cytokines and alteration in the expression of metabolizing enzymes. It has been reported that IL-6 and TNFα cause downregulation of hepatic cytochrome CYP3A4 and CYP2C8 in human [118][119]. Infliximab which is an approval monoclonal antibody targets TNFα. Consequently, the downregulation of CYP3A1 was reversed in rat model of arthritis [120].

Similar outcomes were found when lipoglycans (LPS) was injected to animal model. It was showing a reduction in the expression of CYP1A2, 2A1, 2C6, 2C7, 2C11, 2C19, 2C23, and 3A2 in rats [121]. The initiating event is the release of pro inflammatory cytokine, TNFα, which is triggered by LPS. Subsequently, TNFα simulates the release of IL-6 and many other cytokines that initiate the inflammation process [121].

1.8. Lidocaine

1.8.1. Pharmacological action of lidocaine

Lidocaine is an aminoamide. It is commonly utilized for both topical and local injection anesthesia as well as a cardiac antiarrhythmic agent [122]. It can also be used for the management of extensive pain via either central or peripheral administration [123]. Based on the literature, the effective analgesic plasma concentrations of lidocaine during intravenous infusion were 1.1 to 4.2 µg/ml [135] [136]. The underline mechanism is that lidocaine blocks sodium channel, thus limits the ability of nerve cells to pass the pain signals [124].

Central nervous system (CNS) adverse effects might occur at lidocaine plasma concentration of 3 to 6 µg/ml. Objective signs of toxicity including tinnitus, visual disturbance usually develops at 6 to 8 µg/ml, and serious signs of toxicity such as seizures and obtundations are frequently appear at concentrations greater than 8 µg/ml [143].

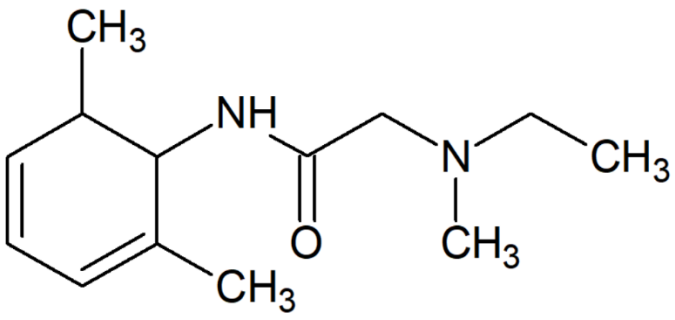

Figure 4: Chemical structure of lidocaine

1.8.2. Pharmacokinetics of lidocaine

Generally, the peak plasma concentrations of lidocaine are directly correlated to the administered dose and the rate of absorption which depends on the vascularity of the site of administration [125]. Oral administration is not a recommended route for lidocaine as it is extensively metabolized before reaching the systemic circulation through first pass effect [126]. Intramuscular administration demonstrates better bioavailability than oral route especially because it avoids the first pass effect [127] [128].

After intravenous bolus administration, blood concentrations of lidocaine decrease rapidly as lidocaine's large volume of distribution [129]. The reported volume of central compartment (V_1) following single-bolus dose in young health subjects was 0.49 L/kg and steady state volume of distribution (V_{ss}) was 2.7 L/kg [130] [129]. The affinity of drug to bind to plasma proteins and body tissue is a key determinant of the volume of distribution [131] [132]. Thus, variations in the plasma proteins binding and diseases induced changes are crucial determinants of lidocaine pharmacokinetics [133][134].

Lidocaine is primary metabolized in the liver through CYP450 system to form active metabolites including Monoethylglycinexylidide (MEGX) and Glycinexylidide (GX) [137] [138]. Those pharmacological active metabolites have up to 90% and 26% of antiarrhythmic potency of lidocaine, respectively [139]. It has been reported that CYP3A4, CYP1A2 are responsible for microsomal MEGX formation in human [138] [151](figure 5).

The mean half-life and systemic clearance of lidocaine following a single intravenous bolus of 25 -200 mg in young and healthy male subjects is 1.6 ± 0.18 hours and 15.6 ± 4.6 ml/min/kg, respectively [140][141][129][142]. It was reported a significant prolongation of elimination

half-life of lidocaine in obese individuals compared to control group (2.69 ± 0.2 vs 1.62 ± 0.06 hour) [224]. Thus, it is critical to assess the pharmacokinetics profile of lidocaine among obese individuals. Above 95% of administered lidocaine dose is excreted in the urine as metabolites and parent drug [143].

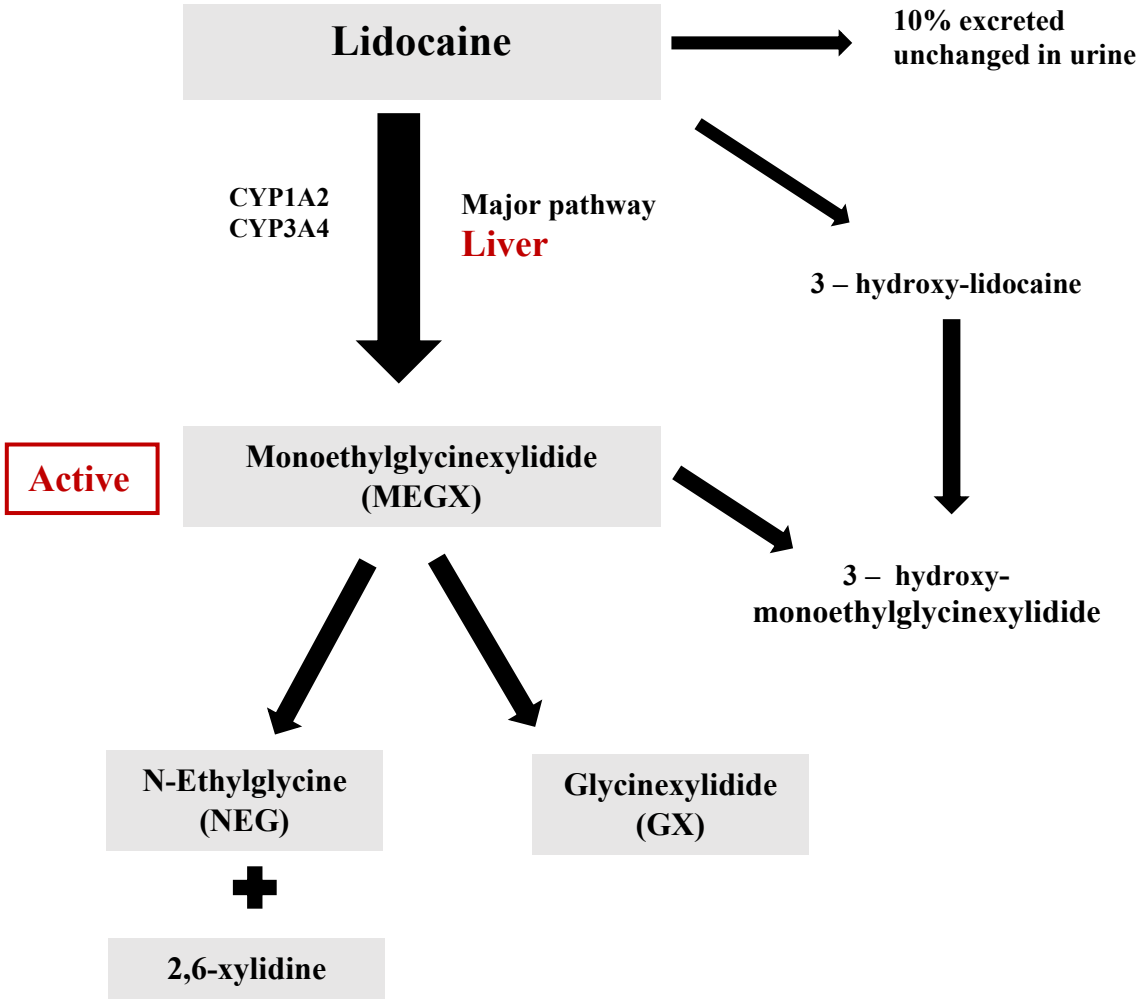

Figure 5: Lidocaine metabolism in human liver [226]

1.9. Propofol

1.9.1. Pharmacological action of propofol

Propofol is clinically used for the induction and maintenance of general anesthesia as well as used for the sedation for patients in the intensive care unit (ICU) [144]. It also has anxiolytic effect when the administered dose does not reach the sedation level . It works on activation of γ -aminobutyric acid ($GABA_A$) receptors, inhibition the N-methyl-D-aspartate (NMDA) receptors and modulation of calcium-ion channels. The most common undesirable effects of propofol are cardiorespiratory depression and dose dependent hypotension [145].

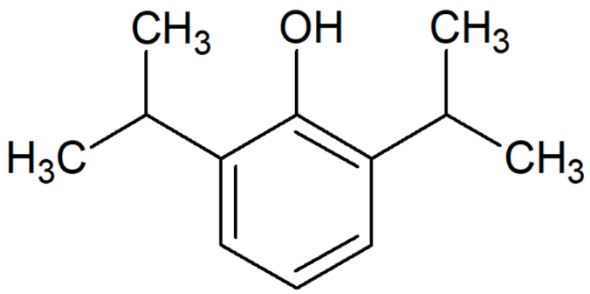

Figure 6: Chemical structure of propofol

1.9.2. Pharmacokinetics of propofol

The plasma concentrations of propofol decline rapidly after a single bolus injection as it is extensively distributed into the body tissues. The volume of distribution in the central compartment range from 13 to 76 L [146].

Liver is considered as a predominate organ for the clearance of propofol [201]. UGT 1A9 is a predominant enzyme involves in metabolism of propofol in human, but it is expected that different UGT isoforms are involved in metabolism of propofol in rats as UGT1A9 is deficient in rats [151]. Because of potential drug interaction when it is co-administered with other medication, the propofol metabolism by cytochrome P450 was investigated. It was found that hydroxylation reaction accounts for a maximum 47%. CYP2C9 was involved in metabolism high proportion of propofol. Another oxidative metabolism of propofol are CYP2A6, 2C8, 2C18, 2C19 and 1A2 [147] (Figure 7). Propofol glucuronide, 4-(2,6-diisopropyl-1-1,4-quinol)-sulphate, and 1-or4(2,6-diisopropyl-1,4-quinol)-glucuronide are the major metabolites of propofol [208].

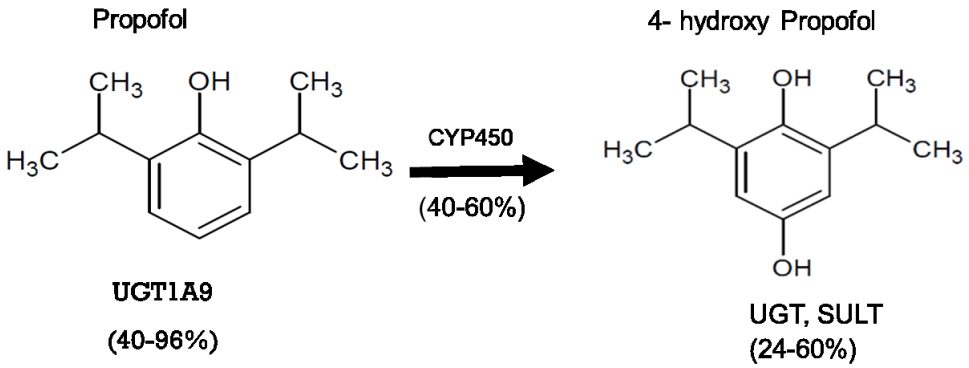

Figure 7: propofol metabolism

Urine is a key route of metabolite elimination of propofol in all species including human [202]. The metabolic pathway of propofol is species dependent. Indeed, in human, it was reported over 80% of given dose appeared in the urine. Less than 0.5% of administered dose is excreted unchanged in the urine, and up to 73% of propofol is glucuronidated and at almost less than

50% of metabolites are hydroxylated in humans [201]. In rats, however, more than half of the administered dose recovered from bile duct cannula after bolus and infusion of propofol [202].

In human, the half life of propofol was ranged from 1.5 to 1.8 hour when its pharmacokinetic profile follows two compartments [146]. The major metabolite of propofol is glucuronic acid (over 50%) [147].

The impact of age on propofol half life and clearance was evaluated. It was noticed that there was no significant difference in the half life between elderly patients (above 65 years old) and young patients (less than 35 years old). However, propofol clearance was significantly impaired [146].

1.10. Effect of obesity on PK of some drugs

Drugs (IV)	Some reported changes in PK (Obese vs. Control subject)*	Ref
Daptomycin	↑ CL	[238]
Verapamil	↑ $t_{1/2}$ ↑ Vd	[239]
Prednisolone	↑ CL	[240]
Carbamazepine [a]	↑ $t_{1/2}$ ↑ Vd	[241]
Bisoprolol	↑ $t_{1/2}$ ↑ Vd	[242]
Sufentanil	↑ $t_{1/2}$ ↑ Vd	[243]
Cimetidine	↑ CL	[244]
Caffeine [a]	↑ Vd	[245]

* $t_{1/2}$ (h) Vd (L) CL (L/h), [an] Oral administration.

1.11. Rationale, Hypotheses, Objectives

1.11.1. Rationale

Obese patients pose significant challenges to anesthesiologists in terms of dose accuracy of anesthetics due to potentially altered pharmacokinetics. The dosing of medications in such patients remains poorly studied and understood. There are limited studies that been conducted to investigate the influence of obesity on pharmacokinetics profile of anesthetics. Although propofol and lidocaine are most frequently used in these patience, the appropriate dosing scalars remains controversial. Notably, there are some cases that have been reported regarding propofol infusion syndrome (propofol toxicity) in obese individuals leading to a rare complication with potentially fatal results. The most recommendations are based on small independent studies, case reports, and expert opinion. Applying manufacturer standard kinetics and dosing recommendations in the obese patient may result in toxicity or treatment failure, leading to increased morbidity, mortality, and hospital length of stay.

As it was mentioned in detail in the introduction the pathophysiological changes that are associated with obesity, it is crucial to investigate the impact of obesity on kinetic constants of hepatic microsomes and the enzyme activities that are primary involved in metabolism of these anesthetic agents.

1.11.2. Hypotheses

1. Obesity causes a general reduction in the expression and functional activities of enzymes involved in drug metabolism
2. Female and male rodents differ in these responses.
3. Normalization of a high fat to normal diet leads to normalization of protein expression and enzyme activity

1.11.3. Objectives

1. To develop a sensitive and validated reverse phase HPLC-UV assay for the determination of lidocaine concentration in human serum.
2. To adopt the developed assay to study pharmacokinetics of lidocaine in patients given the drug after gastrointestinal surgery as well as the enzyme kinetics in animal model.
3. To study the impact of diet induced obesity on phase I and phase II drug metabolizing enzymes (DMEs) and proteins expression in liver
4. To investigate whether switching to normal diet after a relatively long period of high fat diet consumption would render a positive impact

Chapter 2

Materials and Method

2.1. Materials:

2.1.1. Assay development

Lidocaine HCl (0.4% in 5% dextrose for injection USP (Baxter Healthcare Corporation, Deerfield, IL, USA) was utilized to develop a High-Performance Liquid Chromatography Assay Method for the determination of Lidocaine in human serum. Procainamide HCl was obtained from Sigma- Aldrich (St Louis, MO, USA). Ethyl ether, acetonitrile, water (all HPLC grade), triethylamine, potassium phosphate (monobasic) and sulfuric acid were purchased from Caledon Laboratories Ltd (Georgetown, ON, Canada).

2.1.2. Microsomal incubation

Lidocaine HCl (Xylocaine® 2%, injection USP; AstraZeneca Canada Inc) was utilized as a source of lidocaine. Nicotinamide adenine dinucleotide phosphate tetrasodium (NADPH). Magnesium chloride hexahydrate. Propofol (2,6-Diisopropylphenol, 97%) (Alfa Aesar by Thermo Fisher Scientific, Canada) was used as a source of propofol. Thymol was purchased from Sigma- Aldrich (St Louis, MO, USA). Uridine 5´_diphosphoglucuronic acid trisodium salt (UDPGA) (St Louis, MO, USA). Acetonitrile and Methanol (HPLC grade) were purchased from EM Scientific (Gibbstown, NJ). Dimethyl sulfoxide (DMSO) was ordered from Sigma- Aldrich (St Louis, MO, USA).

2.1.3 Western blot

Page Ruler Plus Protein Ladder was from Thermo Scientific (Grand Island, NY), and bovine serum albumin from Fisher Scientific (Ottawa, Canada). Bromophenol blue, ammonium persulfate, b-mercaptoethanol, 40% acrylamide, N,N,N',N' tetramethylethylenediamine, and nitrocellulose membrane were purchased from Bio-Rad Laboratories (Hercules, CA).

Primary antibodies for rat cytochrome P450 (CYP)1A2 (1:1000 dilution, sc-53241) , CYP3A4 (1:1000 dilution, sc-53246) and CYP2E1(1:1000 dilution, were purchased from Santa Cruz

Biotechnology, Inc. (Santa Cruz, CA). Similar primary antibodies react with mice and was used to detect cyp3a41, cyp1a2, and cyp2e1.

Primary antibodies for rat cytochrome P450 (CYP)2D1 (1:500 dilution, ab22590) and CYP2C12 (1:1000 dilution, ab22596) were obtained from Abcam (Toronto, ON). The primary antibody beta-actin (1:1000 dilution, sc-1615) and secondary antibodies (m-IgG_k "1:1000 dilution, sc-516102-CM", donkey anti-goat "1:1000 dilution, sc-2020", and mouse anti-rabbit "1:1000 dilution, sc-2357" IgG peroxidase) were purchased from Santa Cruz Biotechnology, Inc. (Santa Cruz, CA). Chemiluminescence Western blotting detection reagents were from GE Healthcare Life Sciences (Piscataway, NJ).

2.2. Methods

2.2.1. Animal model of obesity

For lidocaine study, all experimental procedures involving animals were approved by the University of Alberta Health Sciences Animal Policy and Welfare Committee. Male and Female Sprague-Dawley rats of 3-4 weeks of age were purchased from Science Animal Support Services (SASS) (Canada). Two different study designs were conducted. The first study has dietary phase lasted 14 weeks, the rats weighed approximately 100 g. In the second study design, the dietary phase lasted 18 weeks, the rats weighed approximately 140 g. The rats were housed 2 per cage in a temperature-controlled room with 12-h dark/light cycle. Female Sprague Dawley rats (n=8 total) and male Sprague Dawley rats (n=8 total) were started on a 14 week course of 45% high fat rat chow with water. At the end of the 14 week period, half of the animals were euthanized under isoflurane. In the remaining rats, the diet was switched to normal rat chow (fat content 13.4%). Four weeks after, those rats were euthanized.

For each of the 14 and 18 week groups, control rats (n=4 each) were included where the diet was 13.4% fat content. Free access to food and fluids was permitted throughout the entire period. Rat weights and food consumption were measured twice per week for female rats. For male rats, the weights were reported one a week and the food intake was examined in the last few weeks of the study as the model had been well studied before [152]. Table 3 lists the dietary compositions of each diet.

After euthanasia (following a 6 hour period of food restriction with water ad libitum) blood was collected in tubes containing anticoagulant with plasma being separated by centrifugation at 3000 g for 10 min. Livers, kidneys, hearts and small intestine were collected. All samples were kept at -80˚C until being used for biochemical assay, enzyme kinetics and protein determinations.

Table 3

Composition of the Dietary Components Used for rats Study

Nutritional Component	**Calories Provided %**	
	Standard Chow 3.35 Kcal/g	High-Fat Chow (HF)* 4.6 Kcal/g
Protein	29.8	19
Carbohydrate	56.8	36
Fat	13.4	44.8

* (HF; Teklad Custom Diet (45/Fat), TD.06415, ENVIGO)

For the propofol study, the source of the microsomal protein was from the same rats previously used in a published report [152]. In brief, Sprague-Dawley male rats aged 4 weeks were fed three different dietary components. Each group consisted of 4 rats fed the diets for 14 weeks. The diets were either a high fat diet as rat pellets (45% kcal of fat, Harlan Laboratory, Inc.) with normal water or a 13% w/v high fructose corn syrup (HFCS) with standard rat chow or a

combination of both (HFCS-HFD) with the control group being fed on a standard rodent diet (13.4 % kcal of fat) and normal drinking water.

The livers of these rats were collected after they were euthanized. All tissue specimens were kept at -80 °C until needed.

Other animal model was used to induce obesity and/or type 2 diabetes. This model includes five to six-week-old C57Bl/6J male and female mice [Jackson Laboratory, Bar Harbor, ME, USA; stock no. 000664; Tg(ACTA1-cre/Esr1*)2Kesr]. Three diverse groups of male mice including lean, obese and type 2 diabetic mice (T2D) were involved in the study while female mice consisted of lean and obese groups. Lean mice fed a low-fat diet (LFD) (10% kcal from lard, Research Diets D12450J) whilst obese and T2D mice fed a high fat diet HFD (60% kcal from lard, Research Diets D12492). During the dietary phase of T2D mice, they were administered a single injection of streptozotocin 90 mg/kg during week 5. Dietary phase in all groups lasted 10 weeks followed by euthanizing process. Liver samples were harvested to do the analysis. Table 4 lists the dietary compositions of each diet.

Teklad standard ("normal") chow and the research diets LFD differ in the micronutrient composition which might cause the difference in the results. The primary different between the regular chow and the LFD is the present or the absent of phytoestrogen and the sucrose compositions [246]. The disaccharide, sucrose, is found profoundly in the LFD while it is absent in the ordinary chow. Phytoestrogen micronutrient, on the other hands, is found in a high percentage in the standard chow but is not absent in the LFD. It was reported that phytoestrogen would affect the appetite, motor activity and lipid metabolism [247, 248].

Table 4

Composition of the Dietary Components Used in the C57BL/6J Mice Study

Nutritional Component	Calories Provided %	
	Standard Chow 3.85 Kcal/g	High-Fat Chow (HF) 5.24 Kcal/g
Protein	20	20
Carbohydrate	70	20
Fat	10	60

2.2.2. Preparation of microsomes

For the lidocaine study, liver tissue from each rat (n=4) was homogenized separately in cold sucrose solution (0.25 M in distilled water) by using a homogenizer (0.5 g of each tissue in 2.5 mL of sucrose). The homogenized solution was centrifuged at 1000 ×g for 10 min to remove nuclei and large cellular debris. The supernatants were transferred to new tubes and further centrifuged at 15,000 ×g for 10 minutes to remove organelle fraction. Centrifugation continued again by transferring supernatants which contain cytosol and microsomes to new tubes at 100,000 ×g for 1 hour to precipitate the microsomes. Then the pellets were resuspended in sucrose 0.25 M solution and stored at -80° C. [153]

For propofol, the same procedures for microsomes preparation of lidocaine was adopted; however, pooled livers of all groups (n=3) (n1=rat1+rat2, n2=rat3+rat4, n3= rat4+rat1) rats were used. This was done for ethical reasons, to maximize the ability to use the materials from the rats to study other drugs, in addition to propofol, in further experiments beyond the scope of this thesis.

2.2.3. Lowry assay for protein concentration in microsomal preparation

Bovine serum albumin (BSA) was utilized as a stock solution for constructing a calibration curve to determine the protein concentration in microsomes samples. The following reagents were involved in assaying the protein concentration in liver samples that was prepared from different animal models. Reagent A comprising of 1mL of sodium and potassium tartrate 2% in double distilled water, 1mL of $CuSO_4$ 1% in double distilled water, and 20 mL of Na_2CO_3 anhydrous 10% in 0.5 M NaOH. Reagent B consisting of 1:10 diluted solution of folin-phenol reagent in double distilled water. The BSA stock solution of 1 mg/ml was used for setting up standard solutions with distinct concentrations (0.6, 0.5, 0.4, 0.3, 0.2, 0.1, and 0 mg/mL) of BSA in double distilled water.

To determine of unknown protein concentrations, 248 µL of double distal water was added to the mixture of 2 µL of protein sample (unknown concentration of protein) or 250 µL of each standard solution followed by adding 250 µL of reagent A. Those mixtures were incubated for 10 min at room temperature. Afterward, 750 µL of reagent B was added to each of the test tubes under continuous vortex mixing, and samples incubated at 50 °C for 10 min. After 10 min incubation, 200 µL of each mixture were transferred to a well in the ELISA plate and analyzed using a plate reader at 550 nm. [154]

2.2.4. Development of reverse phase HPLC-UV assay of lidocaine in human plasma

2.2.4.1. Instrumentation and chromatographic condition

The chromatographic system consisted of a Waters (Milford, MA, USA) 600 E multi-solvent delivery system pump, an autosampler with a variable injection valve (Waters 717), and a

UV–visible tunable absorbance detector (Waters 486). The chromatograms were recorded using EZStart software (Scientific Software, Pleasanton, CA, USA) in a Windows-based computer system for data collection and processing. The chromatographic separation of lidocaine and procainamide (internal standard) were achieved using a 150 × 4.6 mm i.d., 3.5 μm particle size Alltima C18-column (Alltech, Deerfield, IL, USA) attached to a pre-guard column (Grace Alltech All-Guard™ Guard Cartridges, 7.5 mm 5 μm, Deerfield, IL, USA). The mobile phase consisted of a mixture of acetonitrile and phosphate solution (25 mM KH2PO4-3 mM sulfuric acid-3.6 mM triethylamine) in a ratio of 12:88 (v/v). The mobile phase was degassed prior to use by filtering it under vacuum pressure through a 0.45 μm pore size nylon filter, then pumped at a flow rate of 0.9 mL/min at room temperature. Immediately after injection, the UV detection wavelength was set at 277 nm (the UVmax for procainamide). At 4 min post-injection, the UV detector was programmed to switch to a wavelength of 210 nm (the UVmax for lidocaine). The total analytical run time was <13 min.

2.2.4.2. Standard and stock solutions

The stock drug solution was 0.4% lidocaine HCl in 5% dextrose for injection. The working standard solutions were prepared daily from the stock solution by serial dilution with HPLC grade water to provide final concentrations of 40, 4 and 0.4 μg/mL lidocaine. The internal standard (IS) stock solution was prepared by dissolving 17 mg of procainamide HCl in 100 mL of water. All stock solutions were refrigerated between use. For the construction of a standard curve, samples of (0.25 mL) were prepared by adding lidocaine HCl equivalent to 50, 125, 250, 500, 1000, 2000, 2500 and 5000 ng/mL.

2.2.4.3. Extraction procedure

A one-step liquid–liquid extraction step was used to extract lidocaine from human serum. After adding 50 µL volume of the IS stock solution and 200 µL of 1M NaOH to 0.25 mL of human serum, 3 mL of diethyl ether was added. This was followed by vortex mixing of tubes for 30 s and centrifugation at 3000 g for 3 min. The organic solvent layer was pipetted to new tubes, then evaporated to dryness in vacuo. The dried residues were reconstituted using 150 µL of HPLC grade water with up to 75 µL being injected into the chromatographic system.

2.2.4.4. Recovery

Recovery was determined with lidocaine HCl concentrations of 50 and 1000 ng/mL and with an IS concentration of 0.17 mg/mL in human serum. The extraction efficiency was determined using five replicates of each concentration and comparing the extracted peak heights of analyte in the extracted samples to the peak heights of the same amounts of analyte directly injected into the HPLC without extraction.

2.2.4.5. Calibration, accuracy and validation

The assay was validated, generally using the guidelines published by the EMA [155]. The calibration curves were quantified by using peak height ratios of lidocaine HCl (concentration range from 50 to 5000 ng/mL) to IS versus the nominal lidocaine concentration. Intra-day validation was assessed at four different concentrations of lidocaine HCl (50, 250, 500 and 2000 ng/mL) per day in five replicates. This step was repeated on three separate days for determination of inter-day validation. For each daily run, an independent set of calibration curves samples was prepared. Accuracy and precision were assessed using the mean intra- and inter-day percentage error and percent coefficient of variation (CV%), respectively. Calibration curves were weighted by a factor of concentration $^{-2}$ due to the wide range of

concentrations (50–5000) used in the calibration curves. Intraday, accuracy and precision of the assay were determined using a range of concentrations of lidocaine HCl. The selected concentrations were 50, 250, 500 and 2000 ng/mL of lidocaine HCl in human serum. Each concentration had five replicates. To permit the assessment of interday accuracy and precision in human serum, the assay was repeated on three separate days. For each daily run, a set of calibration samples separate from the validation samples were prepared to permit the quantification of the peak height ratios of lidocaine to IS. Precision was assessed by percentage coefficient of variation (CV%), while accuracy was represented by determining the mean intra- or inter-day percentage error.

2.2.4.6. Applicability

For the standard curve and validation samples, the serum was obtained from two healthy individuals on two separate occasions. For two of the samplings, each individual was asked to refrain from ingesting any caffeine-laden foods or drinks for 24 h before sampling. The method was employed to determine the lidocaine concentration in human serum from one surgical patient after the injection of lidocaine as a reservoir within the rectus sheath (200 mg single dose). The patient provided written consent, and the study was approved by the University of Alberta Health Research Ethics Board. After the injection of the dose, blood samples were drawn serially into serum collection tubes until 24 h from the time of dosing. The blood samples were left for 30 min to clot, then centrifuged for 10 min. The serum was then separated and frozen at −20 °C

2.2.5. Microsomal incubation of control and obese rats with lidocaine

The formation kinetics of monoethylglycinexylidide (MEGX) were characterized when lidocaine was exposed to liver microsomes of control and high fat fed male and female rats. The initial step was dissolving lidocaine HCl in water (HPLC grade) to provide a nominal concentration 100, 250, 1000, 2000, 5000, and 10000 μM. It followed by drying process to get ride of the water and have concentrated drug. The incubation mixture contained 5 mM magnesium chloride hexahydrate dissolved in 0.5 mM potassium phosphate buffer (pH=7.4). Each incubation, in final volume of 0.25 mL, contained 1 mg/mL of protein from non-pooled liver microsomes. The reaction was started with the addition of 1 mM NADPH after a 5 min pre-equilibration period. All incubations were performed at 37ºC in a shaking water bath (50 rpm) for 10 min. The oxidative reaction was ended by addition of 0.2 ml 1 M NaOH to terminate the reaction. Followed by adding internal standard, procainamide, and extraction process.

2.2.5.1. Standard and Stock Solutions

The stock drug solution was lidocaine HCl (Xylocaine® 2%). The working standard solutions were prepared daily from the stock solution by serial dilution with HPLC grade water to provide final concentrations of 2, 0.2, 0.02 g/ml lidocaine. The different concentration of lidocaine solution for standard curve and microsomal incubation were dried using vacuo before initiating the experiment. The internal standard (IS) stock solution was prepared by dissolving 17 mg of procainamide HCl in 100 mL of water. All stock solutions were refrigerated between use. For the construction of a standard curve, samples (0.25 mL) were prepared by adding lidocaine HCl equivalent to 25- 20000 μM.

2.2.5.2. Extraction Procedure and HPLC conditions

Identical HPLC conditions and extraction procedure at section 2.2.4.1 and 2.2.4.3 were used with minor changes in the flow rate (0.8 ml/min) with run time < 15 min. The volume of injection for reconstituted dried residues was up to 40 µL.

2.2.6. Microsomal incubation of control and obese rats with propofol

The enzyme kinetics of propofol was determined when propofol was incubated with liver microsomes of control and obese rats. In this experiment, the source of the microsomal protein was obtained from the rats previously published [152]. In the beginning, propofol was diluted with DMSO to acquire a desirable concentration of propofol to be incubated (5, 10, 25, 50, 100, 250, 500, and 1000 µM). The incubation mixture contained 5 mM magnesium chloride hexahydrate dissolved in 0.5 mM potassium phosphate buffer (pH=7.4). Each incubation, in final volume of 0.25 mL, contained 1 mg/mL of protein from pooled liver microsomes. The reaction was started with the addition of 2 mM UDPGA after a 5 min pre-equilibration period. All incubations were performed at 37ºC in a shaking water bath (50 rpm) for 10 min. The glucuronidation reaction was terminated by addition of 0.75 ml cold acetonitrile. Followed by adding internal standard, thymol, and directly inject the sample to the HPLC on the same day.

2.2.6.1. Standard and Stock Solutions for microsomal incubation with propofol

The stock drug solution was 97% propofol solution. The working standard solutions were prepared daily from the stock solution by serial dilution with DMSO to provide final concentrations of 93.3, 9.3, 0.93, 0.09, 0.01 and 0.001 g/mL propofol. The internal standard

(I.S) stock solution was prepared by dissolving 10 mg of thymol in 100 mL of acetonitrile. A standard curve was developed, samples of (0.25 mL) were prepared by adding propofol equivalent to 2.5 to 2000 μM.

2.2.6.2. HPLC conditions for assaying propofol concentrations

The chromatographic system consisted of a Waters (Milford, MA, USA) 600 E multi-solvent delivery system pump, an autosampler with a variable injection valve (Waters 717), and a scanning fluorescence detector. The chromatograms were recorded using EZStart software (Scientific Software, Pleasanton, CA, USA) in a Windows-based computer system for data collection and processing. Separation of propofol and thymol (internal standard) was achieved successfully on a 4.6 mm × 15 cm, 5 μm particle size Alltima C18-column (Alltech, Deerfield, IL, USA) attached to a pre-guard column (Grace Alltech All-Guard™ Guard Cartridges, 7.5 mm 5 μm, Deerfield, IL, USA) using a mixture of acetonitrile and double distal water in a ratio of 60:40 (v/v) as the mobile phase. The mobile phase was degassed prior to use by filtering it under vacuum pressure through a 0.45 μm pore size nylon filter, then pumped at a flow rate of 1 mL/min at room temperature.

The excitation and emission wavelengths were set at 270 and 310 respectively. The total analytical run time was < 10 min.

2.2.7. Western blotting

2.2.7.1. Protein sample preparation

2X loading buffer which contains 0.5 M tris HCL (pH 6.8), 10% SDS, 1.5% bromophenol blue, glycerol and B meracptoethanol was been adding to protein samples to denature the

proteins. For CYP450s and UGTs, 45 µg microsomal proteins were dissolved in 2X loading buffer and then boiled for 5 min at 100 C^0.

2.2.7.2. Western Blot Analysis

Proteins in each denatured sample were separated by 10% SDS-polyacrylamide gel (SDS-PAGE) and electrophoretically transferred to a nitrocellulose membrane. Then, membranes were blocked for an hour at room temperature by 5% BSA diluted in Tris-Buffered Saline Tween-20 (TBST) which consist of Tris-base (TBS), 5% bovine serum albumin, 0.15 M sodium chloride, 3 mM potassium chloride, and 0.5% Tween-20. Thereafter, the blocking solution was discarded, and the blots were rinsed thrice in a washing buffer (0.1% Tween-20 in Tris-buffered saline). Subsequently, the membranes were incubated with primary antibody over night in cold room at 4 C^0. The primary antibody solution was removed, and blots were washed as previously described, followed by incubation with secondary antibody for 1 h at room temperature. Rinsing with washing buffer was then applied to remove the extra secondary antibody. Lastly, the protein bands were detected using enhanced chemiluminescence (ECL). The intensity of protein band relative to β-actin bands intensity were quantified using Image-J software (National Institutes of Health, Bethesda, MD, http://rsb.info.nih.gov/ij).

2.2.8. Data analysis

2.2.8.1. Fitting procedure

Lidocaine data is expressed as Mean±SD unless otherwise indicated. To determine the kinetic constants for MEGX formation by liver microsomal preparations. Michaelis-Menten models for single enzyme was fitted to MEGX formation rates using the Solver routine program in

Microsoft Excel. The total sum of squares and Akaike information criteria were used to judge the quality of fitness and to guide in model selection.

For liver microsomes of the control and high fat diet fed rats incubated with lidocaine, a single enzyme model was used and the intrinsic clearance (CLint) for MEGX formation was calculated by determining the quotient of Vmax to Km. This model uses the following equation:

$$V = \frac{Vmax \times [S]}{km + [S]}$$

Where V is the rate of MEGX formation, Vmax is the maximal formation rate of MEGX, Km is the affinity constant, [S] is lidocaine concentration.

Propofol study: liver microsomes from different rat groups (control, HF, HFCS, combination HFCS-HF) were incubated with different concentrations of propofol. Each group has a different enzyme kinetics. Control group, for example, follow a two enzymes model. This model consists of a single saturable and a second linear component. The intrinsic clearance (CLint1) for propofol consumption was calculated (Vmax/Km) whereas CLint2 acquired from the Solver program.

This model uses the following equation:

$$V = \frac{Vmax1 \times [S]}{Km1 \times [S]} + (Clint2 \times [S])$$

Km1 and Vmax1 represent the kinetic constants for the saturable enzyme while CLint2 shows the ratio of Vmax over Km for the non-saturable (over the range of concentrations used) enzyme. [S] is propofol concentration.

Regarding HF and HFCS+HF groups, the metabolism of propofol best conformed to a one enzyme model (Michaelis-Menten equation). Similarly, HFCS alone group showed that Michaelis-Menten equation using shape factor was the best fit to the resulted data. CLint was calculated by determining the quotient of Vmax to Km.

This model uses the following equation:

$$V = \frac{Vmax \times [S]^n}{[km]^n + [S]^n}$$

Where V is the rate of propofol consumption and n is the shape factor required to fit sigmoidal shapes. [S] is propofol concentration.

2.2.8.2. Statistics

A one-way ANOVA followed by post-hoc test was used to analyze the data following a normal distribution (ANOVA with Bonferroni correction, $p<0.05$). Student's unpaired t tests was used as applicable way to assess the significance of differences between groups. Sigma Plot 11.0 (Systat software, Inc. Chicago, IL) and Microsoft Excel (Microsoft, Redmond, WA) were used in statistical analysis of data. The level of significance was set at $p < 0.05$.

Chapter 3: Results

3 .1. Development of an HPLC-UV assay for the determination of lidocaine in human serum

The chromatographic retention times were ~10 min for lidocaine and 2.5 min for IS (Figure 8). The chromatography displayed symmetrical peak shapes and high specificity, with a baseline resolution of IS and lidocaine. For both analytes, there was an absence of interference (IFN) from endogenous components in serum (Figure 8). It was of note that the chromatograms from the serum of the healthy volunteers used in the assay development had a significant peak present that eluted at about 6.4 min, which was not seen in the patient serum sample obtained at 10 min. However, this did not interfere with the analysis of lidocaine, nor the internal standard.

The average recoveries were 97.7 ± 21.0 and 81.0 ± 2.4% for 50 and 1000 ng/mL lidocaine HCl in serum, respectively. The average extraction recoveries for IS at the concentration used in the assay was 55.4 ± 4.1%. There were excellent linear relationships (>0.9995) noted between the peak height ratios and lidocaine HCl concentrations over ranges of 50–5000 ng/mL serum. From regression analysis of the concentration vs. peak height ratios of lidocaine to IS, the observed average slopes and intercepts were 0.00024 and 0.0011, respectively. The mean correlation coefficient of regression (r^2) for the serum standard curves were 0.9995. The CV of intra-and inter-day assessments were less than 15% (Table 5). The mean inter-day error in human serum was less than 9%.

The validation assessments revealed that the assay was precise and possessed low bias. Overall, all intraday measures for mean error and CV% of the lowest concentration were less

than 15%, and for the other concentrations only one fell above 10% (day three of the 216 ng/mL concentration). Except for the lowest concentration, all of the interday measures of CV% were less than 10%. All interday measures for mean error were less than 10%.

When it was tested for applicability in the patient samples, lidocaine serum concentrations could be measured for the full 24 h period following administration of the lidocaine dose. The observed maximal concentration was 1644 ng/mL, which occurred at 0.5 h post-dose (Figure 10). The correlations between the BMI and the lidocaine half life, clearance, and volume distribution were examined (Figure 11-13).

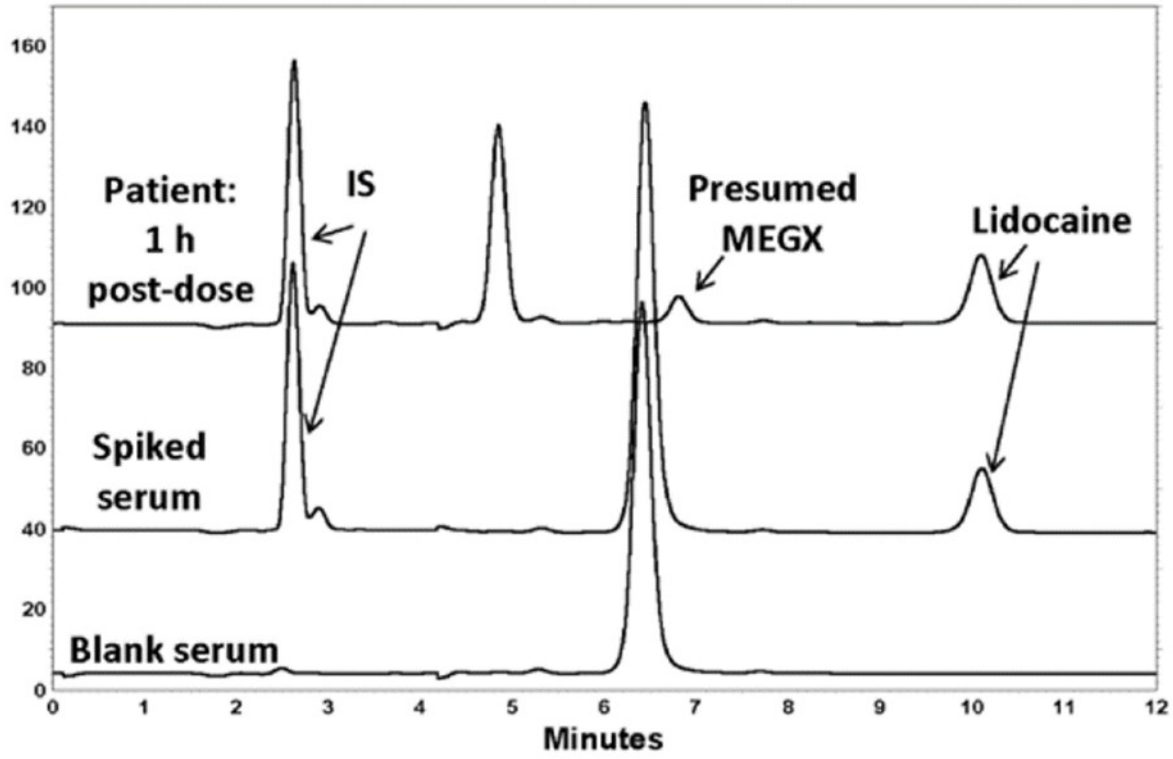

Figure 8: HPLC-UV chromatograms of blank (drug-free) serum from a healthy volunteer, volunteer serum spiked with 1000 ng/mL of lidocaine, and serum obtained 1 h after a 200 mg injection of lidocaine. The peak in the patient sample appearing at 6.8 min in the patient sample was presumed to be the lidocaine metabolite, monoethylglycinexylidide (MEGX). The peak at ~6.4 min was presumed to be from food components ingested by the volunteers who were not fasted.

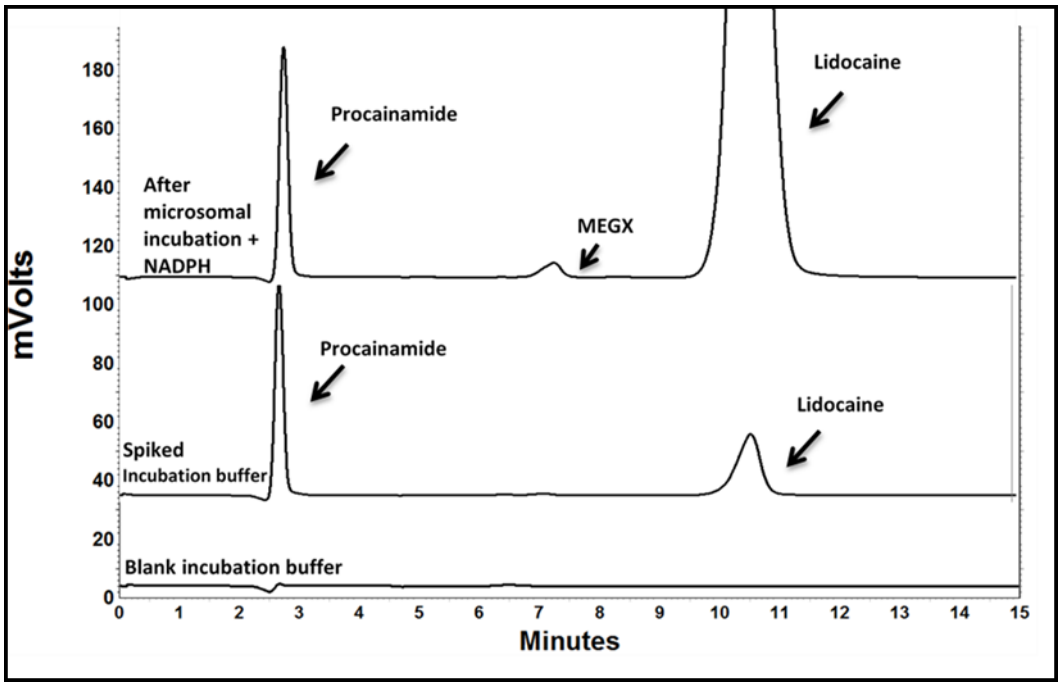

Figure 9: HPLC-UV chromatograms of blank incubation buffer, spiked incubation buffer, and after microsomal incubation with NADPH.

Table 5. Validation data for the assay of lidocaine in human serum, n=5

Nominal Concentration of Lidocaine*, ng/ml	Intraday			Interday		
	Mean ± SD ng/ml (CV%)			Mean ± SD ng/ml (CV%)	CV%	Error%
43.3	45.9±4.54 (9.90)	38.5±5.37 (14.0)	40.8±6.05 (14.8)	41.7±5.32	12.9	-3.57
216	2158±11.5 (5.35)	220±9.60 (4.35)	226±26.6 (11.8)	221±15.9	7.16	1.99
433	379±28.7 (7.56)	395±25.6 (6.46)	407±38.5 (9.47)	394±30.9	7.83	-8.97
1731	1489±60.5 (4.06)	1704±43.3 (2.53)	1635±47.1 (2.87)	1609±50.3	3.16	-7.02

*To convert to lidocaine HCl salt, divided by 0.865

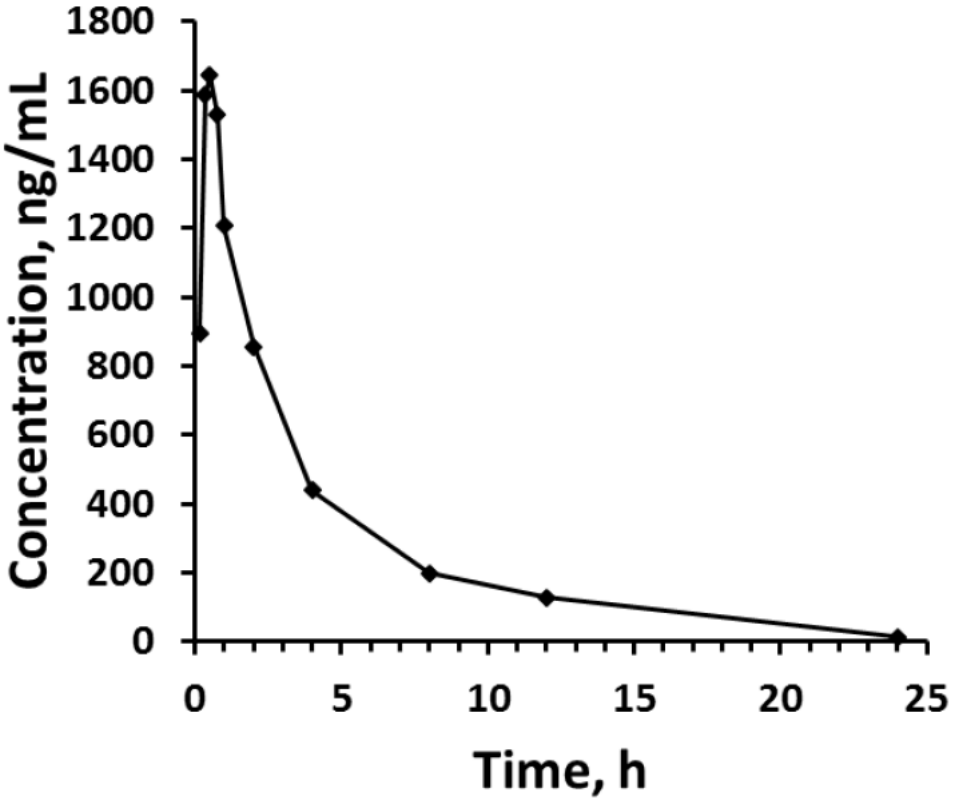

Figure 10: Serum lidocaine concentration vs. time profiles after rectus sheath injection of 200 mg lidocaine HCl to the patient volunteer

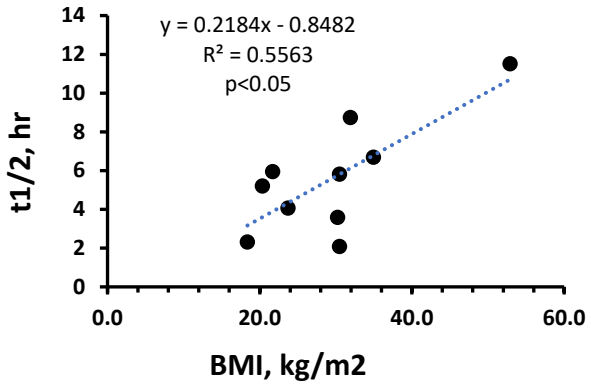

Figure 11: Body mass index (BMI) vs. half life ($t_{1/2}$) of administered lidocaine in patients after major abdominal procedure. Increasing of the body mass index was associated with a significant increase of the half life ($p < 0.05$)

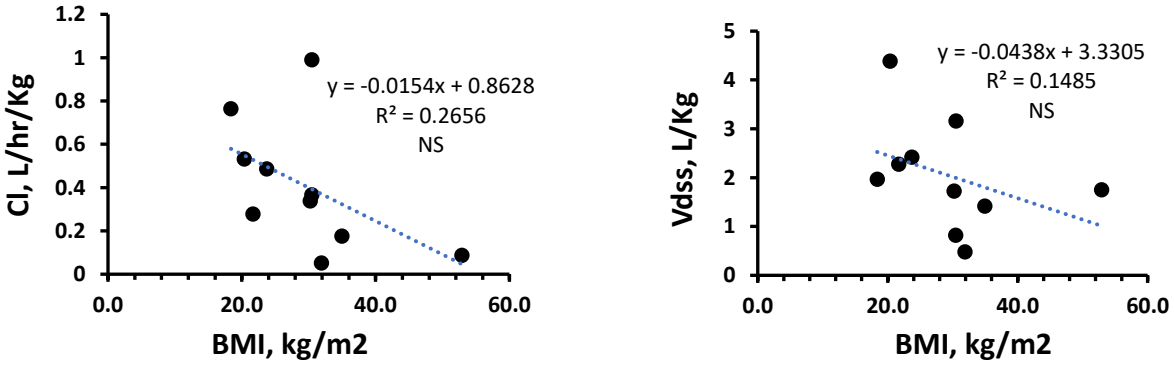

Figure 12: Body mass index (BMI) vs. clearance (Cl**)** and volume of distribution (Vdss**)** of administered lidocaine in patients after major abdominal procedure. The correlation between BMI and Cl as well as Vdss was not significant (NS).

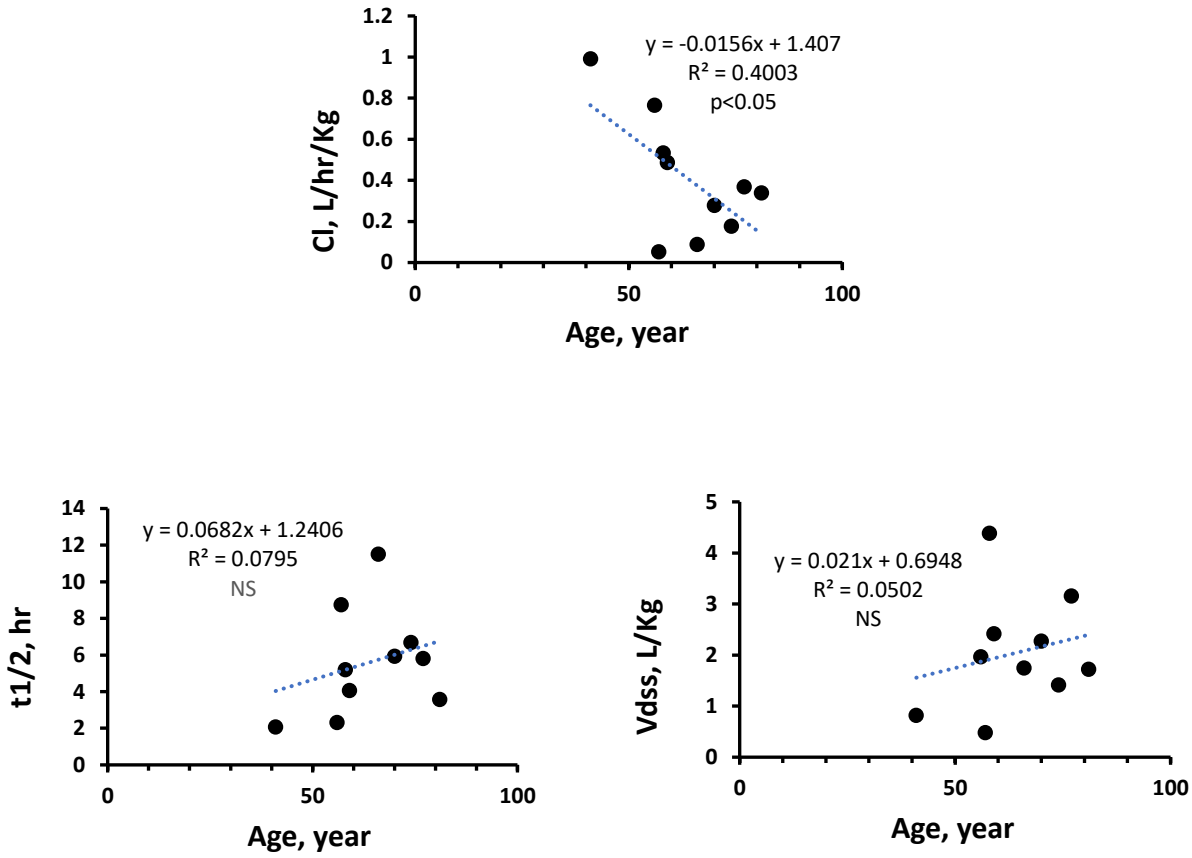

Figure 13: Age vs. pharmacokinetics parameters (Cl, $t_{1/2}$, Vdss) of lidocaine in patients after major abdominal procedure. While the individual matures in age, the lidocaine clearance decreases ($p < 0.05$). In contrast, getting older will not affect the drug half life and its volume of distribution significantly (NS).

3.2. Body weight and caloric intake

Body weight for rats involved in lidocaine studies

There was a significant increase in the body weight of rats fed high caloric diets compared to control rats. After 14 weeks on high fat diet, male rats gained remarkable weight about the double comparing to female rats by the end of this study (Figure 14). The weights of HF fed rats differed significantly from control group in the week 4 and week 3 for male and female rats respectively. These differences increased consistency until the end of the study (14 weeks). By the end of the study, the final average body weights were 656 and 841 g for the control and HF male groups and 355 and 427 g for the control and HF female groups (Figure 14).

Despite the reduction in the food intake (g/day) among male and female fed high fat diet, the calorie intake was significantly higher than control groups (Figure 16)(Figure 17).

Similar results were observed for 18 weeks study plan where the rats started with high fat diet for 14 weeks then they switched to normal chow for 4 weeks. There was a significant increase in the body weight for rats fed HF diet. The body mass was consistently growing until the end of 14 weeks. After substituting HF diet with standard chow, it was noted a reduction in body weight of male rats, but the reduction in the weight was not statistically significant compared to control group. Of note, the obese male rats were resistance to lose weight in a short period (4 weeks) even though they consumed a similar portion of standard chow that control group did (Figure 15)(Figure 16). Noteworthy, female rats exhibited different outcomes pattern. Female rats who were fed HF diet gained a significant body weight compared to control groups

in the first 14 weeks. When the food was switched to standard chow after 14 weeks of HF diet, worth to note that food intake for obese female rats remarkably reduced compared to control group (Figure 16). In other words, they consumed about the half calories that control group had in the last four weeks (week 15 -18) of standard diet which leaded to reduce their average body weights from 424 g on week 14 to 373 g on the 18 weeks (Figure 17). The last achieved average weight (373 g) was in the line with average weight of control group by the end of 18 weeks study plan (Figure 15).

With comparing the food intake per day for control groups of male and female rats, it was noted that the female rats consumed less amount of food compared to male rats. This difference was statistically significant (Figure 16).

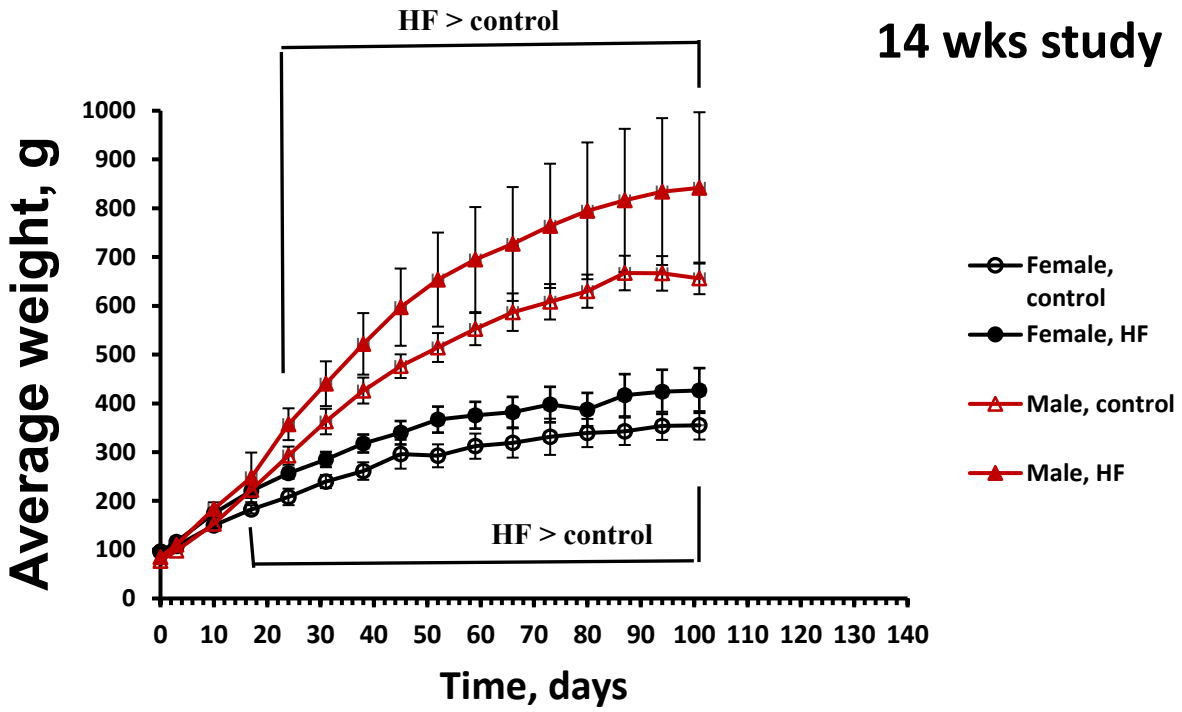

Figure 14: Weekly average weight gain (g) of all groups. Rats were fed on: (Control) standard diet + normal drinking water and high fat (HF) diet + normal drinking water as described in the 'Experimental methods' section. Values are means ± SD (n 4). From 4 weeks on, male rats on HF diet gained weight significantly greater ($p < 0.05$) than the control groups. From 3 weeks onwards, female rats on HF diet had a significant weight than the control group ($p < 0.05$).

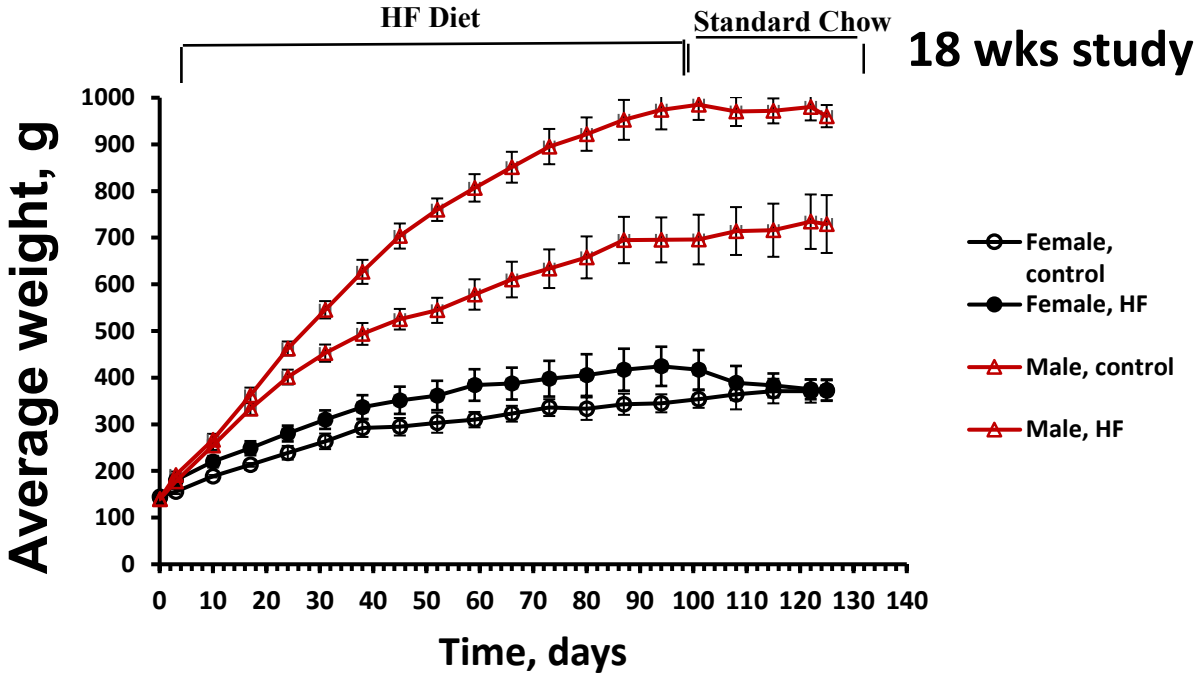

Figure 15: Weekly average weight gain (g) of all groups. Rats were fed on: (Control) standard diet + normal drinking water and high fat (HF) diet + normal drinking water as described in the 'Experimental methods' section. Values are means ± SD (n 4). For first 14 weeks, HF rats were fed high caloric diet followed by normal diet in the last 4 weeks. From 2 weeks onwards until week 14, rats fed HF diet gained a significant body weight ($p < 0.05$). Obese female rats had a remarkable reduction in the body weight by the end of 18 weeks study ($p < 0.05$).

(A)

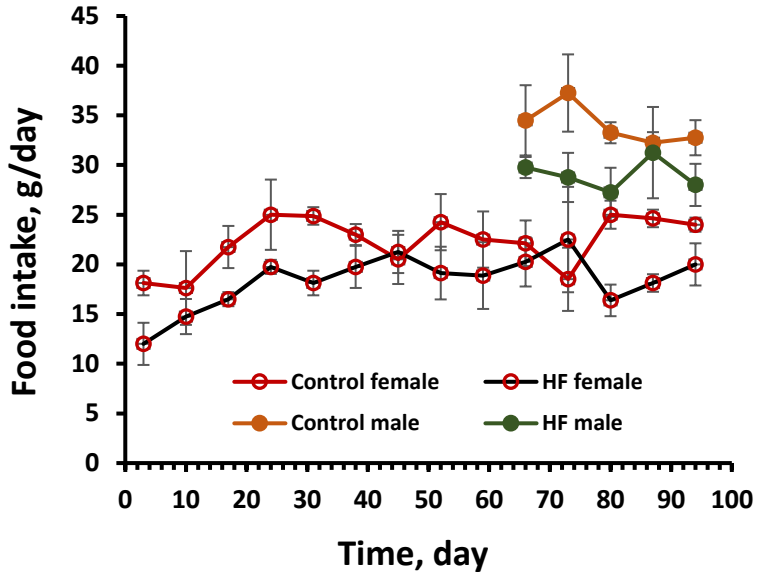

(B)

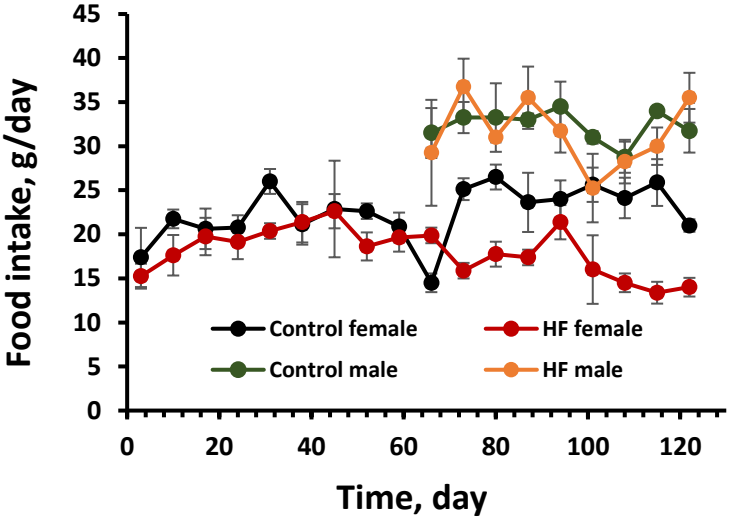

Figure 16: Average food consumed per rat from each group. Groups were fed either: standard diet or HF diet for 14 weeks (A) and for 18 weeks (B) as described in the 'Experimental methods' section. Values are Means ± SD (n 4).

(A)

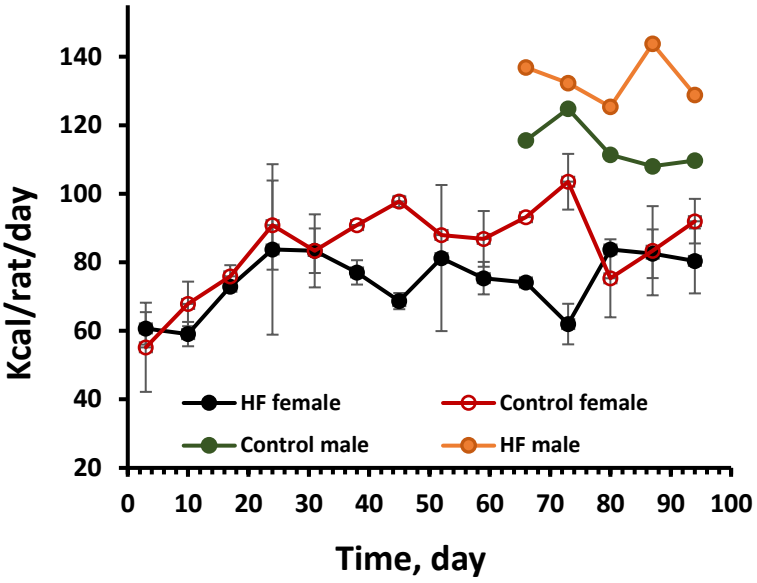

(B)

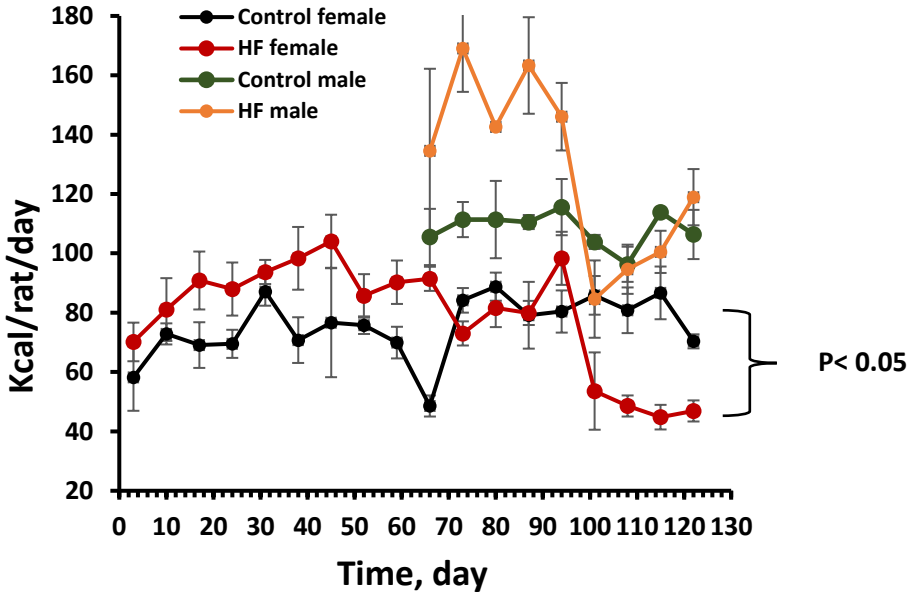

Figure 17: Daily caloric intake (Kcal/day/rat) of all groups. Groups were fed either: standard diet or HF for 14 weeks (A) and for 18 weeks (B) as described in the 'Experimental methods' section. Values are Means ± SD (n 4).

Body weight for rats involved in propofol studies

All the data related to the body weights, food intake and Kcal/day was already interpreted and published by Abdussalam et al. [152]

3.3. Incubation of liver microsomal protein with lidocaine for control and HF diet fed female rats

For microsomal incubation, 1 mg protein per ml was used. This concentration was adopted from Von et al. who used this concertation to study lidocaine metabolism in different species including Sprague-Dawley rats [225].

After incubation of lidocaine (100 – 10000 µM) for 10 min with 1 mg/ml of microsomes, the formation rate of MEGX was determined for lean and obese female rats on 14- and 18- week dietary course. The pattern of MEGX formation for 14-week and 18-week study were illustrated (Figure 18-20) and (Figure 21-23) respectively. Those kinetic parameters of MEGX formation was determined after fitting the data to Michaelis-Menten equation. Furthermore, clearance plots were used to determine those kinetic parameters (Table 6). For female rats who were on 14-week study, there was a statistically significant reduction in V_{max} of HF fed group compared to control group. Interestingly, female rats who were on standard chow after 14 week of HF diet did not show any significant difference in Vmax compared to control group. Other kinetic parameters including Cl_{int} and K_m did not differ significantly between all groups.

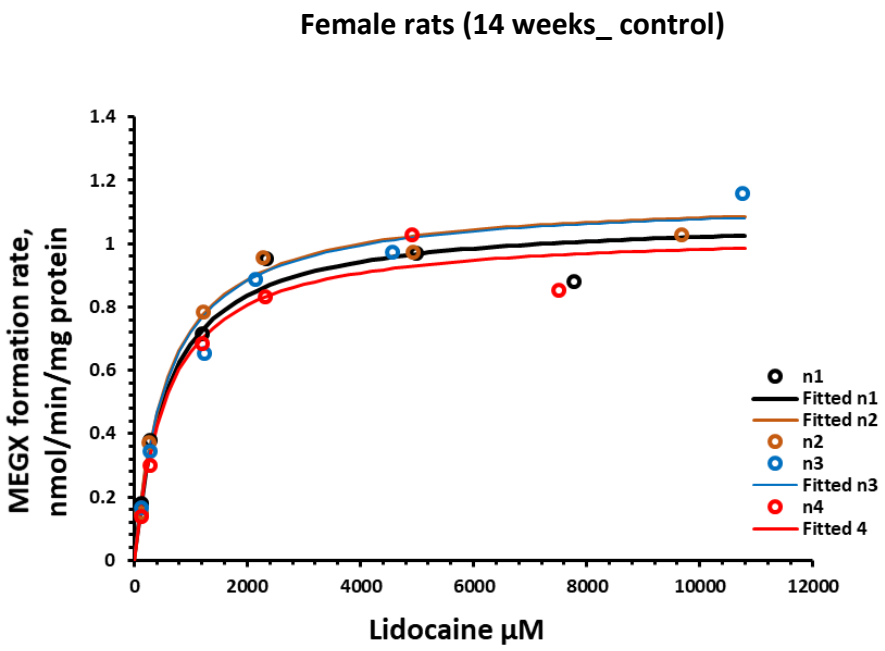

Figure 18: MEGX formation rates from lidocaine in hepatic microsomes of 14-week female rats (control group). Each "n" (n1, n2, n3 and n4) represents different microsomal preparation from different rats and each "n" is a separate run for the experiment. The fitted n1, n2, n3 and n4 represent the predicted data for each "n" obtained by the best-fit model of the tested non-linear pharmacokinetics models

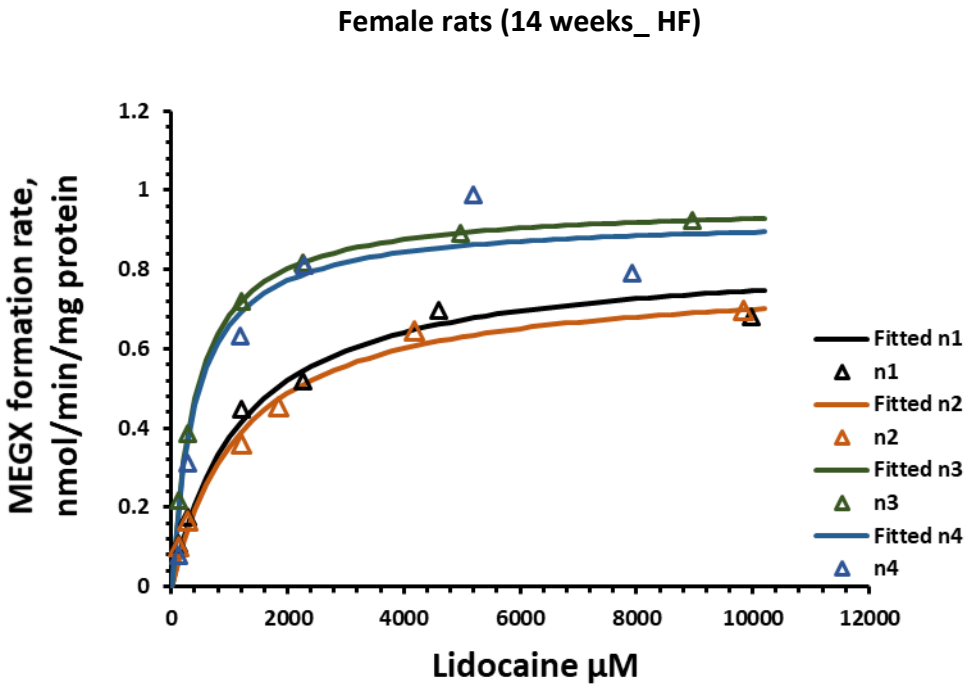

Figure 19: MEGX formation rates from lidocaine in hepatic microsomes of 14-week female rats (HF group). Each "n" (n1, n2, n3 and n4) demonstrates different microsomal preparation from different rats and each "n" is a separate run for the experiment. The fitted n1, n2, n3 and n4 represent the predicted data for each "n" obtained by the best-fit model of the tested non-linear pharmacokinetics models.

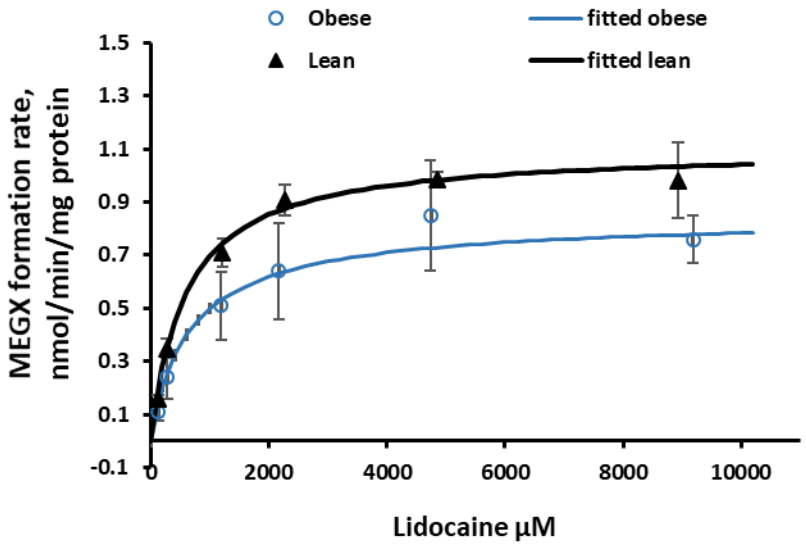

Figure 20: MEGX formation rates (Mean±SD), (n=4) from lidocaine in liver microsomes of control and obese female rats (14-week female rats). 1 mg/ml of protein was incubated with 100 – 10,000 µM of lidocaine for 10 min. MEGX formation rates were calculated using HPLC. The one enzyme model was fitted to the data.

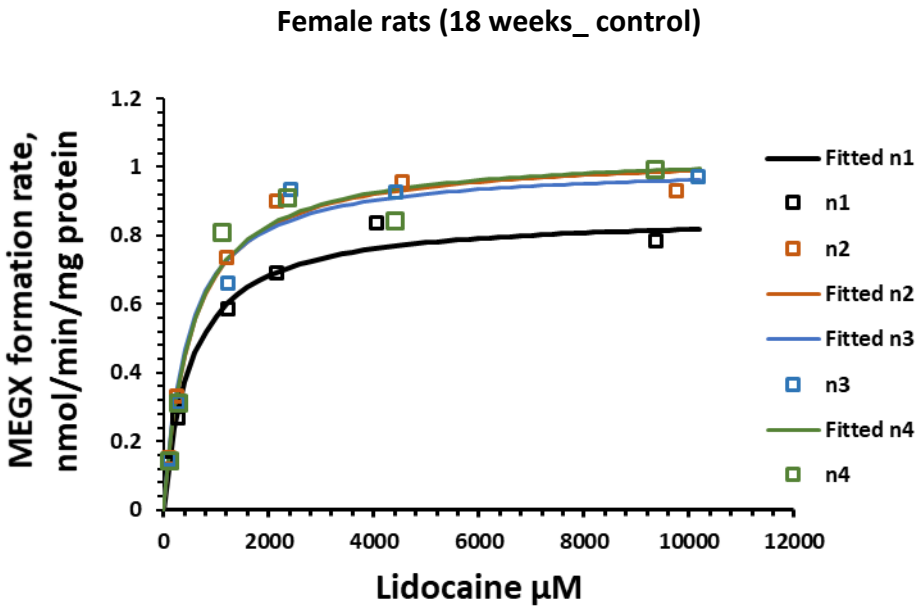

Figure 21: MEGX formation rates from lidocaine in hepatic microsomes of 18-week female rats (control group). Each "n" (n1, n2, n3 and n4) represents different microsomal preparation from different rats and each "n" is a separate run for the experiment. The fitted n1, n2, n3 and n4 represent the predicted data for each "n" obtained by the best-fit model of the tested non-linear pharmacokinetics models

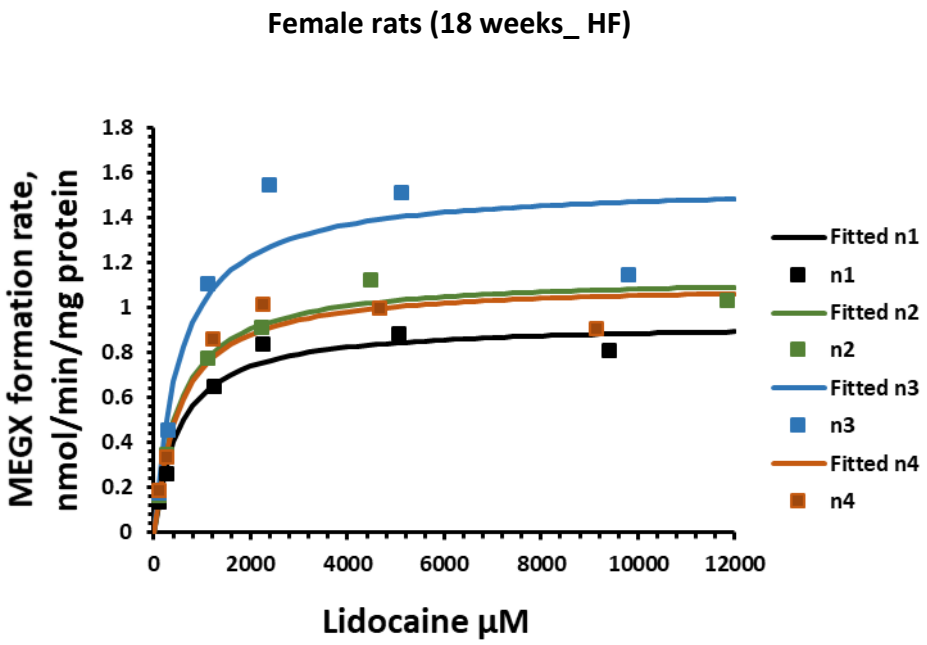

Figure 22: MEGX formation rates from lidocaine in hepatic microsomes of 18-week female rats (HF group). Each "n" (n1, n2, n3 and n4) demonstrates different microsomal preparation from different rats and each "n" is a separate run for the experiment. The fitted n1, n2, n3 and n4 represent the predicted data for each "n" obtained by the best-fit model of the tested non-linear pharmacokinetics models

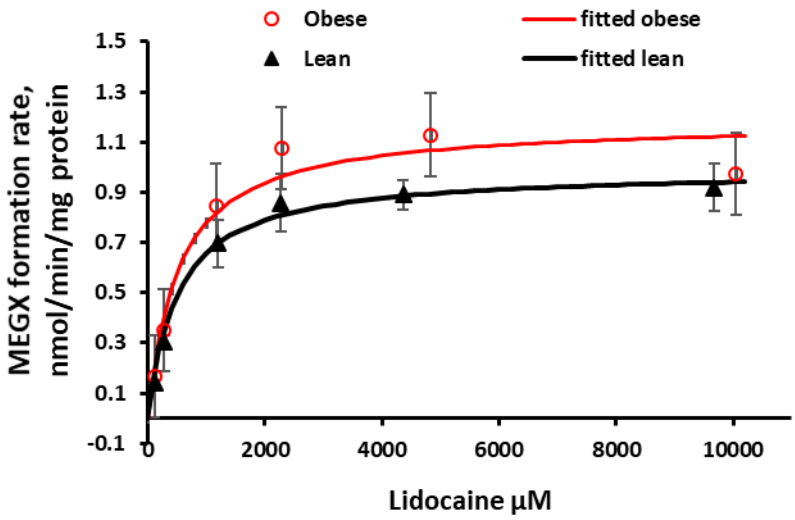

Figure 23: MEGX formation rates (Mean±SD), (n=4) from lidocaine in liver microsomes of control and obese female rats (18-week female rats). 1 mg/ml of protein was incubated with 100 – 10,000 µM of lidocaine for 10 min. MEGX formation rates were calculated using HPLC. The one enzyme model was fitted to the data.

	14 weeks study		18 weeks study	
Parameter	**Lean**	**Obese**	**Lean**	**Obese**
V_{max} nmol/min/mg protein	**1.10±0.05**	**0.86±0.17[a]**	**1.04±0.09**	**1.23±0.28**
K_m, mM	**0.66±0.087**	**0.71±0.1**	**0.68±0.02**	**0.67±0.08**
Cl_{int} µL/min/mg protein	**1.67±0.2**	**1.25±0.4**	**1.51±0.12**	**1.82±0.33**

Table 6: Kinetic constants (Mean±SD) for liver microsomes MEGX formation in control and obese rats. Comparisons were done using Student's unpaired t tests. "a" differed significantly from control ($p<0.05$).

3.4. Incubation of liver microsomal protein with propofol for control and obese rats

The glucuronidation rate of propofol with increasing protein concentration from 0.5 to 4 mg/ml was increased linearly suggesting that 1 mg/ml would be the best option to use in microsomal incubations study (Figure 24).

The liver microsomes of high caloric diet fed rats were used to assess the metabolism rate of propofol. Those rats were confirmed to be obese based on their body weight, caloric intake, and plasma biochemistry including cholesterol, triglycerides and leptin compared to control group.

Upon incubation of propofol (5 – 1000 μM) for 10 min with 1mg/ml of microsomes, the metabolism rate of propofol was calculated for lean and obese male rats who were on 14-week dietary phase.

The consumption of propofol by the microsomes was calculated by measuring the concentration difference between incubation of the drug with the microsomes at zero time (no metabolism) and at 10 minutes after incubation (time required for the metabolism). Then the consumption rates were plotted against the propofol concentrations (Figure 25-29). Each group has a different kinetic pattern. The kinetic parameters of propofol for control group were fitting the data to two enzymes models. Michaelis-Menton equation using shape factor was best fitted to calculate the PK parameters of HFCS group while Michaelis-Menton equation was best fitted to HF and HF/HFCS groups. In comparison with control group, HF group exhibited a significant reduction in Vmax while HFCS and HF/HFCS showed a significant induction of Vmax values. There was a significant different in the values of Km among the control and high caloric group, HF < HF/HFCS < Control. Although there was no statistically

significant different in Clint between the control and HF group, HF/HFCS demonstrated a significant induction of Clint (Table 7).

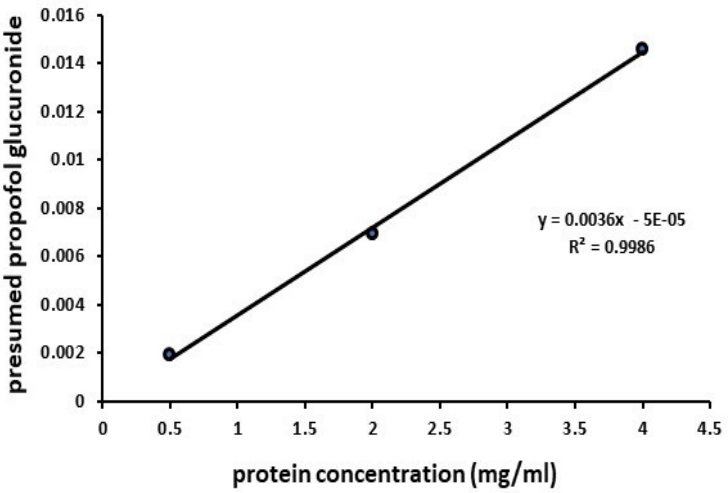

Figure 24: Linearity of propofol metabolism in different protein concentration of microsomes (250 µM of propofol was incubated with 0.5, 2 and 4 mg/mL hepatic microsomes).

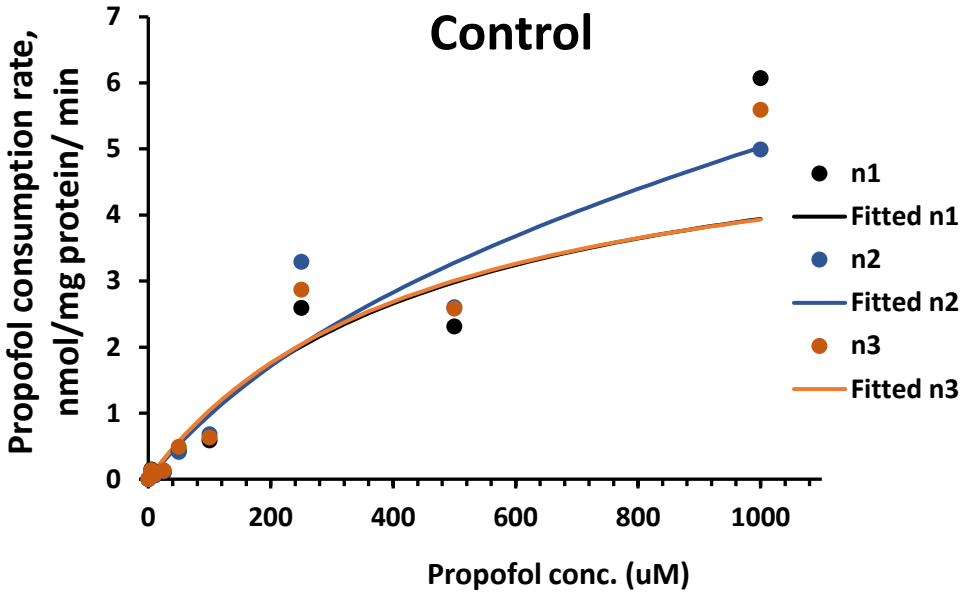

Figure 25: Propofol consumption rates in hepatic microsomes of control group. Each "n" (n1, n2 and n3) demonstrates different microsomal preparation from different rats and each n is pooled liver microsomes. The fitted n1, n2 and n3 represent the predicted data for each n obtained by the best-fit model of the tested non-linear pharmacokinetics models (two enzymes models).

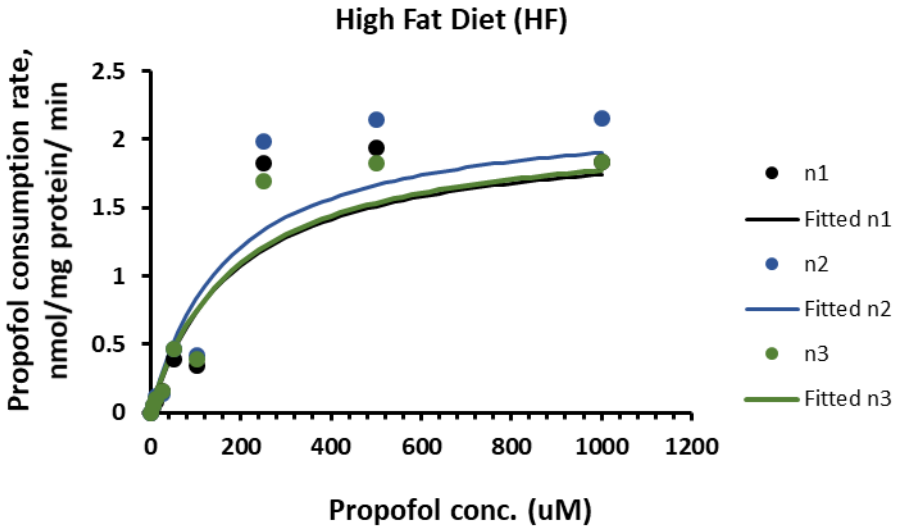

Figure 26: Propofol consumption rates in hepatic microsomes of HF group. Each "n" (n1, n2 and n3) demonstrates different microsomal preparation from different rats and each n is pooled liver microsomes. The fitted n1, n2 and n3 represent the predicted data for each n obtained by the best-fit model of the tested non-linear pharmacokinetics models (Michaelis-Menton kinetic).

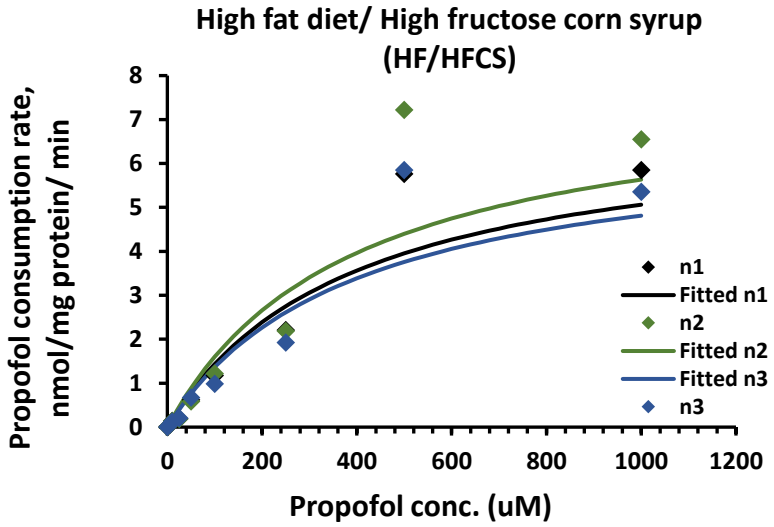

Figure 27: Propofol consumption rates in hepatic microsomes of HF/HFCS group. Each "n" (n1, n2 and n3) demonstrates different microsomal preparation from different rats and each "n" is pooled liver microsomes. The fitted n1, n2 and n3 represent the predicted data for each n obtained by the best-fit model of the tested non-linear pharmacokinetics models (Michaelis-Menton kinetic).

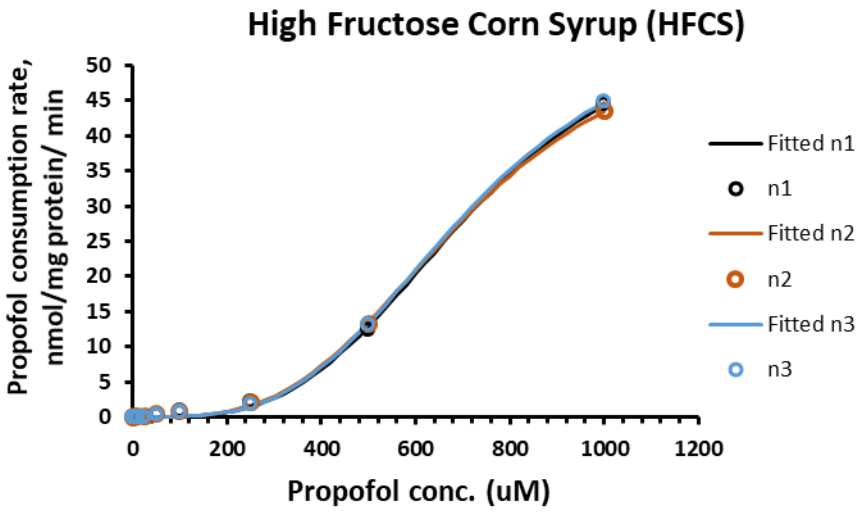

Figure 28: Propofol consumption rates in hepatic microsomes of HFCS group. Each "n" (n1, n2 and n3) demonstrates different microsomal preparation from different rats and each "n" is pooled liver microsomes. The fitted n1, n2 and n3 represent the predicted data for each "n" obtained by the best-fit model of the tested non-linear pharmacokinetics models (Michaelis-Menton kinetic with shape factor).

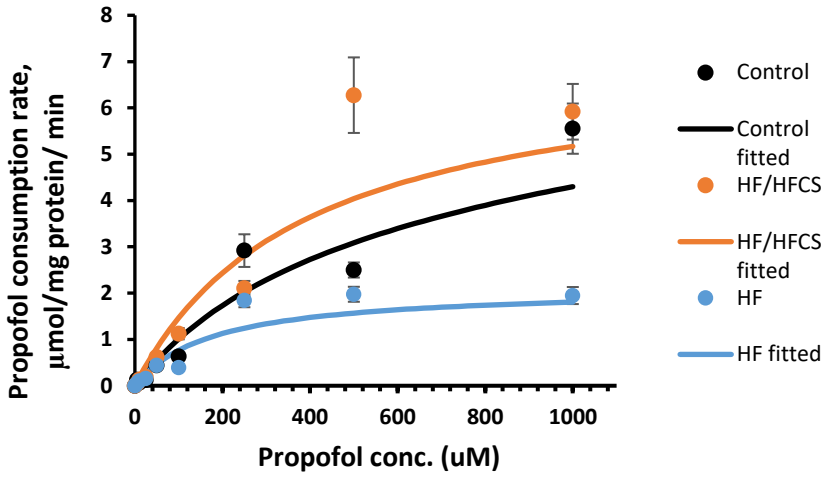

Figure 29: Propofol consumption rate (Mean±SD), (n=3) using liver microsomes of control and obese male rats. 1 mg/ml of protein was incubated with 5 – 1000 µM of lidocaine for 10 min. Each group has a distinct enzyme kinetics that fit to the data.

Parameter	Propofol consumption rate			
	Liver			
	Control	HF+HFCS	HF	HFCS
Vmax (nmol/min/mg)	5.23 ± 0.75	7.18 ± 0.58	2.12 ± 0.08	57.85±1.09
Km (µM)	458.51 ± 12.8	389.6 ±0.01	177.3 ± 9.1	711.3±7.85
CLint (µL/min/mg)	11.5 ± 1.78 *	18.4 ± 1.5 *	12.02 ± 1.12	81.32±0.94
CL2 (µL/min/mg)	0.71 ± 1.17	_	_	_
Shape factor, n	_	_	_	3.43±0.03

Table 7: Kinetic constants (Mean±SD) for liver microsomes propofol metabolism in control and obese rats. * Group showing this symbol is not different from one another. Where no symbol appears, there is a significant different from other group (ANOVA with Bonferroni correction, $p < 0.05$).

3.5. Western blot result

To investigate weather the HF diet and normalization of a high fat to normal diet would change the protein expression in female rats, the microsomal proteins were prepared from those rats' liver of control and obese group. The proteins expression of P450 including CYP2E1, CYP3A1, CYP1A2, CYP2C12, and CYP2D1 were determined using western blot analysis. In 14-week dietary phase where the female rats on HF diet, there was a significant reduction in the protein levels of CYP3A1, CYP1A2 and CYP2C12 in comparison to control group (Figure 30). Interestingly, this reduction in the protein's expression was normalized when female rats were given a standard chow for 4 weeks after 14 weeks of HF diet (Figure 31). The protein expression of CYP2D1 was examined among obese male Sprague Dawley that were on high caloric diet for 14 weeks (Figure 32). In the HF rats, CYP2D1 expression was downregulated. However, in the rats given HFCS alone or HFCS+HF had relatively larger increase in CYP2D1 compared to control group (Figure 32). The expression of UGT1A1 was also determined in those obese rats (Figure 33). All groups fed high caloric diet demonstrated significant reduction in the expression of UGT1A1 (Figure 33).

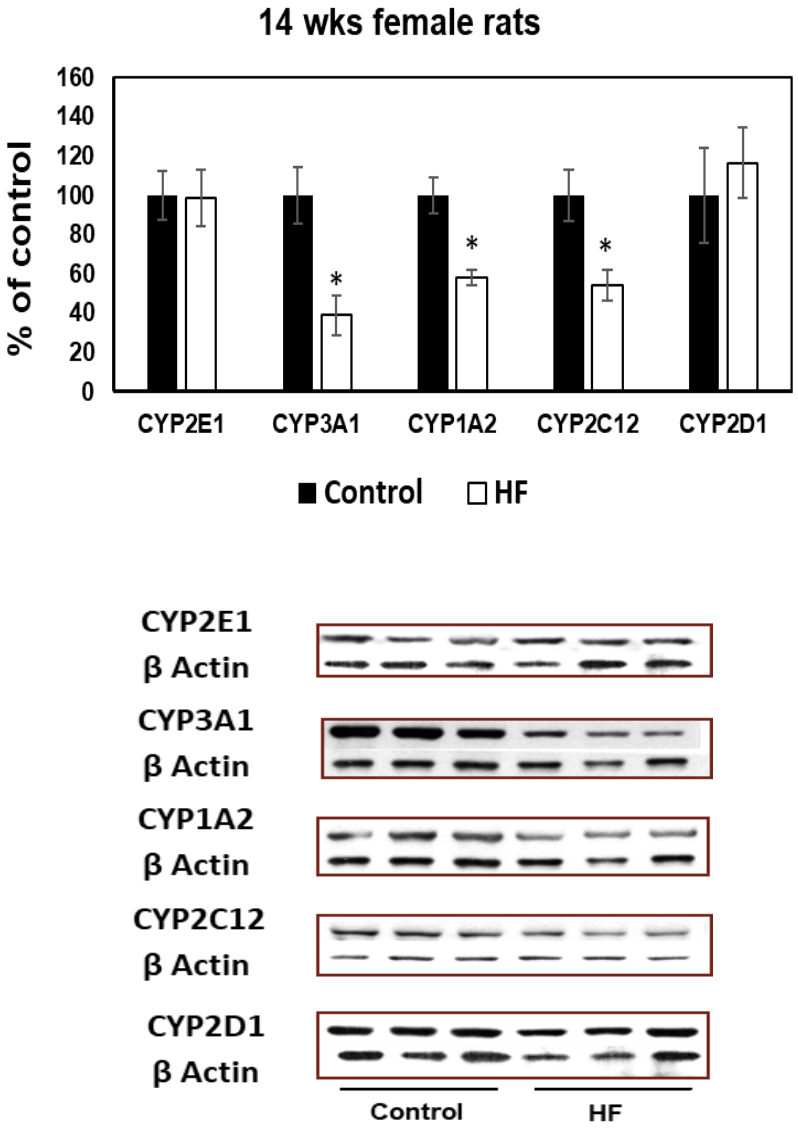

Figure 30: Effect of HF diet on the protein expression of metabolizing enzymes in liver of female rat. CYP2E1, CYP3A1, CYP1A2, CYP2C12, and CYP2D1 proteins were detected using the enhanced chemiluminescence method. The intensity of bands was normalized to β actin signals. Data are presented in fold of control (mean ± S.E.M., n = 4). * $p < 0.05$ compared to control using unpaired Student t-test.

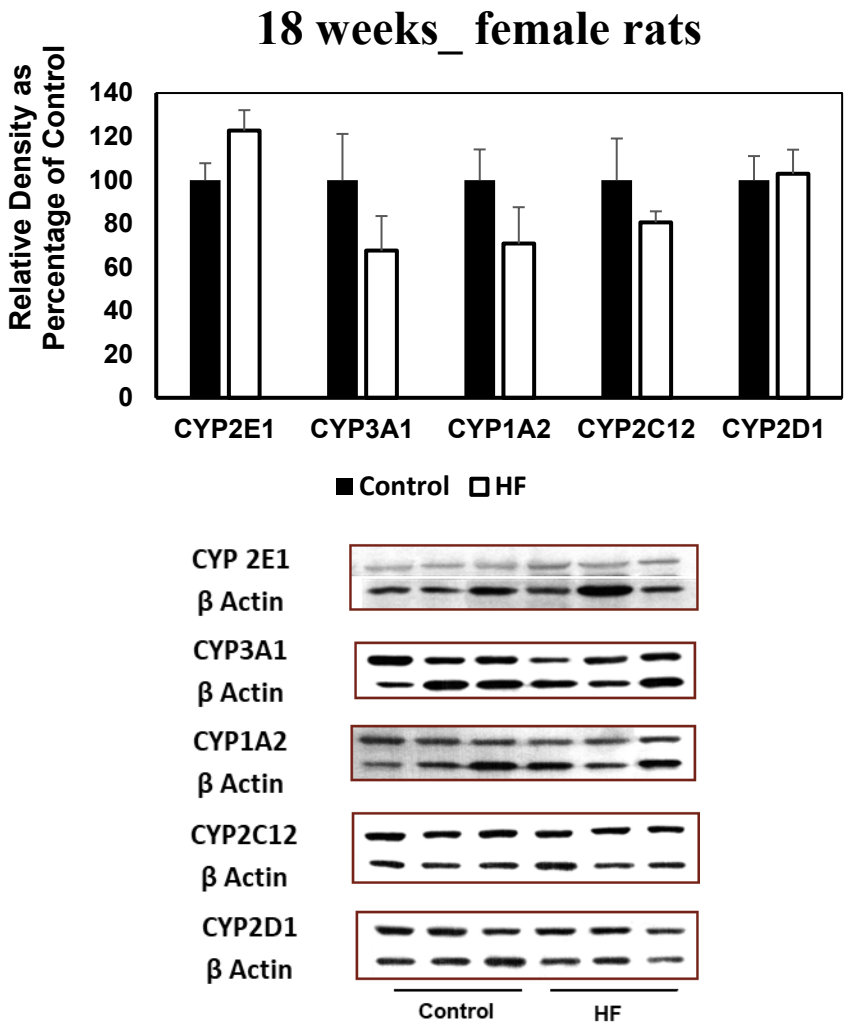

Figure 31: Effect of diet normalization on the protein expression of metabolizing enzymes in liver of female rat. CYP2E1, CYP3A1, CYP1A2, CYP2C12, and CYP2D1 proteins were detected using the enhanced chemiluminescence method. The intensity of bands was normalized to β actin signals. Data are presented in fold of control (mean ± S.E.M., n = 4). There was no statistically significant difference between HF and control group (unpaired Student t-test).

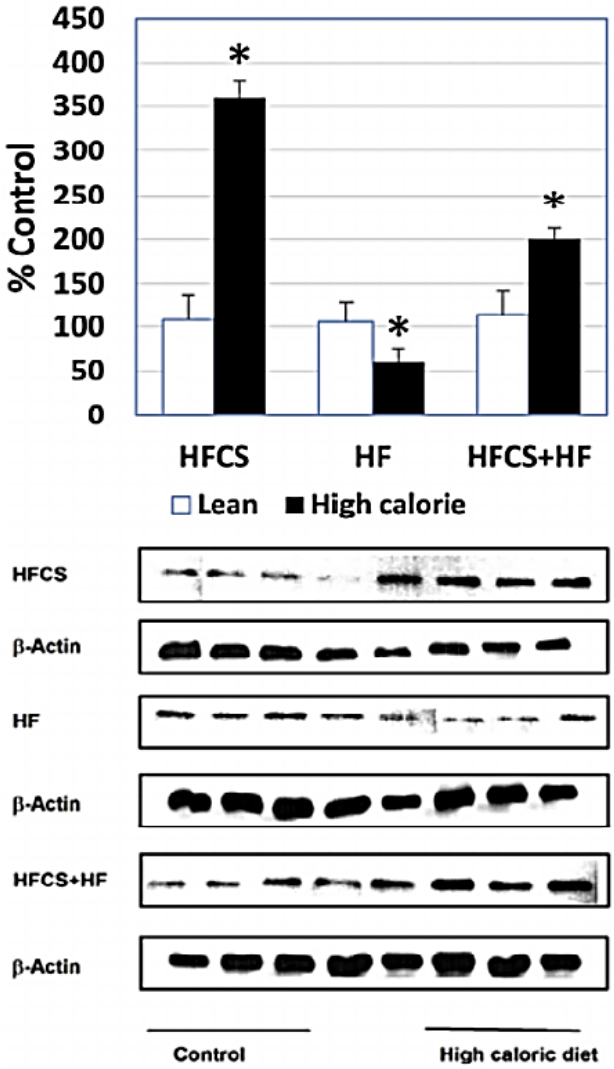

Figure 32: Rat CYP2D1 expression measured using western blot in lean control rats versus those fed either HFCS, HF, or combination (HF+HFCS) diet for 14 weeks (mean + SD., n = 4)**.** * Significant difference between the lean control and high calorie fed dietary group.

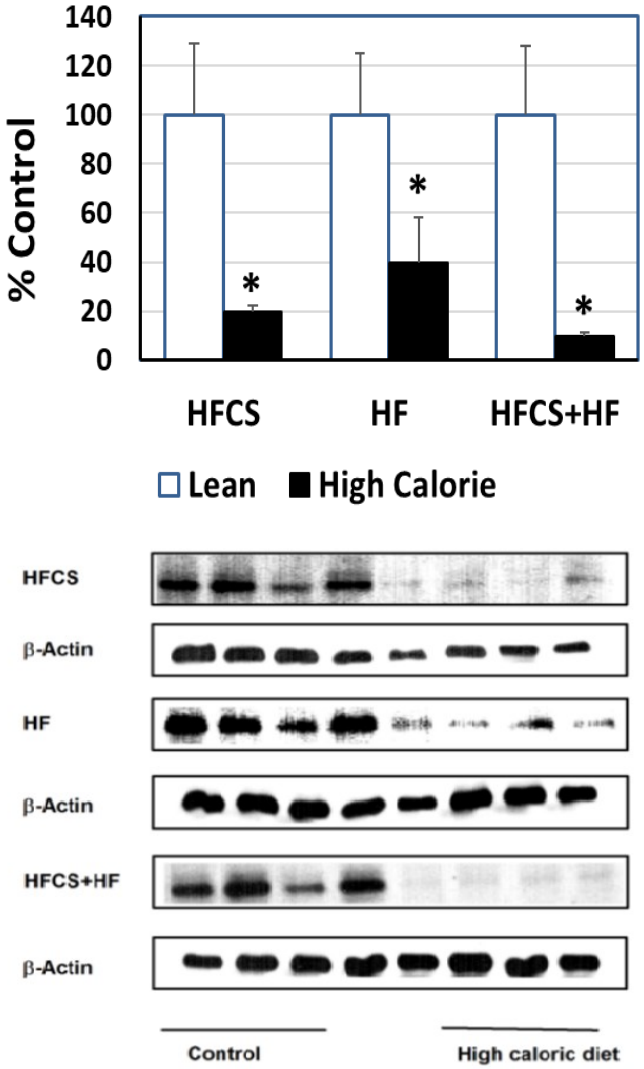

Figure 33: Rat UGT1A1 expression measured using western blot in lean control rats versus those fed either HFCS, HF, or combination (HF+HFCS) diet for 14 weeks (Mean + SD, n = 4)**.** *Significant difference between the lean control and high calorie fed dietary group.

The proteins level of cyp3a41, cyp1a2, and cyp2e1 were evaluated for C57B1/6J mice. For obese male mice who were on HF diet, it was noted that the expression of cyp3a41 was significantly low whereas cyp2e1 was significantly high. Similarly, the level of cyp3a41 was markedly low in diabetic male mice. For female mice, there was not any significant changes in the protein expression of cyp3a41 in treated groups compared to control group. The protein expression of cyp2e1 was more than double higher in HF female mice than control group. There was a reduction in the expression of cyp1a2 almost half the percentage of control group (Figure 34-36).

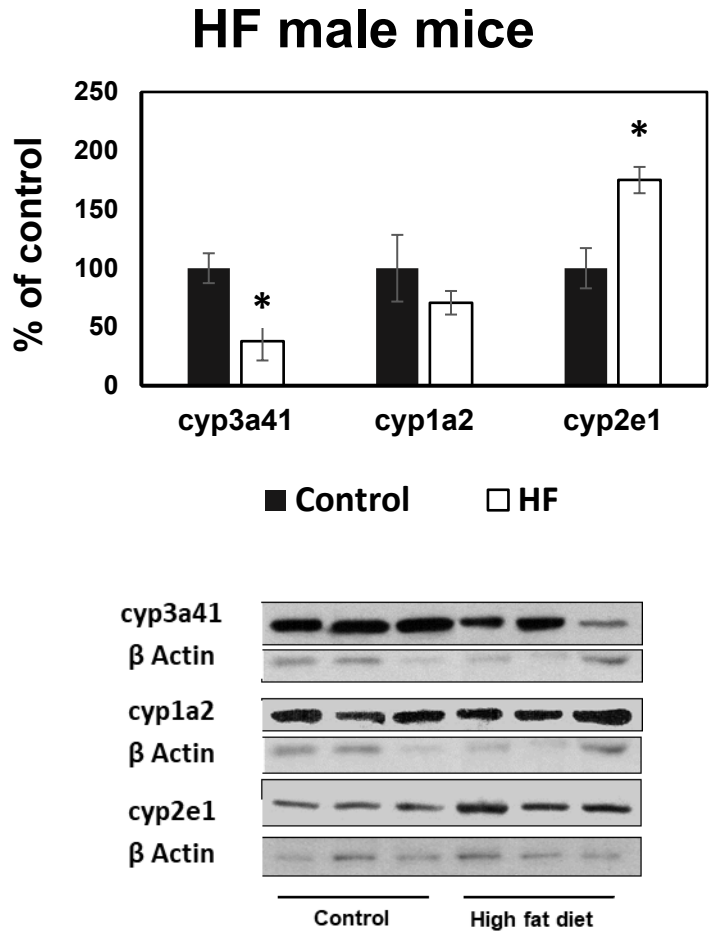

Figure 34: Effect of HF diet on the protein expression of metabolizing enzymes in liver of HF male mice. Cyp3a41, cyp1a2, and cyp2e1 proteins were detected using the enhanced chemiluminescence method. The intensity of bands was normalized to β actin signals. Data are presented in fold of control (mean ± S.E.M., n = 3). * $p < 0.05$ compared to control using unpaired Student t-test.

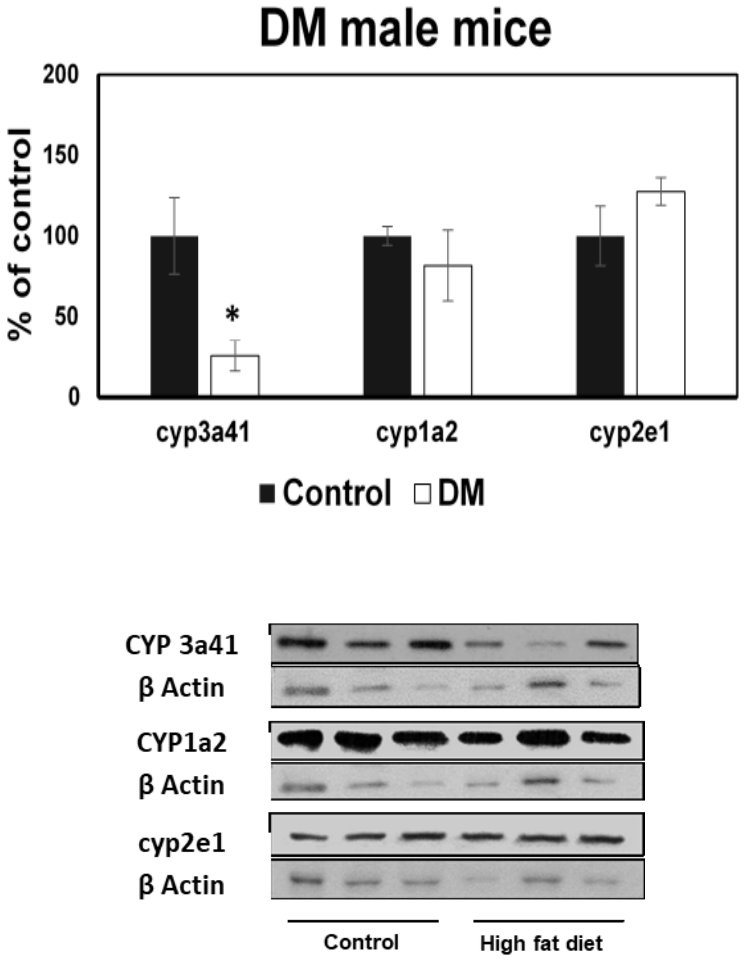

Figure 35: Effect of HF diet on the protein expression of metabolizing enzymes in liver of diabetic male mice. Cyp3a41, cyp1a2, and cyp2e1 proteins were detected using the enhanced chemiluminescence method. The intensity of bands was normalized to β actin signals. Data are presented in fold of control (mean ± S.E.M., n = 3). * $p < 0.05$ compared to control using unpaired Student t-test.

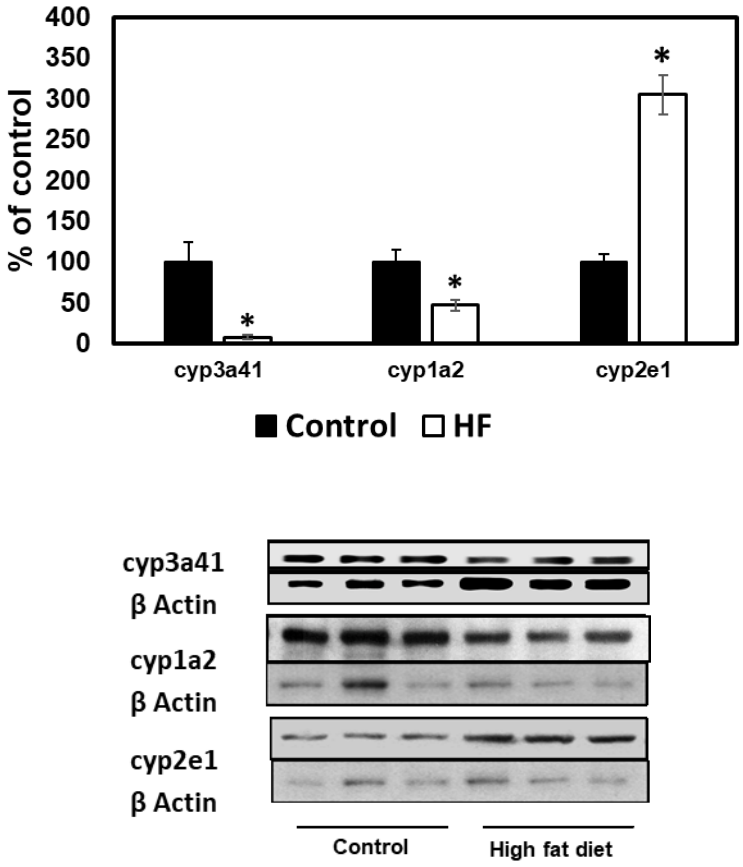

Figure 36: Effect of HF diet on the protein expression of metabolizing enzymes in liver of HF female mice. Cyp3a41, cyp1a2, and cyp2e1 proteins were detected using the enhanced chemiluminescence method. The intensity of bands was normalized to β actin signals. Data are presented in fold of control (mean ± S.E.M., n = 3). * $p < 0.05$ compared to control using unpaired Student t-test.

Chapter 4: Discussion

Serious medical comorbidities are associated with obesity, many of which require pharmacological intervention. Obesity is associated with pathophysiological changes that might affect the pharmacokinetics of drugs, and obesity is a highly prevalent condition. Although there is some data on the pharmacokinetic changes that might accompany obesity, considering the entire scope of what is published on obesity, the scope of knowledge in pharmacokinetic changes has been modest at best. This is an important area because pharmacokinetic changes can have a direct impact on a drug's safety and effectiveness.

Several research efforts have been reported the influence of obesity on phase I and phase II metabolizing enzymes. Those studies usually assessed the expression of proteins, mRNA levels and the functional activity of drug metabolizing enzymes. What we have done in our lab was to investigate and evaluate the impact of obesity on proteins expression as well as enzymes activities that involved in metabolism of most commonly used drugs.

To mimic the modern lifestyle diets, we implemented different sources of high caloric diet in our animal models to induce the obesity. High fat chow and high fructose corn syrup equivalent were used for this purpose. The male and female Sprague Dawley rats were fed rich caloric diet for different time intervals. At the end of high calorie dietary phase, it was noted that all rats gained weight significantly compared to the control group. What was novel in our study design was that we also changed the diet after the high calorie phase to observe the potential for reversibility of any changes in expression and/or enzyme activity.

For assessing enzymes activities in obese rats, we used substrates that are mainly metabolized by phase I and phase II enzymes and are widely used in clinical practice. The widely used local anesthetic and antiarrhythmic agent, lidocaine, was used as it is primarily metabolized by CYPs, CYP3A4 in humans and it's equivalent, CYP3A1, in rats. The sedative/anesthetic

agent propofol is commonly used in general anesthesia, intensive care units and caesarean section. It is metabolized by CYP (phase I) and UDP-glucuronosyltransferase (UGT) (phase II).

4.1. Development of an HPLC-UV assay for the determination of lidocaine in human serum

The HPLC method described here represents an accurate and precise avenue to determine the concentration of lidocaine in 0.25 mL volumes of human serum. The volumes of serum required are at the lower end of those volumes used by other analytical methods [156-169]. Additionally, the reported validated lower limits of quantitation are frequently greater than 50 ng/mL [157-159, 162-163, 166-167]. The lowest validated quantifiable concentration was found in the literature to be 10 ng/mL, though a serum volume of 1 mL was required [160]. Sintov et al. reported that the validated lower limit of quantification by using fluorescence detector was 25 ng/mL, which also required larger volumes of specimen up to 1 mL and derivatization following the extraction process [164], thereby adding elements of expense and time into sample preparation. The lower limit of quantitation (LLQ) in the current method is comparable to 50 ng/ml by the GC-MS method [156]. Alkaline conditions were used to force lidocaine into its free base form, which promotes its extraction into a suitable organic solvent [164]. For the extraction of lidocaine from biological matrices, different solvents have been used in HPLC methods. These include an ethyl acetate/hexane/methanol mixture [166], dichloromethane [157], ethyl acetate [159, 163], and a mixture of diethyl ether/dichloromethane [160]. Qin et al. had previously used diethyl ether as an extraction solvent for local anesthetics in human plasma, including procaine, ropivacaine, tetracaine,

bupivacaine, including lidocaine [161]. The extraction of lidocaine from plasma in their hands was virtually complete, similar to what we had found. For this reason, we adopted the extraction method of Qin for use in the currently described assay method. Qin et al. had used carbamazepine as their internal standard. Due to its late elution time compared to procainamide [161], we chose to use procainamide instead. Although its recovery was less than that of lidocaine, it nevertheless extracted very consistently and provided excellent standard curves and validation indices. Procainamide would be an unlikely interfering substance in a patient as while it is chemically similar to lidocaine, it is not a popular antiarrhythmic currently, nor is it used as an anesthetic agent. The disadvantage of procainamide is that it requires that the UV detector possess the ability to program a change in wavelength after the elution of the internal standard. In terms of mobile phase composition, acetonitrile and phosphate solution are the most common components in most of the reported studies [156-157, 160, 161-169]. Only Tam et al. and Qin et al. supplemented the mobile phase with 0.15% and 0.16% of triethylamine (TEA), respectively [159, 161], while Chen et al. supplied the mobile phase with 1% diethylamine [158]. In the current method, 0.15% of triethylamine was added as it improved the peak symmetries and reduced the peak tailing of the compounds of interest, as has been noted for other compounds [170,171]. From the literature, the retention time for the compound of interest ranged from 3.6 to less than 13 min (156 -169). The measured serum concentrations in the patient were in accordance with measures of plasma concentrations observed previously in patients administered the same dose of lidocaine HCl as depot parenteral injections [172]. The presence of a peak at 6.4 min was noticed in HPLC-UV chromatograms of blank (drug-free) human serum. Unfortunately, the appearance of this peak in the blank serum (with or without a caffeine-free period) virtually

coincided with the elution of monoethylglycylxylidide (MEGX), a major metabolite of lidocaine [173]. In the first sample taken from the patient 10 min after the dose, although lidocaine was present, there was no peak observed eluting between 6 and 7 min. In later timed samples, such as 1 h after dosing (Figure 8) a peak virtually coinciding with MEGX was apparent. However, because in the volunteer serum, a large, mostly interfering peak was present, it was not possible to quantify the MEGX concentrations in the serum of the patient using the chromatographic conditions optimal for lidocaine elution. The patient differed from those subjects contributing volunteer serum in that the patients were required to fast before the surgery. Hence, it is possible that the peak in the healthy serum was from a food component, as none of the healthy volunteers had consumed any medications before contributing the blood for serum. The assay of metabolite was not a primary aim of this study, so we did not further pursue assay work as it would have meant a longer analytical run time for lidocaine, our primary analyte of interest. We did check for the elution of caffeine, and indeed it eluted at the same time as the large interfering peak in the serum of the volunteers who drank caffeine, but it was still present even after a 24 h caffeine fast. Therefore, it most likely derived from some other component of food, or perhaps a metabolite of caffeine that is of sustained presence in serum. The patient also received other medications during surgery, and we believe that one of these may have been represented by the peak at 4.8 min (Figure 8), as it was not also seen in the volunteer serum, none of whom ingested any other drugs orally. In the in vitro metabolism study of lidocaine in rat microsomes, there were no interfering peaks present in the samples that would interfere with the assay of MEGX.

The assay was then used in a clinical study to assess the pharmacokinetics of lidocaine after rectus sheath administration. We were fortunate to have had included in the study population

10 patients of wide range of age and BMI. Hence, the relationships between the pharmacokinetic data (t½, and weight normalized CL/F and Vd/F) and the body metrics of age and BMI was evaluated. Two significant relationships were observed (Figure 11, 13), BMI vs. t½ (positive) and age vs. CL/F (negative). In rats, decreases in hepatic blood flow occur with higher age and body weight, as are levels and activities of CYP3A isoforms (involved in lidocaine metabolism) [174-176]. General anesthesia is associated with reduction in the hepatic and portal blood flow, particularly in older patients (>55 y) [177-179], and the average age of patients involved in this study was 63.9 y. Therefore, it is possible that hepatic blood flow was lower at the time of lidocaine injection and during at least part of the postsurgical recovery period, which may have contributed to a lower CL/F.

Other factor contributes to reduction of lidocaine clearance is that surgery is associated with significant increases in the circulating plasma concentrations of α1 acid glycoprotein, a major binding protein of lidocaine in plasma [180-181].

Aging by itself is associated with reduced liver size and hepatic blood flow [182]. Indeed, lidocaine CL has been found to be lower in elderly subjects compared to young subjects [183].

4.2. Rat model of obesity

Previously published studies have reported alterations in pharmacokinetics properties of some drugs among obese population; however, there were some contradictions between the findings of those studies [184 -187, 43, 65, 109). In our project, we studied the impact of obesity on the activities of liver enzymes and proteins expressions of metabolizing enzymes that are involved in metabolism of commonly used drugs in the clinic. Based on other studies our laboratory has completed in male rats, we hypothesized that obesity would associate with down-regulation in the expression and functional activities of number of CYPs enzymes and UGT. In addition, there are some differences in the responses among female and male rodents as well as normalization of a high fat to normal diet leads to normalization of protein expression and enzyme activity. To investigate our hypothesis, we developed an animal model where the rats were fed a diet that mimics Western-lifestyle food. The first model was focusing on feeding the male and female rats HF diet only. The second model, previously developed in our lab, was emphasising on include HF diet and high fructose corn syrup in the diet.

4.3. Validation of the animal model: The effect of high caloric diet on body weight

In the recent developed model, all rats that were feed HF diet for 14 weeks gained a significant weight compared to control group. The end average weight for male rats was remarkably high (28% higher) compared to control group (842 vs. 656 g) (Figure 14) with average Kcal intake per day was 114 for control group and 134 for obese rats (18% higher) (Figure 17(A)). In female rats, the end average weight (20% higher) and average Kcal/day (13% higher) for

female rats were significantly higher than control group (427 vs. 355 g and 85 vs. 75 Kcal/day) (Figure 14) (Figure 17(A)).

Male and female rats had similar average weight in the beginning of the "14 weeks study" and had identical composition of fat and standard diet. Interestingly, female rats gained less weight than male rats. Schemmel et al. indicated similar outcomes and exhibited the influence of sex and age on the body weight. The body weights were statistically different between male and female sprague dawley rats, female rats showed lower weight than male rats. Equivalently, age led to a significant increase in body mass [188].

In the 18 weeks arm, both male and female rats gained significant weight than control group when they were on HF diet in the first 14 weeks of study. By the end of 14 week, the measured mean weights for obese and lean male rats was 985 and 696 g, respectively (42% larger in HF rats) (Figure 15). Similarly, HF female rats gained more weight than lean one (424 vs 345 g, 23% higher) (Figure 15). Impressive outcomes were observed when the diet plan was switched to low caloric diet (standard chow). For obese male rats, the average body weight hit a plateau over the last 4 weeks after the diet switch (Figure 15). Indeed, obese male rats consumed similar average amounts of normal chow to that in the control group did (30 g/day obese rats vs. 31 g/day lean rats) ((Figure 16(B))). Thus, there was minor reduction in weight of obese male rats as result of low caloric intake per day. For obese female rats, there was a remarkable reduction in their weights over the last 4 weeks after the dietary switch. Their average weights dropped from 424 g at week 14, to 373 g, at week 18 (Figure 15). The significant decline in their weight matched the significant reduction in the average food intake per day after switching the food to low caloric diet (Figure 16 (B)). The average food intake in obese female rats was about 15 g/day while in control group was about 24 g/d which represents a 40%

reduction in the food intake. This significant reduction lead to overlapping of average weight of control and obese female rats by the end of the 18 week study arm (Figure 15). Thus, low and high caloric diets, respectively, had apparent catabolic and anabolic effects as measured by the body weights of the rats.

As previously observed [152], the rats were fed high caloric diet for 14 weeks. The average recorded weight after 14 weeks of dietary phase for HFD-HFCS, HFD, HFCS, and control groups was 802, 789, 719, and 639 g respectively. All groups had a remarkable increase in caloric intake in comparison to control group [152]. Regarding visceral fat mass, all high caloric fed rats gained a significant fat mass compared to control group, with highest fat mass gain occurred in HF group. In addition, some of biochemical markers that are characteristic feature associated with obesity in the plasma were studied in those groups. Compared to control group, both HF and HF-HFCS fed groups had a significant increase in cholesterol plasma levels whilst HFCS fed group demonstrated upward trend in plasma cholesterol levels. High caloric fed groups had upward tendency in the mean plasma levels of triglyceride compared to control group, yet this was significant only for HFD-HFCS and HFCS groups. HF group is the only group that experienced significant increase in the level of HDL [152]. The obese animal model was characterised with hyperinsulinemia with a small elevation of plasma glucose and without any significant changes in the biomarkers of liver injury including alanine aminotransferase (ALT) and aspartate aminotransferase (AST) [152]. Thus, the impact of other factors such as diabetes and liver injury on drug metabolizing enzymes in obese rats were omitted.

4.4. Fitting procedure for microsomal incubation study

Computer-aided nonlinear curve fitting is commonly used to determine the pharmacokinetics parameters. Many models are available to assess the goodness of fit of provided data sets to the model. Most models of metabolism are curved relationships in practice. For our purposes, to solve nonlinear programming problems, "Generalized reduced gradient algorithm" available to us as part of the Solver routine in Microsoft Excel was used. It is used as an iterative algorithm to arrive at solution based on the sum of least squares estimation via providing an initial value to get the required Michaelis-Menton parameters. The process was repeated many times using different initial values to arrive at the best estimates of the values.

Several models were implemented and tested when the enzyme kinetics for lidocaine metabolism, MEGX formation, and propofol metabolism were determined. The study was done on liver tissue of normal and high caloric diet. The utilized models were simple Michaelis-Menton kinetics, sigmoidal Michaelis-Menton kinetics with the shape factor and two enzyme (one saturable, the other not) system [189].

To select which model fits best to the experimental results, the Akaike Information criterion (AIC) was applied. AIC is commonly employed in analyzing clinical and pharmacokinetic data. It is based on maximum likelihood estimation and it selects the model that minimizes mean squared error of prediction as well as minimizes maximum possible risk in finite sample sizes [190]. The model with the smallest AIC value (negative value) is an indication of the most appropriate model and fits the actual data [191].

$$AIC = N \ In \ R_e + 2p$$

Where N is the number of data points, R_e is the residual sum of squares and p is the number of parameters estimated by the model (for example, for the simple Michaelis-Menton model, p is 2 as Vmax and km are the only estimated parameters).

4.5. The effect of diet induced obesity on the metabolism of lidocaine in female Sprague-Dawley rats

The kinetic constants including Vmax, Km, CLint were determined in female rats after 14- and 18-weeks dietary phase. Those parameters were determined after each phase. When we compared control and HF groups, it was noticed that the Vmax of MEGX was significantly lower in obese female rats compared to lean ones (Figure 20). In contrast, other parameters such as Km and CLint were not changed between treated and control groups (Table 6). This suggests an impact of obesity on the responsible enzyme's expression because lidocaine is principally metabolized via CYP3A4 and CYP1A2 in human liver [138, 150, 192]. Thus, any potential changes in these enzymes would in turn influence their activities.

To confirm our finding regarding the reduction of lidocaine metabolism in obese rats, we determined the expression of the presumed enzymes involved in the metabolism of lidocaine (CYP3A4 and CYP1A2) to MEGX using immunoblotting technique. We found a significant reduction in the protein expression of CYP3A1 and CYP1A2. Our findings are largely correlated with several completed studies on human (CYP3A4) who had NAFLD and obese male rats (CYP3A1) which demonstrated a significant reduction in activities of these enzymes

and their proteins expression [193, 152]. No study has been developed to examine the influence of obesity on CYP1A2 in obese female rats.

The second study design where the female rats were on dietary phase for 18 weeks. During the 18 weeks, they were fed HF diet for 14 weeks followed by 4 weeks of normal diet. Then, similar experiments that were conducted on the previously discussed 14 weeks study were also applied on 18 weeks study. Interestingly, after comparing the kinetic constants (Vmax, Km, Clint) between obese and lean female rats, there was no statistically significant difference between two groups (Table 6). Impressively, the reduction in the protein expression of xenobiotic-metabolizing enzymes in 14 weeks study (CYP3A1 & CYP1A) was normalized after the dietary switch (Figure 31).

The underling mechanism for repression of CYP3A1 and CYP1A2 is the involvement of transcriptional factors [195, 196]. It was reported that cytokines including IL-6, IL-4 and TNFα play a role in down-regulation the expression of drug metabolizing enzymes. These proteins are expressed from the adipose tissue, and it is known the obese individuals have a massive adipose tissue mass. Thus, obesity is associated with abundant release of these cytokines [197].

Regarding the correlation of CYP3A4 and inflammatory signal, CYP3A4 which is a major xenobiotic-metabolizing enzyme is negatively regulated by IL-6. This down-regulation occurs as result of activation of the glycoprotein receptor gp130 by IL-6 which initiates cytoplasmic signal transduction cascades. Another mechanism is that IL-6 moderately induces the mRNA of transcriptional factor C/EBPβ (CCAAT-enhancer binding protein β) [195]. Consequently, these intracellular changes lead to downregulation of CYP3A4. One of the studies has examined the effect of inflammatory cytokines on the gene expression of CYP1A2 that was

tested on adult human hepatocyte. It was found that the present of IL-6, TNF-α, IL-4, IL-1β and INF-γ were capable to reduce the mRNA expression of CYP1A2 up to 70% [196]. However, Barker et al. has reported a reduction in the rates of the transcription of CYP1A2 gene expression in isolated rat hepatocytes which was induced by IL-1 but not IL-6 or TNF in the presence of 2,3,7,8-tetrachlorodibenzo-p-dioxin, which is CYP1A2 inducer [198]. Suppression of transcriptional factors, AhR and Arnt, by Kupffer cells which produce proinflammatory cytokines lead to downregulation of CYP1A2 [199]. There is no study has been conducted to evaluate the effects of dietary-induced obesity on transcriptional regulation of CYP1A2.

The information about the effects of dietary-induced obesity on transcriptional regulation of drug-metabolizing enzymes is scarce and little known. In our study, we believe that the switching to a normal diet countered the impact of obesity on the protein expression alterations. The normalization of the protein levels might relate to reduction in the mass of adipose tissue which was noted the weights of obese female rats was reduced significantly to match the weight of control group. Thus, reduction in the expression of inflammatory cytokines is expected. Other potential mechanisms would be normalization of biochemical markers.

4.6. The effect of diet induced obesity on the metabolism of propofol in rats' liver

For the propofol study, we utilized the previously developed animal model (male Sprague Dawley rats) in our lab [152]. Those rats were fed high caloric diet (HF, HFCS, and combination HFCS+HF).

Different concentrations of propofol up to 1000 µM were incubated with liver microsomes. This wide range of concentration was adopted from Mukai et al. Mukai et al demonstrated that the kinetics of propofol glucuronidation fit a biphasic model [151] which is in line with what we found. In our study, the reported Vmax from the control group was 5.23±0.75 nmol/mg protein/ min. Even though Mukai et al. reported the Vmax for low and high affinity phases to be 2.07±0.37 and 0.58±0.12 nmol/min/mg protein respectively, it is crucial to consider the strain and age differences of rats. In our experiment, we used male Sprague dawley rats which were 18 weeks old by the end of the study. In contrast, Mukai et al. used male Wistar rats who were younger age than our rats (8-10 weeks) when the experiment was conducted [151]. Similar study by Shimizu examined the kinetics parameters of propofol on male Wistar rats with similar age (7-8 weeks). However, this study demonstrated that enzyme kinetics of propofol best fit Michaelis-Menton kinetics and Vmax was 0.39±0.02 nmol/min/mg protein [200].

No studies have been conducted to examine the kinetic constant of propofol in obese rats. In our experiment, we found that rats fed HF diet exhibited significant reduction in glucuronidation of propofol compared to control group (2.12±0.08 vs. 5.23±0.75 nmol/min/mg protein) (Figure 29). In contrast, the group that drank high fructose corn syrup in conjunction with HF diet and HFCS alone showed the opposite effect on glucuronidation

activity, indicative of significant induction in the glucuronidation pathway (Figure 28) (Figure 29).

It was reported that over 70% of propofol is glucuronidated and at almost less than 50% of metabolites are hydroxylated in humans [201]. Based on what was mentioned about propofol metabolism in section 1.9.2., it is metabolized to inactive substrate via different UGTs and CYPs isoforms. CYP2C9 [201, 204] and UGT1A9 [151, 203] are predominate enzymes involve in metabolism of propofol in human. We observed that UGT1A1 protein expression was remarkably reduced among all different types of high caloric diet (over 50% reduction) (Figure 33). Ghose R et al reported a reduction in the RNA level of *ugt1a1* in male mice fed a HF diet (60% kcal fat) [207]. There is limited literature on the impact of obesity on the expression of phase II enzymes.

4.7. The effect of diet induced obesity on the expression levels of CYP and UGT enzymes in the liver

4.7.1. Expression levels of CYP enzymes in the liver of female Sprague Dawley rats

We examined the protein expression of the following enzymes CYP3A1, CYP1A2, CYP2C12, CYP2E1, and CYP2D1. Regarding CYP3A1 expression, it was significantly reduced in female rats about 60% (Figure 30). There is no previous study that assesses the expression of CYP3A1 in female rat, the result here match what was reported in obese human and male Sprague Dawley rats [193, 152]. The possible explanation for the reduction of CYP3A1 was mentioned in detail in the section 4.5.1. CYP1A2 expression was reduced significantly in obese female rats compared to lean female rats (about 40% reduction) (Figure

30). No published study has examined the influence of high caloric diet on CYP1A2 expression in female Sprague Dawley rats. Elam et al, revealed that CYP1A2 gene expression was significantly reduced in the livers of morbidly obese women [205]. One study that was done on male Zucker rats showed induction in CYP1A2 expression; however, there was no a clear statement or Figure to show if they used a housekeeping gene to normalize the bands reading of CYP1A2 in their study [194].

Wright et al. found, interestingly, that IL-1 but not IL-6 in female rats was associated with down-regulation of *CYP2C12* mRNA and protein expressions using in vivo and in vitro assessments[206]. Eventhoug this study was not conducted on obese female rats, it is expected to observe similar outcome on the expression of CYP2C12 in obese female rats given that inflammatory stimuli are commonly associated with obesity. In our study, protein expression of CYP2C12 was reduced significantly about 40% comparing to control group (Figure 30). CYP2D1 was not changed in obese female rats comparing with control group (Figure 30). In contrast, male Sprague-Dawley rats fed HF diet demonstrated a significant reduction about 40% in the CYP2D1 level (Figure 32).

There is a correlation between diets rich in fat and the expression of CYP2E1 in the liver. At cellular level (Figure 37), anti-apoptotic protein Bax inhibitor-1 (BI-1) has a critical role in minimizing endoplasmic reticulum (ER) stress and production of reactive oxygen species (ROS) which are triggered by increasing free fatty acid consumption. In addition, it was reported that the hepatic expression of BI-1 improve both glucose and insulin intolerance in mice fed HF diet via increasing tyrosine phosphorylation of IR, IS1/2, and increasing Akt (Protein kinase B) phosphorylation. A significant reduction of CYP2E1 activity and related lipid peroxidation were noted in liver of BI-1 overexpressing mice as BI-1 is an inhibitor of

IRE-1α as well as the association of CYP2E1 with CPR. However, the interaction between BI-1 and IRE-1α was impaired under free fatty acid stress. Thus, constant consumption of HF diet associates with induction of CYP2E1 and stimulation of IRE-1α and PERK signaling transduction [209].

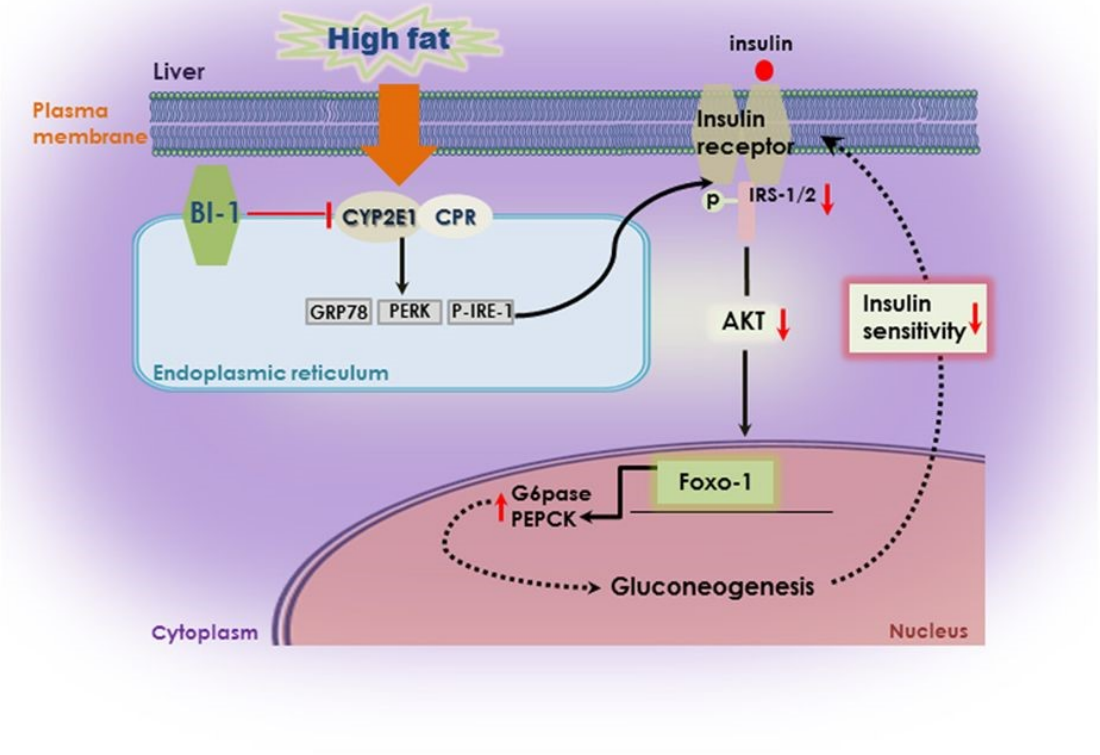

Figure 37: Correlation between high fat consumption and CYP2E1 activity as well as the relationships between obesity induced by HF diet and insulin resistance [209].

4.7.2. Expression levels of CYP enzymes in the liver of male and female mice

CYP2E1 is an inducible protein as various pathophysiological conditions contribute to enhance its level. It was reported that hepatic CYP2E1 is frequently prompted in obesity and

other related metabolic diseases. The enhancement of CYP2E1 protein expression and/ or activity was reported in the context of obesity, diabetes, fatty liver, and non-alcoholic steatohepatitis (NASH) in both human [212-217] and rodents [218-223]. Wide range of factors that exacerbate the expression of CYP2E1 are fatty acid, insulin resistance, inflammatory cytokines and some adipose hormones. Fatty acids such as palmitic and oleic acids are capable to induce mRNA and/or protein levels of CYP2E1 in human hepatocytes [216,217]. Moreover, experimental animals were on high-fat diets exhibited enhancement of hepatic CYP2E1 expression and activity as a compensatory mechanism to get ride of excess fatty acids. The hepatic expression of CYP2E1 is down-regulated by insulin through alteration its mRNA stability. However, some metabolic pathways such as gluconeogenesis and lipogenesis are resistant to insulin. Thus, insulin-mediated down regulation of CYP2E1 mRNA level would be impaired. Similarly, glucagon which is commonly high in obesity and insulin resistance is capable to induce CYP2E1 mRNA levels. Regarding to hormonal factor, obesity is frequently associated with alteration in the secretion of adipose hormones (leptin and adiponectin). Adiponectin level is commonly reduced in obese patients while leptinemia is induced in obesity. Inflammatory cytokines ,in particular, IL-4 induces the expression of CYP2E1 [70].

From the analysis of the liver samples of the mice, the level of cyp2e1 in obese male and female mice was significantly higher than lean mice. These findings were in the line with those reported earlier in the protein expressions of male ICR mice and ob/ob female mice [Figure 34-36] [211]. There was upwards trend in cyp2e1 expression in diabetic mice, but it was not significant (Figure 35).

Cyp3a41 is mouse homologue of human CYP3A4, which metabolize a significant proportion of xenobiotics [60]. There was a significant reduction in the protein expressions of cyp3a4 in

obese and diabetic male mice as well as in female mice [Figure 34-36]. Similar results were observed by Yoshinari et al, where the cyp3a isoforms drastically diminished at both proteins and mRNA levels of obese male mice [210].

The protein expression of cyp1a2 that was determined in obese and diabetic male mice appeared lower than control group, but it was not significantly. Yoshinari et al, demonstrated similar outcomes as there was no remarkable reduction in protein expression of cyp1a2 after 5 weeks on HF diet while its mRNA level was diminished significantly [210].

4.8. Conclusion

- A new assay for lidocaine was developed.
- There are correlations between lidocaine's half life and body mass index and an inverse relationship between its clearance and age.
- Diet induce obesity is associated with reduction in the hepatic microsomal rate of hydroxylation.
- The protein expression of the most CYPs including CYP3A1, CYP1A2 and CYP2C12 were diminished after relative long period consumption of HF diet.
- Even though high fat diet itself revealed a reduction in the expression of CYP2D1, other type of energy dense food that contains sucrose demonstrated induction in its expression.
- Propofol glucuronidation was high among HFCS and HF+HFCS groups while HF group showed opposite effect.

- One of UGT isoforms (UGT1A1) revealed significant reductions after consumption of high caloric diet
- Normalization of a high fat to normal diet leads to normalization of protein expression and enzyme activity
- There is gender and species difference in response to hypercaloric diets

4.9. Future directions

Western blot and microsomal incubation for male rats will be determined to assess the expression and functional activities of enzymes involved in lidocaine metabolism. Immunoinhibition study will be conducted to determine the predominant CYPs and UGTs involve in lidocaine and propofol metabolism in rats. In addition, real-time PCR primers for lidocaine metabolic enzymes in male and female rats before and after diet switching will be assessed. In order to investigate the possible mechanism for our observation, plasma and liver biochemistry including glucose, insulin, leptin, lipid profile will be examined.

References

1. Twells LK, Gregory DM, Reddigan J, Midodzi WK. Current and predicted prevalence of obesity in Canada: a trend analysis. CMAJ Open 2014 Mar 3;2(1): E18-26.

2. McCormack GR, Friedenreich C, McLaren L, Potestio M, Sandalack B, Csizmadi I. Interactions between Neighbourhood Urban Form and Socioeconomic Status and Their Associations with Anthropometric Measurements in Canadian Adults. Journal of environmental and public health 2017;2017.
3. Arroyo-Johnson C, Mincey KD. Obesity Epidemiology Worldwide. Gastroenterol Clin North Am 2016 Dec;45(4):571-579.
4. Mathieu P, Poirier P, Pibarot P, Lemieux I, Després JP. Visceral obesity. Hypertension. 2009 Apr 1;53(4):577-84.
5. Emerging Risk Factors Collaboration. Separate and combined associations of body-mass index and abdominal adiposity with cardiovascular disease: collaborative analysis of 58 prospective studies. The Lancet 2011;377(9771):1085-1095.
6. Rosenblum J., Venkatesh RD. Obesity. In: Goldstein MA, editor. The MassGeneral Hospital for Children Adolescent Medicine Handbook. Second edition. Boston, MA, USA: Goldstein MA; 2011. P. 68-69.
7. Phillips CM, Tierney AC, Perez-Martinez P, Defoort C, Blaak EE, Gjelstad IM, et al. Obesity and body fat classification in the metabolic syndrome: impact on cardiometabolic risk metabotype. Obesity 2013;21(1)
8. Hu FB. Sedentary lifestyle and risk of obesity and type 2 diabetes. Lipids 2003;38(2):103-108.
9. Ludwig DS. Dietary glycemic index and obesity. J Nutr 2000 Feb;130(2S Suppl):280S-283S.
10. Roberts SB. High-glycemic Index Foods, Hunger, and Obesity: Is There a Connection? Nutr Rev 2000;58(6):163-169.
11. Knibbe CA, Brill MJ, van Rongen A, Diepstraten J, van der Graaf, Piet Hein, Danhof M. Drug disposition in obesity: toward evidence-based dosing. Annu Rev Pharmacol Toxicol 2015; 55:149-167.
12. Jain R, Chung S, Jain L, Khurana M, Lau S, Lee J, et al. Implications of obesity for drug therapy: limitations and challenges. Clinical Pharmacology & Therapeutics 2011;90(1):77-89.
13. American Diabetes Association, American Psychiatric Association, American Association of Clinical Endocrinologists, North American Association for the Study of Obesity. Consensus development conference on antipsychotic drugs and obesity and diabetes. Diabetes Care 2004 Feb;27(2):596-601

14. Vincent HK, Heywood K, Connelly J, Hurley RW. Obesity and weight loss in the treatment and prevention of osteoarthritis. PM&R 2012;4(5):S59-S67
15. Poulain M, Doucet M, Major GC, Drapeau V, Series F, Boulet LP, et al. The effect of obesity on chronic respiratory diseases: pathophysiology and therapeutic strategies. CMAJ 2006 Apr 25;174(9):1293-1299
16. Cheymol G. Effects of obesity on pharmacokinetics. Clin Pharmacokinet 2000;39(3):215-231
17. Das UN. Obesity: genes, brain, gut, and environment. Nutrition 2010;26(5):459-473.
18. Muluke M, Gold T, Kiefhaber K, Al-Sahli A, Celenti R, Jiang H, et al. Diet-induced obesity and its differential impact on periodontal bone loss. J Dent Res 2016;95(2):223-229
19. Bocarsly ME, Powell ES, Avena NM, Hoebel BG. High-fructose corn syrup causes characteristics of obesity in rats: increased body weight, body fat and triglyceride levels. Pharmacology Biochemistry and Behavior 2010;97(1):101-106
20. Lutz TA, Woods SC. Overview of animal models of obesity. Current protocols in pharmacology 2012;58(1):5.61. 1-5.61. 18.
21. Bates SH, Kulkarni RN, Seifert M, Myers MG. Roles for leptin receptor/STAT3-dependent and-independent signals in the regulation of glucose homeostasis. Cell metabolism 2005;1(3):169-178.
22. Chua SC,Jr, Chung WK, Wu-Peng XS, Zhang Y, Liu SM, Tartaglia L, et al. Phenotypes of mouse diabetes and rat fatty due to mutations in the OB (leptin) receptor. Science 1996 Feb 16;271(5251):994-996.
23. Expert Panel Members, Jensen MD, Ryan DH, Donato KA, Apovian CM, Ard JD, et al. Executive summary: guidelines (2013) for the management of overweight and obesity in adults: a report of the American College of Cardiology/American Heart Association Task Force on Practice Guidelines and the Obesity Society published by the Obesity Society and American College of Cardiology/American Heart Association Task Force on Practice Guidelines. Based on a systematic review from the Obesity Expert Panel, 2013. Obesity 2014;22(S2):S5-S39.
24. Hamdy O, Ledbury S, Mullooly C, Jarema C, Porter S, Ovalle K, et al. Lifestyle modification improves endothelial function in obese subjects with the insulin resistance syndrome. Diabetes Care 2003 Jul;26(7):2119-2125.
25. Wadden TA, Volger S, Tsai AG, Sarwer DB, Berkowitz RI, Diewald L, et al. Managing obesity in primary care practice: an overview with perspective from the POWER-UP study. Int J Obes 2013;37(S1):S3.
26. Wadden TA, West DS, Neiberg RH, Wing RR, Ryan DH, Johnson KC, et al. One-year weight losses in the Look AHEAD study: factors associated with success. Obesity 2009;17(4):713-722
27. Brocks DR, Ben-Eltriki M, Gabr RQ, Padwal RS. The effects of gastric bypass surgery on drug absorption and pharmacokinetics. Expert opinion on drug metabolism & toxicology 2012;8(12):1505-1519.
28. Buchwald H, Oien DM. Metabolic/bariatric surgery worldwide 2011. Obesity Surg 2013;23(4):427-436

29. Goldstein MA. The MassGeneral Hospital for children adolescent medicine handbook. : Springer; 2011
30. Adams TD, Davidson LE, Litwin SE, Kolotkin RL, LaMonte MJ, Pendleton RC, et al. Health benefits of gastric bypass surgery after 6 years. JAMA 2012;308(11):1122-1131
31. Hanley MJ, Abernethy DR, Greenblatt DJ. Effect of obesity on the pharmacokinetics of drugs in humans. Clin Pharmacokinet 2010;49(2):71-87.
32. Barras M, Legg A. Drug dosing in obese adults. Australian prescriber 2017;40(5):189.
33. Van Kralingen S, Diepstraten J, Peeters MY, Deneer VH, Van Ramshorst B, Wiezer RJ, et al. Population pharmacokinetics and pharmacodynamics of propofol in morbidly obese patients. Clin Pharmacokinet 2011;50(11):739-750
34. Brill MJ, Houwink AP, Schmidt S, Van Dongen EP, Hazebroek EJ, van Ramshorst B, et al. Reduced subcutaneous tissue distribution of cefazolin in morbidly obese versus non-obese patients determined using clinical microdialysis. J Antimicrob Chemother 2013;69(3):715-723.
35. Brocks DR, Hamdy DA, Ben-Eltriki M, Patel JP, El-Kadi AO. Effect of rat serum lipoproteins on mRNA levels and amiodarone metabolism by cultured primary rat hepatocytes. J Pharm Sci 2013;102(1):262-270.
36. Brill MJ, Diepstraten J, van Rongen A, Van Kralingen S, van den Anker, John N, Knibbe CA. Impact of obesity on drug metabolism and elimination in adults and children. Clin Pharmacokinet 2012;51(5):277-304.
37. Tripathi K. Essentials of medical pharmacology. JP Medical Ltd; 2013
38. Bowman S, Hudson S, Simpson G, Munro J, Clements J. A comparison of the pharmacokinetics of propranolol in obese and normal volunteers. Br J Clin Pharmacol 1986;21(5):529-532.
39. Flechner SM, Kolbeinsson ME, Tam J, Lum B. The impact of body weight on cyclosporine pharmacokinetics in renal transplant recipients. Transplantation 1989 May;47(5):806-810.
40. Cheymol G, Weissenburger J, Poirier JM, Gellee C. The pharmacokinetics of dexfenfluramine in obese and non-obese subjects. Br J Clin Pharmacol 1995 Jun;39(6):684-687.
41. Kees MG, Weber S, Kees F, Horbach T. Pharmacokinetics of moxifloxacin in plasma and tissue of morbidly obese patients. J Antimicrob Chemother 2011;66(10):2330-2335.
42. Brill MJ, Houwink AP, Schmidt S, Van Dongen EP, Hazebroek EJ, van Ramshorst B, et al. Reduced subcutaneous tissue distribution of cefazolin in morbidly obese versus non-obese patients determined using clinical microdialysis. J Antimicrob Chemother 2013;69(3):715-723.
43. Sanderink G, Le Liboux A, Jariwala N, Harding N, Ozoux M, Shukla U, et al. The pharmacokinetics and pharmacodynamics of enoxaparin in obese volunteers. Clinical Pharmacology & Therapeutics 2002;72(3):308-318.
44. Clauson PG, Linde B. Absorption of rapid-acting insulin in obese and nonobese NIDDM patients. Diabetes Care 1995 Jul;18(7):986-991.

45. Jusko WJ, Gretch M. Plasma and tissue protein binding of drugs in pharmacokinetics. Drug Metab Rev 1976;5(1):43-140.
46. Blouin RA, Warren GW. Pharmacokinetic considerations in obesity. J Pharm Sci 1999;88(1):1-7.
47. Mahmood I. Prediction of clearance and volume of distribution in the obese from normal weight subjects. Clin Pharmacokinet 2012;51(8):527-542.
48. Jusko WJ, Gretch M. Plasma and tissue protein binding of drugs in pharmacokinetics. Drug Metab Rev 1976;5(1):43-140.
49. Abernethy DR, Greenblatt DJ, Divoll M, Harmatz JS, Shader RI. Alterations in drug distribution and clearance due to obesity. J Pharmacol Exp Ther 1981 Jun;217(3):681-685.
50. Lemmens HJ, Bernstein DP, Brodsky JB. Estimating blood volume in obese and morbidly obese patients. Obesity Surg 2006;16(6):773-776.
51. Blouin RA, Warren GW. Pharmacokinetic considerations in obesity. J Pharm Sci 1999;88(1):1-7.
52. Van Kralingen S, Diepstraten J, Peeters MY, Deneer VH, Van Ramshorst B, Wiezer RJ, et al. Population pharmacokinetics and pharmacodynamics of propofol in morbidly obese patients. Clin Pharmacokinet 2011;50(11):739-750.
53. Diepstraten J, Chidambaran V, Sadhasivam S, van Oud-Alblas HB, Inge T, van Ramshorst B, et al. An Integrated Population Pharmacokinetic Meta-Analysis of Propofol in Morbidly Obese and Nonobese Adults, Adolescents, and Children. CPT: pharmacometrics & systems pharmacology 2013;2(9):1-8.
54. Armenti VT, Boullata JI. Handbook of Drug-nutrient Interactions. : Humana Press; 2010.
55. Jones AW. Profiles in drug metabolism and toxicology: Richard Tecwyn Williams (1909–1979). Drug Metab Rev 2015;47(4):401-405.
56. Moretto M, Kupski C, Mottin CC, Repetto G, Toneto MG, Rizzolli J, et al. Hepatic steatosis in patients undergoing bariatric surgery and its relationship to body mass index and co-morbidities. Obesity Surg 2003;13(4):622-624.
57. Matteoni CA, Younossi ZM, Gramlich T, Boparai N, Liu YC, McCullough AJ. Nonalcoholic fatty liver disease: a spectrum of clinical and pathological severity. Gastroenterology 1999;116(6):1413-1419.
58. Harnois F, Msika S, Sabaté J, Mechler C, Jouet P, Barge J, et al. Prevalence and predictive factors of non-alcoholic steatohepatitis (NASH) in morbidly obese patients undergoing bariatric surgery. Obesity Surg 2006;16(2):183-188.
59. Donato MT, Lahoz A, Jimenez N, Perez G, Serralta A, Mir J, et al. Potential impact of steatosis on cytochrome P450 enzymes of human hepatocytes isolated from fatty liver grafts. Drug Metab Dispos 2006 Sep;34(9):1556-1562.
60. Evans WE, Relling MV. Pharmacogenomics: translating functional genomics into rational therapeutics. Science 1999 Oct 15;286(5439):487-491.
61. Canaparo R, Nordmark A, Finnström N, Lundgren S, Seidegård J, Jeppsson B, et al. Expression of Cytochromes P450 3A and P-Glycoprotein in Human Large Intestinse in

Paired Tumour and Normal Samples. Basic & clinical pharmacology & toxicology 2007;100(4):240-248.
62. Guengerich FP. Cytochrome p450 and chemical toxicology. Chem Res Toxicol 2007;21(1):70-83.
63. Jelić D, Antolović R. From erythromycin to azithromycin and new potential ribosome-binding antimicrobials. Antibiotics 2016;5(3):29.
64. Hunt CM, Westerkam WR, Stave GM, Wilson JA. Hepatic cytochrome P-4503A (CYP3A) activity in the elderly. Mech Ageing Dev 1992;64(1-2):189-199.
65. Abernethy DR, Greenblatt DJ, Divoll M, Smith RB, Shader RI. The influence of obesity on the pharmacokinetics of oral alprazolam and triazolam. Clin Pharmacokinet 1984;9(2):177-183.
66. Michaut A, Moreau C, Robin M, Fromenty B. Acetaminophen-induced liver injury in obesity and nonalcoholic fatty liver disease. Liver International 2014;34(7):e171-e179.
67. Lucas D, Farez C, Bardou L, Vaisse J, Attali J, Valensi P. Cytochrome P450 2E1 activity in diabetic and obese patients as assessed by chlorzoxazone hydroxylation. Fundam Clin Pharmacol 1998;12(5):553-558.
68. Millonig G, Wang Y, Homann N, Bernhardt F, Qin H, Mueller S, et al. Ethanol-mediated carcinogenesis in the human esophagus implicates CYP2E1 induction and the generation of carcinogenic DNA-lesions. International journal of cancer 2011;128(3):533-540.
69. Abernethy DR, Greenblatt DJ, Divoll M, Shader RI. Enhanced glucuronide conjugation of drugs in obesity: studies of lorazepam, oxazepam, and acetaminophen. J Lab Clin Med 1983;101(6):873-880.
70. Aubert J, Begriche K, Knockaert L, Robin M, Fromenty B. Increased expression of cytochrome P450 2E1 in nonalcoholic fatty liver disease: mechanisms and pathophysiological role. Clinics and research in hepatology and gastroenterology 2011;35(10):630-637.
71. Begriche K, Massart J, Robin M, Bonnet F, Fromenty B. Mitochondrial adaptations and dysfunctions in nonalcoholic fatty liver disease. Hepatology 2013;58(4):1497-1507.
72. Ayano G. Clinical Pharmacology & Biopharmaceutics. 2016.
73. Zanger UM, Raimundo S, Eichelbaum M. Cytochrome P450 2D6: overview and update on pharmacology, genetics, biochemistry. Naunyn Schmiedebergs Arch Pharmacol 2004;369(1):23-37.
74. Ingelman-Sundberg M. Genetic polymorphisms of cytochrome P450 2D6 (CYP2D6): clinical consequences, evolutionary aspects and functional diversity. The pharmacogenomics journal 2005;5(1):6.
75. Cheymol G, Woestenborghs R, Snoeck E, Ianucci R, Le Moing J, Naditch L, et al. Pharmacokinetic study and cardiovascular monitoring of nebivolol in normal and obese subjects. Eur J Clin Pharmacol 1997;51(6):493-498.
76. Lefebvre J, Poirier L, Poirier P, Turgeon J, Lacourciere Y. The influence of CYP2D6 phenotype on the clinical response of nebivolol in patients with essential hypertension. Br J Clin Pharmacol 2007;63(5):575-582.

77. Schrenk D, Brockmeier D, Mörike K, Bock K, Eichelbaum M. A distribution study of CYP1A2 phenotypes among smokers and non-smokers in a cohort of healthy Caucasian volunteers. Eur J Clin Pharmacol 1998;53(5):361-367.
78. Plowchalk DR, Yeo KR. Prediction of drug clearance in a smoking population: modeling the impact of variable cigarette consumption on the induction of CYP1A2. Eur J Clin Pharmacol 2012;68(6):951-960.
79. Hammond D, Fong GT, Borland R, Cummings KM, McNeill A, Driezen P. Text and graphic warnings on cigarette packages: findings from the international tobacco control four country study. Am J Prev Med 2007;32(3):202-209.
80. Rostami-Hodjegan A, Nurminen S, Jackson PR, Tucker GT. Caffeine urinary metabolite ratios as markers of enzyme activity: a theoretical assessment. Pharmacogenetics 1996 Apr;6(2):121-149.
81. Rasmussen BB, Brøsen K. Theophylline has no advantages over caffeine as a putative model drug for assessing CYP1A2 activity in humans. Br J Clin Pharmacol 1997;43(3):253-258.
82. Caraco Y, Zylber-Katz E, Berry EM, Levy M. Caffeine pharmacokinetics in obesity and following significant weight reduction. Int J Obes Relat Metab Disord 1995 Apr;19(4):234-239.
83. Abernethy D, Todd EL, Schwartz JB. Caffeine disposition in obesity. Br J Clin Pharmacol 1985;20(1):61-66.
84. Jusko WJ, Gardner MJ, Mangione A, Schentag JJ, Koup JR, Vance JW. Factors affecting theophylline clearances: age, tobacco, marijuana, cirrhosis, congestive heart failure, obesity, oral contraceptives, benzodiazepines, barbiturates, and ethanol. J Pharm Sci 1979;68(11):1358-1366.
85. Blouin RA, Elgert JF, Bauer LA. Theophylline clearance: effect of marked obesity. Clinical Pharmacology & Therapeutics 1980;28(5):619-623.
86. Abernethy DR, Greenblatt DJ. Ibuprofen disposition in obese individuals. Arthritis & Rheumatism: Official Journal of the American College of Rheumatology 1985;28(10):1117-1121.
87. Abernethy DR, Greenblatt DJ. Phenytoin disposition in obesity: determination of loading dose. Arch Neurol 1985;42(5):468-471.
88. Flockhart DA. Drug interactions and the cytochrome P450 system. Clin Pharmacokinet 1995;29(1):45-52.
89. Abernethy DR, Greenblatt DJ., Divoll M, Shader RI. Prolonged accumulation of diazepam in obesity. The Journal of Clinical Pharmacology 1983;23(8-9):369-376.
90. Abernethy DR, Greenblatt DJ, Divoll M, Shader RI. Prolongation of drug half-life due to obesity: studies of desmethyldiazepam (clorazepate). J Pharm Sci 1982;71(8):942-944.
91. Strolin Benedetti M, Whomsley R, Baltes E. Involvement of enzymes other than CYPs in the oxidative metabolism of xenobiotics. Expert opinion on drug metabolism & toxicology 2006;2(6):895-921.

92. Rashidi M, Beedham C, Smith JS, Davaran S. In vitro study of 6-mercaptopurine oxidation catalysed by aldehyde oxidase and xanthine oxidase. Drug metabolism and pharmacokinetics 2007;22(4):299-306.
93. Chiney MS, Schwarzenberg SJ, L'aurelle AJ. Altered xanthine oxidase and N-acetyltransferase activity in obese children. Br J Clin Pharmacol 2011;72(1):109-115.
94. Gibson GG, Skett P. Pathways of drug metabolism. Introduction to drug metabolism: Springer; 1996. p. 1-34.
95. Oda S, Fukami T, Yokoi T, Nakajima M. A comprehensive review of UDP-glucuronosyltransferase and esterases for drug development. Drug metabolism and pharmacokinetics 2015;30(1):30-51.
96. Kiang TK, Ensom MH, Chang TK. UDP-glucuronosyltransferases and clinical drug-drug interactions. Pharmacol Ther 2005;106(1):97-132.
97. Tchernof A, Lévesque É, Beaulieu M, Couture P, Després J, Hum DW, et al. Expression of the androgen metabolizing enzyme UGT2B15 in adipose tissue and relative expression measurement using a competitive RT–PCR method. Clin Endocrinol (Oxf) 1999;50(5):637-642.
98. Mutlib AE, Goosen TC, Bauman JN, Williams JA, Kulkarni S, Kostrubsky S. Kinetics of Acetaminophen Glucuronidation by UDP-Glucuronosyltransferases 1A1, 1A6, 1A9 and 2B15. Potential Implications in Acetaminophen− Induced Hepatotoxicity. Chem Res Toxicol 2006;19(5):701-709.
99. Abernethy DR, Divoll M, Greenblatt DJ, Ameer B. Obesity, sex, and acetaminophen disposition. Clinical Pharmacology & Therapeutics 1982;31(6):783-790.
100. Barshop NJ, Capparelli EV, Sirlin CB, Schwimmer JB, Lavine JE. Acetaminophen pharmacokinetics in children with nonalcoholic fatty liver disease. J Pediatr Gastroenterol Nutr 2011 Feb;52(2):198-202.
101. Kim MS, Wang S, Shen Z, Kochansky CJ, Strauss JR, Franklin RB, et al. Differences in the pharmacokinetics of peroxisome proliferator-activated receptor agonists in genetically obese Zucker and sprague-dawley rats: implications of decreased glucuronidation in obese Zucker rats. Drug Metab Dispos 2004 Sep;32(9):909-914.
102. Mallick P, Shah P, Gandhi A, Ghose R. Impact of obesity on accumulation of the toxic irinotecan metabolite, SN-38, in mice. Life Sci 2015;139:132-138.
103. Okumura K, Kita T, Chikazawa S, Komada F, Iwakawa S, Tanigawara Y. Genotyping of N-acetylation polymorphism and correlation with procainamide metabolism. Clinical Pharmacology & Therapeutics 1997;61(5):509-517.
104. Christoff PB, Conti DR, Naylor C, Jusko WJ. Procainamide disposition in obesity. Drug Intell Clin Pharm 1983;17(7-8):516-522.
105. Czerwinski M, Gibbs JP, Slattery JT. Busulfan conjugation by glutathione S-transferases alpha, mu, and pi. Drug Metab Dispos 1996 Sep;24(9):1015-1019.
106. Gibbs JP, Gooley T, Corneau B, Murray G, Stewart P, Appelbaum FR, et al. The impact of obesity and disease on busulfan oral clearance in adults. Blood 1999 Jun 15;93(12):4436-4440.
107. Casey G. Metabolism and excretion: eliminating drugs from the body. Nurs N Z 2012 Aug;18(7):20-24.

108. Henegar JR, Bigler SA, Henegar LK, Tyagi SC, Hall JE. Functional and structural changes in the kidney in the early stages of obesity. J Am Soc Nephrol 2001 Jun;12(6):1211-1217.
109. Allard S, Kinzig M, Boivin G, Sörgel F, Lebel M. Intravenous ciprofloxacin disposition in obesity. Clinical Pharmacology & Therapeutics 1993;54(4):368-373.
110. Redinger RN. Fat storage and the biology of energy expenditure. Translational Research 2009;154(2):52-60.
111. Li MD. Leptin and beyond: an odyssey to the central control of body weight. Yale J Biol Med 2011 Mar;84(1):1-7.
112. Hall JE, do Carmo JM, da Silva AA, Wang Z, Hall ME. Obesity-induced hypertension: interaction of neurohumoral and renal mechanisms. Circ Res 2015;116(6):991-1006.
113. Lihn AS, Bruun JM, He G, Pedersen SB, Jensen PF, Richelsen B. Lower expression of adiponectin mRNA in visceral adipose tissue in lean and obese subjects. Mol Cell Endocrinol 2004;219(1-2):9-15.
114. Wang C. Obesity, inflammation, and lung injury (OILI): the good. Mediators Inflamm 2014;2014:978463.
115. Fantuzzi G. Adipose tissue, adipokines, and inflammation. J Allergy Clin Immunol 2005;115(5):911-919.
116. Aguilar-Valles A, Inoue W, Rummel C, Luheshi GN. Obesity, adipokines and neuroinflammation. Neuropharmacology 2015;96:124-134.
117. Hotamisligil GS, Murray DL, Choy LN, Spiegelman BM. Tumor necrosis factor alpha inhibits signaling from the insulin receptor. Proc Natl Acad Sci U S A 1994 May 24;91(11):4854-4858.
118. Aitken AE, Morgan ET. Gene-specific effects of inflammatory cytokines on cytochrome P450 2C, 2B6 and 3A4 mRNA levels in human hepatocytes. Drug Metab Dispos 2007 Sep;35(9):1687-1693.
119. Mimura H, Kobayashi K, Xu L, Hashimoto M, Ejiri Y, Hosoda M, et al. Effects of cytokines on CYP3A4 expression and reversal of the effects by anti-cytokine agents in the three-dimensionally cultured human hepatoma cell line FLC-4. Drug metabolism and pharmacokinetics 2015;30(1):105-110.
120. Harvey RD, Morgan E. Cancer, Inflammation, and Therapy: Effects on Cytochrome P450–Mediated Drug Metabolism and Implications for Novel Immunotherapeutic Agents. Clinical Pharmacology & Therapeutics 2014;96(4):449-457.
121. Morgan ET. Regulation of cytochromes P450 during inflammation and infection. Drug Metab Rev 1997;29(4):1129-1188.
122. Mofenson HC, Caraccio TR, Miller H, Greensher J. Lidocaine toxicity from topical mucosal application: with a review of the clinical pharmacology of lidocaine. Clin Pediatr 1983;22(3):190-192.
123. Challapalli V, Tremont-Lukats IW, McNicol ED, Lau J, Carr DB. Systemic administration of local anesthetic agents to relieve neuropathic pain. Cochrane Database of Systematic Reviews 2005(4).

124. Hondeghem L, Katzung B. Antiarrhythmic agents: the modulated receptor mechanism of action of sodium and calcium channel-blocking drugs. Annu Rev Pharmacol Toxicol 1984;24(1):387-423.
125. Benowitz NL, Meister W. Clinical pharmacokinetics of lignocaine. Clin Pharmacokinet 1978;3(3):177-201.
126. Routledge PA, Shand DG. Presystemic drug elimination. Annu Rev Pharmacol Toxicol 1979;19(1):447-468.
127. Fehmers MC, Dunning AJ. Intramuscularly and orally administered lidocaine in the treatment of ventricular arrhythmias in acute myocardial infarction. Am J Cardiol 1972 Apr;29(4):514-519.
128. Perucca E, Richens A. Reduction of oral bioavailability of lignocaine by induction of first pass metabolism in epileptic patients. Br J Clin Pharmacol 1979;8(1):21-31.
129. Boyes R, Scott D, Jebson P, Godman M, Julian D. Pharmacokinetics of lidocaine in man. Clinical Pharmacology & Therapeutics 1971;12(1):105-116.
130. Nation RL, Triggs EJ, Selig M. Lignocaine kinetics in cardiac patients and aged subjects. Br J Clin Pharmacol 1977;4(4):439-448.
131. Gillette JR. Factors affecting drug metabolism. Ann N Y Acad Sci 1971;179(1):43-66.
132. Wilkinson GR, Shand DG. A physiological approach to hepatic drug clearance. Clinical Pharmacology & Therapeutics 1975;18(4):377-390.
133. Routledge PA, Stargel WW, Wagner GS, Shand DG. Increased alpha-1-acid glycoprotein and lidocaine disposition in myocardial infarction. Ann Intern Med 1980;93(5):701-704.
134. Routledge PA, Shand DG, Barchowsky A, Wagner G, Stargel WW. Relationship between α1-acid glycoprotein and lidocaine disposition in myocardial infarction. Clinical Pharmacology & Therapeutics 1981;30(2):154-157.
135. Koppert W, Weigand M, Neumann F, Sittl R, Schuettler J, Schmelz M, et al. Perioperative intravenous lidocaine has preventive effects on postoperative pain and morphine consumption after major abdominal surgery. Anesthesia & Analgesia 2004;98(4):1050-1055.
136. Herroeder S, Pecher S, Schonherr ME, Kaulitz G, Hahnenkamp K, Friess H, et al. Systemic lidocaine shortens length of hospital stay after colorectal surgery: a double-blinded, randomized, placebo-controlled trial. Ann Surg 2007 Aug;246(2):192-200.
137. Keenaghan JB, Boyes RN. The tissue distribution, metabolism and excretion of lidocaine in rats, guinea pigs, dogs and man. J Pharmacol Exp Ther 1972 Feb;180(2):454-463.
138. Bargetzi MJ, Aoyama T, Gonzalez FJ, Meyer UA. Lidocaine metabolism in human liver microsomes by cytochrome P450IIIA4. Clinical Pharmacology & Therapeutics 1989;46(5):521-527.
139. Strong JM, Mayfield DE, Atkinson Jr AJ, Burris BC, Raymon F, Webster Jr LT. Pharmacological activity, metabolism, and pharmacokinetics of glycinexylidide. Clinical Pharmacology & Therapeutics 1975;17(2):184-194.
140. Rowland M, Thomson PD, Guichard A, Melmon KL. Disposition kinetics of lidocaine in normal subjects. Ann N Y Acad Sci 1971;179(1):383-398.

141. Thomson PD, Melmon KL, Richardson JA, Cohn K, Steinbrunn W, Cudihee R, et al. Lidocaine pharmacokinetics in advanced heart failure, liver disease, and renal failure in humans. Ann Intern Med 1973;78(4):499-508.
142. Bennett PN, Aarons LJ, Bending MR, Steiner JA, Rowland M. Pharmacokinetics of lidocaine and its deethylated metabolite: dose and time dependency studies in man. J Pharmacokinet Biopharm 1982;10(3):265-281.
143. Evans WE, Schentag JJ, Jusko WJ. Applied pharmacokinetics: principles of therapeutic drug monitoring. : Applied Therapeutics, Incorporated; 1992.
144. Shafer SL. Advances in propofol pharmacokinetics and pharmacodynamics. J Clin Anesth 1993;5(6):14-21.
145. Kotani Y, Shimazawa M, Yoshimura S, Iwama T, Hara H. The experimental and clinical pharmacology of propofol, an anesthetic agent with neuroprotective properties. CNS neuroscience & therapeutics 2008;14(2):95-106.
146. Mark S, RENNIE C. Propofol. A review of its pharmacodynamic and pharmacokinetic properties and use as an intravenous anaesthesia. Drug Evaluation 1988;35:334-372.
147. Guitton J, Buronfosse T, Desage M, Flinois J, Perdrix J, Brazier J, et al. Possible involvement of multiple human cytochrome P450 isoforms in the liver metabolism of propofol. Br J Anaesth 1998;80(6):788-795.
148. Hariri N, Thibault L. High-fat diet-induced obesity in animal models. Nutrition research reviews 2010;23(2):270-299.
149. Cheymol G, Poirier J, Barre J, Pradalier A, Dry J. Comparative pharmacokinetics of intravenous propranolol in obese and normal volunteers. The Journal of Clinical Pharmacology 1987;27(11):874-879.
150. Blouin RA, Warren GW. Pharmacokinetic considerations in obesity. J Pharm Sci 1999;88(1):1-7.
151. Mukai M, Isobe T, Okada K, Murata M, Shigeyama M, Hanioka N. Species and sex differences in propofol glucuronidation in liver microsomes of humans, monkeys, rats and mice. Die Pharmazie-An International Journal of Pharmaceutical Sciences 2015;70(7):466-470.
152. Abdussalam A, Elshenawy OH, Bin Jardan YA, El-Kadi AOS, Brocks DR. The Obesogenic Potency of Various High-Caloric Diet Compositions in Male Rats, and Their Effects on Expression of Liver and Kidney Proteins Involved in Drug Elimination. J Pharm Sci 2017 Jun;106(6):1650-1658.
153. Elshenawy OH, El-Kadi AO. Modulation of aryl hydrocarbon receptor-regulated enzymes by trimethylarsine oxide in C57BL/6 mice: In vivo and in vitro studies. Toxicol Lett 2015;238(1):17-31.
154. LOWRY, O. H., ROSEBROUGH, N. J., FARR, A. L., & RANDALL, R. J. (1951). Protein measurement with the folin phenol reagent. The Journal of Biological Chemistry, 193(1), 265-275
155. Guideline on Bioanalytical Method Validation. Available online: http://www.ema.europa.eu/docs/en_GB/document_library/Scientific_guideline/2011/08/WC500109686.pdf (accessed on 15 November 2017).

156. Ohshima T, Takayasu T. Simultaneous determination of local anesthetics including ester-type anesthetics in human plasma and urine by gas chromatography–mass spectrometry with solid-phase extraction. Journal of Chromatography B: Biomedical Sciences and Applications 1999;726(1-2):185-194.
157. Piwowarska J, Kuczyñska J, Pachecka J. Liquid chromatographic method for the determination of lidocaine and monoethylglycine xylidide in human serum containing various concentrations of bilirubin for the assessment of liver function. Journal of Chromatography B 2004;805(1):1-5.
158. Chen L, Liao L, Zuo Z, Yan Y, Yang L, Fu Q, et al. Simultaneous determination of nikethamide and lidocaine in human blood and cerebrospinal fluid by high performance liquid chromatography. J Pharm Biomed Anal 2007;43(5):1757-1762.
159. Tam Y, Tawfik S, Ke J, Coutts R, Gray M, Wyse D. High-performance liquid chromatography of lidocaine and nine of its metabolites in human plasma and urine. Journal of Chromatography B: Biomedical Sciences and Applications 1987;423:199-206.
160. Lotfi H, Debord J, Dreyfuss MF, Marquet P, Ben Rhaiem M, Feiss P, et al. Simultaneous determination of lidocaine and bupivacaine in human plasma: application to pharmacokinetics. Ther Drug Monit 1997 Apr;19(2):160-164.
161. Qin W, Jiao Z, Zhong M, Shi X, Zhang J, Li Z, et al. Simultaneous determination of procaine, lidocaine, ropivacaine, tetracaine and bupivacaine in human plasma by high-performance liquid chromatography. Journal of Chromatography B 2010;878(15-16):1185-1189.
162. Bhusal P, Sharma M, Harrison J, Procter G, Andrews G, Jones DS, et al. Development, validation and application of a stability indicating HPLC method to quantify lidocaine from polyethylene-co-vinyl acetate (EVA) matrices and biological fluids. J Chromatogr Sci 2017;55(8):832-838.
163. Nation RL, Peng GW, Chiou WL. High-performance liquid chromatographic method for the simultaneous determination of lidocaine and its N-dealkylated metabolites in plasma. J Chromatogr 1979 Mar 1;162(3):466-473.
164. Sintov A, Siden R, Levy RJ. Sensitive high-performance liquid chromatographic assay using 9-fluorenylmethylchloroformate for monitoring controlled-release lidocaine in plasma. Journal of Chromatography B: Biomedical Sciences and Applications 1989;496:335-344.
165. Kihara S, Miyabe M, Kakiuchi Y, Takahashi S, Fukuda T, Kohda Y, et al. Plasma concentrations of lidocaine and its principal metabolites during continuous epidural infusion of lidocaine with or without epinephrine. Reg Anesth Pain Med 1999;24(6):529-533.
166. Dusci LJ, Hackett LP. Simultaneous determination of lidocaine, mexiletine, disopyramide, and quinidine in plasma by high performance liquid chromatography. J Anal Toxicol 1985;9(2):67-70.

167. Ter Weijden E, Van den Broek M, Ververs F. Easy and fast LC–MS/MS determination of lidocaine and MEGX in plasma for therapeutic drug monitoring in neonates with seizures. Journal of Chromatography B 2012;881:111-114.
168. Dal Bo L, Mazzucchelli P, Marzo A. Highly sensitive bioassay of lidocaine in human plasma by high-performance liquid chromatography–tandem mass spectrometry. Journal of Chromatography A 1999;854(1-2):3-11.
169. Ochoa-Aranda E, Esteve-Romero J, Rambla-Alegre M, Martinavarro-Domnguez A, Marcos-Toms JV, Bose D. Monitoring disopyramide, lidocaine, and quinidine by micellar liquid chromatography. J AOAC Int 2011;94(2):537-542.
170. Roos RW, Lau-Cam CA. General reversed-phase high-performance liquid chromatographic method for the separation of drugs using triethylamine as a competing base. Journal of Chromatography A 1986;370:403-418.
171. Ruiz-Angel M, Torres-Lapasió J, Carda-Broch S, Garcia-Alvarez-Coque M. Improvement of peak shape and separation performance of β-blockers in conventional reversed-phase columns using solvent modifiers. J Chromatogr Sci 2003;41(7):350-358.
172. Chen, L.; Wang, Q.; Shi, K.; Liu, F.; Liu, L.; Ni, J.; Fang, X.; Xu, X. The Effects of Lidocaine Used in Sciatic Nerve on the Pharmacodynamics and Pharmacokinetics of Ropivacaine in Sciatic Nerve Combined with Lumbar Plexus Blockade: A Double-Blind, Randomized Study. Basic Clin. Pharmacol. Toxicol. 2013, 112, 203–208.
173. Bargetzi MJ, Aoyama T, Gonzalez FJ, Meyer UA. Lidocaine metabolism in human liver microsomes by cytochrome P450IIIA4. Clinical Pharmacology & Therapeutics 1989;46(5):521-527.
174. Subramanian M, Kurawattimath V, Pocha K, Freeden C, Rao I, Thanga Mariappan T, Marathe PH, Vikramadithyan RK, Abraham P, Kulkarni CP, Katnapally P. Role of hepatic blood flow and metabolism in the pharmacokinetics of ten drugs in lean, aged and obese rats. Xenobiotica. 2014 Dec 1;44(12):1108-16.
175. Abdussalam A, Al-Agili M, Al Nebaihi HM, Mayo PR, Gabr RQ, Brocks DR. Dietary-Induced Obesity and Changes in the Biodistribution and Metabolism of Amiodarone in the Rat. Journal of pharmaceutical sciences. 2018 Nov 1;107(11):2938-45.
176. Abdussalam A, Elshenawy OH, bin Jardan YA, El-Kadi AO, Brocks DR. The Obesogenic Potency of Various High-Caloric Diet Compositions in Male Rats, and Their Effects on Expression of Liver and Kidney Proteins Involved in Drug Elimination. Journal of pharmaceutical sciences. 2017 Jun 1;106(6):1650-8.
177. Cowan RE, Jackson BT, Grainger SL, Thompson RP. Effects of anesthetic agents and abdominal surgery on liver blood flow. Hepatology. 1991 Dec;14(6):1161-6.
178. Gelman S. General anesthesia and hepatic circulation. Canadian Journal of Physiology and Pharmacology. 1987 Aug 1;65(8):1762-79.

179. Tunon MJ, Gonzalez P, Jorquera F, Llorente A, Gonzalo-Orden M, Gonzalez-Gallego J. Liver blood flow changes during laparoscopic surgery in pigs. Surgical endoscopy. 1999 Jul 1;13(7):668-72.
180. Easton JA, Hardwicke J, Whitehead PH. The estimation of two alpha1 glycoproteins (orosomucoid and another alpha1 acid glycoprotein) in health and disease. Journal of clinical pathology. 1962 Nov 1;15(6):585-90.
181. Routledge PA, Lazar JD, Barchowsky A, Stargel WW, Wagner GS, Shand DG. A free lignocaine index as a guide to unbound drug concentration. British journal of clinical pharmacology. 1985 Dec 1;20(6):695-8.
182. Woodhouse KW, Wynne HA. Age-related changes in liver size and hepatic blood flow. Clinical pharmacokinetics. 1988 Nov 1;15(5):287-94.
183. Abernethy DR, Greenblatt DJ. Impairment of lidocaine clearance in elderly male subjects. Journal of cardiovascular pharmacology. 1983;5(6):1093-6.
184. Schwartz AE, Matteo RS, Ornstein E, Young WL, Myers KJ. Pharmacokinetics of sufentanil in obese patients. Anesth Analg 1991 Dec;73(6):790-793.
185. Chung EK, Cheatham SC, Fleming MR, Healy DP, Shea KM, Kays MB. Population pharmacokinetics and pharmacodynamics of piperacillin and tazobactam administered by prolonged infusion in obese and nonobese patients. The Journal of Clinical Pharmacology 2015;55(8):899-908.
186. Benedek I, Fiske 3d W, Griffen W, Bell R, Blouin R, McNamara P. Serum alpha 1-acid glycoprotein and the binding of drugs in obesity. Br J Clin Pharmacol 1983;16(6):751-754.
187. Patoine D, Levac X, Pilote S, Drolet B, Simard C. Decreased CYP3A expression and activity in guinea pig models of diet-induced metabolic syndrome: is fatty liver infiltration involved? Drug Metab Dispos 2013 May;41(5):952-957.
188. Schemmel R, Mickelsen O, Gill J. Dietary obesity in rats: body weight and body fat accretion in seven strains of rats. J Nutr 1970;100(9):1041-1048.
189. Venkatakrishnan K, von Moltke LL, Obach R, Greenblatt DJ. Drug metabolism and drug interactions: application and clinical value of in vitro models. Curr Drug Metab 2003;4(5):423-459.
190. Vrieze SI. Model selection and psychological theory: a discussion of the differences between the Akaike information criterion (AIC) and the Bayesian information criterion (BIC). Psychol Methods 2012;17(2):228.
191. Yamaoka K, Nakagawa T, Uno T. Application of Akaike's information criterion (AIC) in the evaluation of linear pharmacokinetic equations. J Pharmacokinet Biopharm 1978;6(2):165-175.
192. Orlando R, Piccoli P, De Martin S, Padrini R, Floreani M, Palatini P. Cytochrome P450 1A2 is a major determinant of lidocaine metabolism in vivo: effects of liver function. Clinical Pharmacology & Therapeutics 2004;75(1):80-88.

193. Jamwal R, de la Monte, Suzanne M, Ogasawara K, Adusumalli S, Barlock BB, Akhlaghi F. Nonalcoholic fatty liver disease and diabetes is associated with decreased CYP3A4 protein expression and activity in human liver. Molecular pharmaceutics 2018.
194. Irizar A, Barnett CR, Flatt PR, Ioannides C. Defective expression of cytochrome P450 proteins in the liver of the genetically obese Zucker rat. European Journal of Pharmacology: Environmental Toxicology and Pharmacology 1995;293(4):385-393.
195. Jover R, Bort R, GÓMEZ-LECHÓN MJ, Castell JV. Down-regulation of human CYP3A4 by the inflammatory signal interleukin-6: molecular mechanism and transcription factors involved. The FASEB Journal 2002;16(13):1799-1801.
196. Abdel-Razzak Z, Loyer P, Fautrel A, Gautier JC, Corcos L, Turlin B, et al. Cytokines down-regulate expression of major cytochrome P-450 enzymes in adult human hepatocytes in primary culture. Mol Pharmacol 1993 Oct;44(4):707-715.
197. Kern PA, Ranganathan S, Li C, Wood L, Ranganathan G. Adipose tissue tumor necrosis factor and interleukin-6 expression in human obesity and insulin resistance. American Journal of Physiology-Endocrinology And Metabolism 2001;280(5):E745-E751.
198. Barker CW, Fagan JB, Pasco DS. Interleukin-1 beta suppresses the induction of P4501A1 and P4501A2 mRNAs in isolated hepatocytes. J Biol Chem 1992 Apr 25;267(12):8050-8055.
199. Wu R, Cui X, Dong W, Zhou M, Simms HH, Wang P. Suppression of hepatocyte CYP1A2 expression by Kupffer cells via AhR pathway: the central role of proinflammatory cytokines. International journal of molecular medicine. 2006 Aug 1;18(2):339-46.
200. Shimizu M, Matsumoto Y, Tatsuno M, Fukuoka M. Glucuronidation of propofol and its analogs by human and rat liver microsomes. Biological and Pharmaceutical Bulletin 2003;26(2):216-219.
201. Guitton J, Buronfosse T, Desage M, Flinois J, Perdrix J, Brazier J, et al. Possible involvement of multiple human cytochrome P450 isoforms in the liver metabolism of propofol. Br J Anaesth 1998;80(6):788-795.
202. Simons PJ, Cockshott ID, Douglas EJ, Gordon EA, Knott S, Ruane RJ. Species differences in blood profiles, metabolism and excretion of 14C-propofol after intravenous dosing to rat, dog and rabbit. Xenobiotica. 1991 Jan 1;21(10):1243-56.
203. Emi Y, Ikushiro S, Iyanagi T. Drug-responsive and tissue-specific alternative expression of multiple first exons in rat UDP-glucuronosyltransferase family 1 (UGT1) gene complex. The Journal of Biochemistry 1995;117(2):392-399.
204. Al-Jahdari WS, Yamamoto K, Hiraoka H, Nakamura K, Goto F, Horiuchi R. Prediction of total propofol clearance based on enzyme activities in microsomes from human kidney and liver. Eur J Clin Pharmacol 2006;62(7):527-533.

205. Elam MB, Cowan Jr GS, Rooney RJ, Hiler ML, Yellaturu CR, Deng X, et al. Hepatic gene expression in morbidly obese women: implications for disease susceptibility. Obesity 2009;17(8):1563-1573.
206. Wright K, Morgan ET. Regulation of cytochrome P450IIC12 expression by interleukin-1 alpha, interleukin-6, and dexamethasone. Mol Pharmacol 1991 Apr;39(4):468-474.
207. Ghose R, Omoluabi O, Gandhi A, Shah P, Strohacker K, Carpenter KC, McFarlin B, Guo T. Role of high-fat diet in regulation of gene expression of drug metabolizing enzymes and transporters. Life sciences. 2011 Jul 4;89(1-2):57-64.
208. Favetta P, Degoute CS, Perdrix JP, Dufresne C, Boulieu R, Guitton J. Propofol metabolites in man following propofol induction and maintenance. British journal of anaesthesia. 2002 May 1;88(5):653-8.
209. Lee G, Oh K, Kim H, Han H, Lee H, Park K, et al. Effect of BI-1 on insulin resistance through regulation of CYP2E1. Scientific reports 2016;6:32229.
210. Yoshinari K, Takagi S, Yoshimasa T, Sugatani J, Miwa M. Hepatic CYP3A expression is attenuated in obese mice fed a high-fat diet. Pharm Res 2006;23(6):1188-1200.
211. Roe A, Howard G, Blouin R, Snawder JE. Characterization of cytochrome P450 and glutathione S-transferase activity and expression in male and female ob/ob mice. Int J Obes 1999;23(1):48.
212. O'Shea D, Davis SN, Kim RB, Wilkinson GR. Effect of fasting and obesity in humans on the 6-hydroxylation of chlorzoxazone: a putative probe of CYP2E1 activity. Clinical Pharmacology & Therapeutics 1994;56(4):359-367.
213. Weltman MD, Farrell GC, Hall P, Ingelman-Sundberg M, Liddle C. Hepatic cytochrome P450 2E1 is increased in patients with nonalcoholic steatohepatitis. Hepatology 1998;27(1):128-133.
214. Niemelä O, Parkkila S, Juvonen RO, Viitala K, Gelboin HV, Pasanen M. Cytochromes P450 2A6, 2E1, and 3A and production of protein-aldehyde adducts in the liver of patients with alcoholic and non-alcoholic liver diseases. J Hepatol 2000;33(6):893-901.
215. Emery MG, Fisher JM, Chien JY, Kharasch ED, Dellinger EP, Kowdley KV, et al. CYP2E1 activity before and after weight loss in morbidly obese subjects with nonalcoholic fatty liver disease. Hepatology 2003;38(2):428-435.
216. Varela NM, Quinones LA, Orellana M, Poniachik J, Csendes A, Smok G, et al. Study of cytochrome P450 2E1 and its allele variants in liver injury of nondiabetic, nonalcoholic steatohepatitis obese women. Biol Res 2008;41(1):81-92.
217. Bell LN, Temm CJ, Saxena R, Vuppalanchi R, Schauer P, Rabinovitz M, et al. Bariatric surgery-induced weight loss reduces hepatic lipid peroxidation levels and affects hepatic cytochrome P-450 protein content. Ann Surg 2010 Jun;251(6):1041-1048.

218. Raucy JL, Lasker JM, Kraner JC, Salazar DE, Lieber CS, Corcoran GB. Induction of cytochrome P450IIE1 in the obese overfed rat. Mol Pharmacol 1991 Mar;39(3):275-280.
219. Zou Y, Li J, Lu C, Wang J, Ge J, Huang Y, et al. High-fat emulsion-induced rat model of nonalcoholic steatohepatitis. Life Sci 2006;79(11):1100-1107.
220. Khemawoot P, Yokogawa K, Shimada T, Miyamoto K. Obesity-induced increase of CYP2E1 activity and its effect on disposition kinetics of chlorzoxazone in Zucker rats. Biochem Pharmacol 2007;73(1):155-162.
221. Begriche K, Lettéron P, Abbey-Toby A, Vadrot N, Robin M, Bado A, et al. Partial leptin deficiency favors diet-induced obesity and related metabolic disorders in mice. American Journal of Physiology-Endocrinology and Metabolism 2008;294(5):E939-E951.
222. Osabe M, Sugatani J, Fukuyama T, Ikushiro S, Ikari A, Miwa M. Expression of hepatic UDP-glucuronosyltransferase 1A1 and 1A6 correlated with increased expression of the nuclear constitutive androstane receptor and peroxisome proliferator-activated receptor alpha in male rats fed a high-fat and high-sucrose diet. Drug Metab Dispos 2008 Feb;36(2):294-302.
223. Baumgardner JN, Shankar K, Hennings L, Badger TM, Ronis MJ. A new model for nonalcoholic steatohepatitis in the rat utilizing total enteral nutrition to overfeed a high-polyunsaturated fat diet. American Journal of Physiology-Gastrointestinal and Liver Physiology 2008;294(1):G27-G38.
224. Abernethy DR, Greenblatt DJ. Lidocaine disposition in obesity. American Journal of Cardiology. 1984 Apr 1;53(8):1183-6.
225. von Bahr C, Hedlund I, Karlen B, Backstrom D, Grasdalen H. Evidence for two catalytically different binding sites of liver microsomal cytochrome P-450: importance for species and sex differences in oxidation pattern of lidocaine. Acta Pharmacol Toxicol (Copenh) 1977 Jul;41(1):39-48.
226. Lauder GR. A Review of Intravenous Lidocaine Infusion Therapy for Paediatric Acute and Chronic Pain Management. InPain Relief-From Analgesics to Alternative Therapies 2017. InTech.
227. Scandlyn MJ, Stuart EC, Rosengren RJ. Sex-specific differences in CYP450 isoforms in humans. Expert opinion on drug Metabolism & toxicology. 2008 Apr 1;4(4):413-24.
228. Cui YJ, Yeager RL, Zhong XB, Klaassen CD. Ontogenic expression of hepatic Ahr mRNA is associated with histone H3K4 di-methylation during mouse liver development. Toxicology letters. 2009 Sep 28;189(3):184-90.
229. Honkakoski P, Negishi M. Regulation of cytochrome P450 (CYP) genes by nuclear receptors. Biochemical Journal. 2000 Apr 15;347(2):321-37.
230. Chen S, Wang K, Wan YJ. Retinoids activate RXR/CAR-mediated pathway and induce CYP3A. Biochemical pharmacology. 2010 Jan 15;79(2):270-6.

231. Phillips JM, Yamamoto Y, Negishi M, Maronpot RR, Goodman JI. Orphan nuclear receptor constitutive active/androstane receptor–mediated alterations in DNA methylation during phenobarbital promotion of liver tumorigenesis. Toxicological sciences. 2006 Dec 16;96(1):72-82.
232. Xu C, Li CY, Kong AN. Induction of phase I, II and III drug metabolism/transport by xenobiotics. Archives of pharmacal research. 2005 Mar 1;28(3):249.
233. Takagi S, Nakajima M, Mohri T, Yokoi T. Post-transcriptional regulation of human pregnane X receptor by micro-RNA affects the expression of cytochrome P450 3A4. Journal of biological chemistry. 2008 Apr 11;283(15):9674-80.
234. Wang, K., Chen, S., Xie, W. & Wan, Y.J. (2008). Retinoids induce cytochrome P450 3A4 through RXR/VDR-mediated pathway. *Biochemical Pharmacology*. Vol.75, No.11, (June 2008), pp. 2204-2213, ISSN 0006-2952.
235. Levi M. Nuclear receptors in renal disease. Biochimica et Biophysica Acta (BBA)-Molecular Basis of Disease. 2011 Aug 1;1812(8):1061-7.
236. Álvarez S, Bourguet W, Gronemeyer H, de Lera ÁR. Retinoic acid receptor modulators: a perspective on recent advances and promises. Expert opinion on therapeutic patents. 2011 Jan 1;21(1):55-63.
237. Czekaj P, Skowronek R. Transcription factors potentially involved in regulation of cytochrome P450 gene expression. InTopics on Drug Metabolism 2012. InTech.
238. Hanley MJ, Abernethy DR, Greenblatt DJ. Effect of obesity on the pharmacokinetics of drugs in humans. Clinical pharmacokinetics. 2010 Feb 1;49(2):71-87.
239. Abernethy DR, Schwartz JB. Verapamil pharmacodynamics and disposition in obese hypertensive patients. Journal of cardiovascular pharmacology. 1988 Feb;11(2):209-15.
240. Milsap RL, Plaisance KI, Jusko WJ. Prednisolone disposition in obese men. Clinical Pharmacology & Therapeutics. 1984 Dec;36(6):824-31.
241. Caraco Y, Zylber-Katz E, Berry EM, Levy M. Carbamazepine Phakmacokinetics in Obese and Lean Subjects. Annals of Pharmacotherapy. 1995 Sep;29(9):843-7.
242. Le Jeunne C, Poirier JM, Cheymol G, Ertzbischoff O, Engel F, Hugues FC. Pharmacokinetics of intravenous bisoprolol in obese and non-obese volunteers. European journal of clinical pharmacology. 1991 Aug 1;41(2):171-4.
243. Schwartz AE, Matteo RS, Ornstein E, Young WL, Myers KJ. Pharmacokinetics of sufentanil in obese patients. Anesthesia and analgesia. 1991 Dec;73(6):790-3.
244. Bauer LA, Wareing-Tran C, Drew Edwards WA, Raisys V, Ferreri L, Jack R, Patchen Dellinger E, Simonowitz D. Cimetidine clearance in the obese. Clinical Pharmacology & Therapeutics. 1985 Apr;37(4):425-30.
245. Abernethy DR, Todd EL, Schwartz JB. Caffeine disposition in obesity. British journal of clinical pharmacology. 1985 Jul;20(1):61-6.
246. Warden CH, Fisler JS. Comparisons of diets used in animal models of high fat feeding. Cell metabolism. 2008 Apr;7(4):277.
247. Torre-Villalvazo I, Tovar AR, Ramos-Barragán VE, Cerbón-Cervantes MA, Torres N. Soy protein ameliorates metabolic abnormalities in liver and adipose tissue of rats fed a high fat diet. The Journal of nutrition. 2008 Mar 1;138(3):462-8.
248. Lephart ED, Porter JP, Lund TD, Bu L, Setchell KD, Ramoz G, Crowley WR. Dietary isoflavones alter regulatory behaviors, metabolic hormones and neuroendocrine function in Long-Evans male rats. Nutrition & metabolism. 2004 Dec;1(1):16.